P-04-103

Forsmark site investigation

Petrography, geochemistry, petrophysics and fracture mineralogy of boreholes KFM01A, KFM02A and KFM03A+B

Jesper Petersson, Johan Berglund,
Peter Danielsson, Anders Wängnerud
SwedPower AB

Eva-Lena Tullborg, Terralogica AB

Håkan Mattsson, Hans Thunehed, Hans Isaksson
GeoVista AB

Hardy Lindroos, MIRAB Mineral Resurser AB

May 2004

Svensk Kärnbränslehantering AB
Swedish Nuclear Fuel
and Waste Management Co
Box 5864
SE-102 40 Stockholm Sweden
Tel 08-459 84 00
+46 8 459 84 00
Fax 08-661 57 19
+46 8 661 57 19

ISSN 1651-4416
SKB P-04-103

Forsmark site investigation

Petrography, geochemistry, petrophysics and fracture mineralogy of boreholes KFM01A, KFM02A and KFM03A+B

Jesper Petersson, Johan Berglund,
Peter Danielsson, Anders Wängnerud
SwedPower AB

Eva-Lena Tullborg, Terralogica AB

Håkan Mattsson, Hans Thunehed, Hans Isaksson
GeoVista AB

Hardy Lindroos, MIRAB Mineral Resurser AB

May 2004

Keywords: KFM01A, KFM02A, KFM03A, KFM03B, Geology, Petrography, Geochemistry, Petrophysics, Fractures, Forsmark, AP PF 400-03-51, Field note Forsmark 61.

Contents

1 Introduction

Since 2002, SKB investigates two potential sites at Forsmark and Oskarshamn for a deep repository in the Swedish Precambrian basement. In order to characterise the rock mass down to a depth of about 1 km at the Forsmark test site area, SKB has initiated a drilling program starting with three deep telescopic boreholes, denoted KFM01A, KFM02A and KFM03A (Figure 1-1). Each borehole starts with 100 m of percussion drilling, followed by core drilling down to about 1000 m depth. To obtain drill cores for the upper 100 m of the boreholes, three additional boreholes were planned adjacent to the telescopic boreholes. In November 2003, at the time of initiating this project, one such borehole, KFM03B, was finished. Material obtained from all four boreholes (KFM01A, KFM02A, KFM03A and KFM03B) have been mapped in detail by the so-called Boremap system /Petersson and Wängnerud, 2003; Petersson et al, 2003, 2004/. Boremap integrates information from drill core mapping, or alternatively, the drill cuttings when a core is not available, with results from BIPS-logging (Borehole Image Processing System). Lithological features are mapped, as well as fractures, and the absolute position and orientation of fractures and lithological boundaries are calculated /Stråhle, 2003/. Following the mapping activities, the drill cores were sampled for more specialized studies, pertaining to the petrograpical, geochemical, petrophysical and mechanical properties of the rock mass.

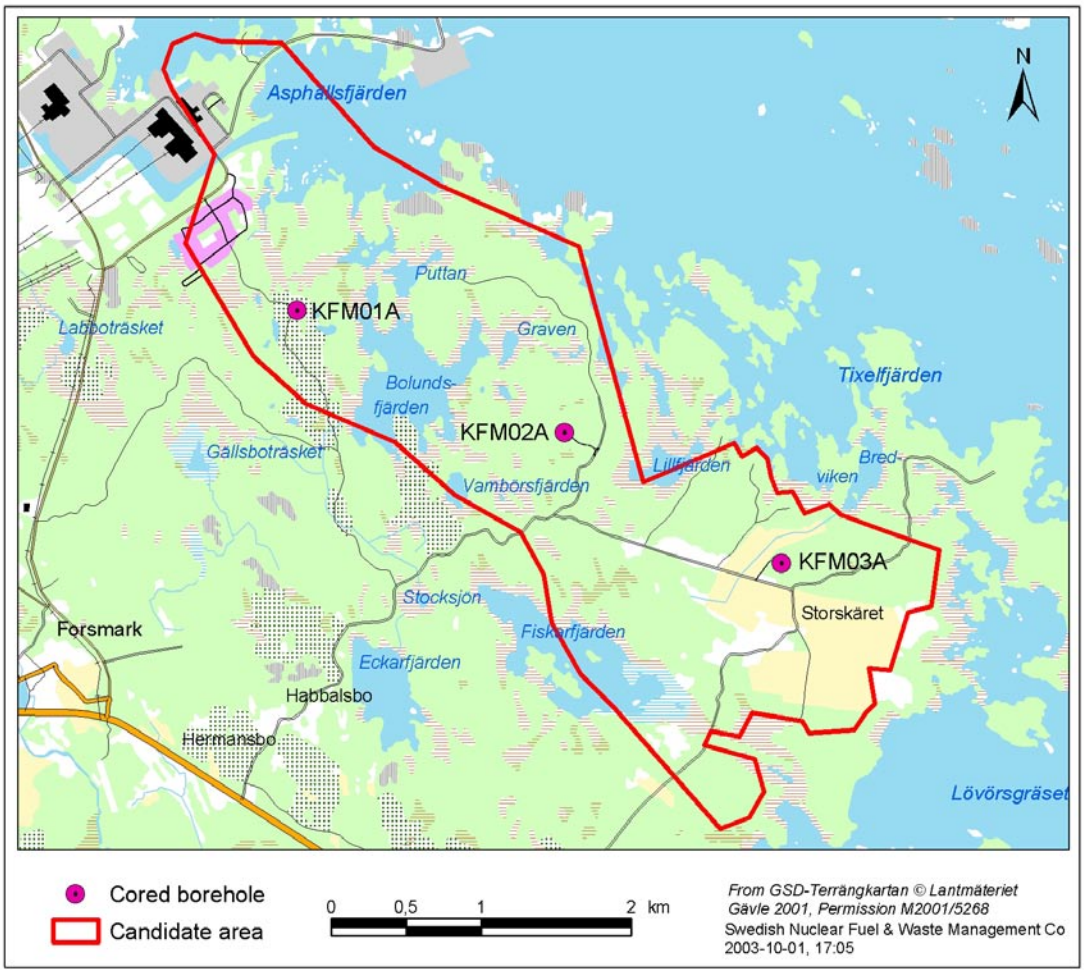

Figure 1-1. *Location of the three, 1 km deep cored boreholes KFM01A, KFM02A and KFM03A in the Forsmark area.*

The purpose of this report is to present the results from the petrographical, geochemical and petrophysical investigations of the first four drill cores obtained from the Forsmark test site area. Although the sampling program mainly dealt with whole-rock samples, it also includes characterisation and identification of a number of fracture filling minerals. The report gives also a brief discussion of the results within each section to aid forthcoming interpretations in a larger context. A more in-depth discussion is, however, beyond the scope of the project. To facilitate comparison with corresponding data for surface bedrock samples given by /Stephens et al, 2003/, the grouping of rock types, the choice of diagrams for data presentation, etc follows that of Stephens et al.

The work has been conducted by a project group, in which Eva-Lena Tullborg (Terralogica AB) has answered for the fracture mineralogy, Håkan Mattsson, Hans Thunehed and Hans Isaksson (GeoVista AB) for the petrophysics, and Jesper Petersson (with assistance from Johan Berglund, Peter Danielsson and Anders Wängnerud; SwedPower AB) for the petrography and geochemistry. Representatives for each discipline have been responsible for the analysis, interpretation and delivery of data. Also included in the report are some trace element analyses made by Hardy Lindroos (MIRAB) to evaluate the gold potential of a highly altered and porous granite (episyenite) in borehole KFM02A. Jesper Petersson has been editor for this report.

2 Objective and scope

The main objective of the project is to obtain petrographical, geochemical and petrophysical data down to a depth of 1 km in the Forsmark area. These initial data from the first four boreholes will serve as a platform for more detailed geological investigations at the test site and are essential for the forthcoming three-dimensional, descriptive modelling. Our ambition has been to include data for all samples from the drill cores, except for those samples taken for mechanical and thermal analysis. However, due to the lack of time and extent of some analyse programs, it was decided that the sections concerning both the petrophysics and the fracture filling mineralogy should be reduced versions of forthcoming, more extensive reports.

A summary of all thin-sections and whole-rock geochemical and petrophysical samples from the four boreholes are given in Table 2-1. Totally, 45 samples were collected for thin-section preparation. Twenty-eight of these underwent modal analysis. Samples which lack modal analysis were either collected to give answer to a specific petrographic question or judged to be too fine/coarse-grained to yield reliable results. Samples for whole-rock geochemical analysis were taken adjacent to all, except for one, of the modally analysed samples. Another seven samples make a total of 34 whole-rock geochemical samples.

Also included in these numbers are 13 thin-sections and 8 whole-rock geochemical samples collected by /Möller et al, 2003/ for a special investigation of a strongly altered and porous interval in borehole KFM02A. These samples are classified as episyenite and shown shaded in Table 2-1. This report includes modal analyses of five of these thin-sections and all whole-rock geochemistry. Five additional samples, analysed for selected trace elements, including gold, were collected from the episyenite in KFM02A, in order to investigate the ore potential.

The petrophysical analysis programme includes gamma-ray spectrometry, density and porosity measurements, as well as analysis of magnetic, electric and electromagnetic properties. The gamma-ray spectrometry was done on the same core sample material used for whole-rock geochemical analysis, whereas samples for the remaining petrophysical analyses were taken adjacent or close to all, except for one, of the 34 geochemical samples (cf Table 2-1).

Several of the fracture filling minerals, which were not identified during the regular mapping of the four boreholes, has been sampled for XRD (X-ray diffractometry) identification. Clay minerals have been paid special attention, as XRD is the most suitable method to distinguish different types of clays. In addition, chemical analyses have been carried out on 12 of the fracture filling samples analysed by XRD.

Table 2-1. Compilation of all thin-sections and geochemical and petrophysical samples analysed from borehole KFM01A, KFM02A, KFM03A and KFM03B. Also included are the rock classification based on macroscopic, modal and chemical classification. • = No modal analysis.

Core	Sampled core section		Rock group	Rock classification			Macroscopic character		
	Thin section	Geochemistry		Macroscopic	Modal	Chemical (QP)	Colour	Structure	Other
KFM01A	109.66	109.60 - 110.06	B	Granite-granodiorite	Monzogranite	Granodiorite	Reddish grey	Foliation	—
	242.44	242.25 - 242.55	C	Granitoid	Granodiorite	Tonalite	Grey	—	—
	317.79	315.85 - 316.25	B	Granite-granodiorite	Granodiorite	Granodiorite	Reddish grey	Foliation	—
	355.33●	355.30 - 355.50	B	Amphibolite	—	Gabbro	—	—	—
	379.90●	—	B	Granite-granodiorite	—	—	—	—	—
	433.03●	432.96 - 433.15	B	Amphibolite	—	Monzogabbro/Gabbro	—	—	—
	—	473.53 - 473.71	B	Amphibolite	—	Gabbro	—	—	—
	477.30●	477.10 - 477.50	B	Granite-granodiorite	Granodiorite	Tonalite	Grey	Foliation	—
	521.27	521.10 - 521.40	C	Granitoid	Granodiorite	Tonalite	Grey	—	—
	528.66●	—	D	Pegmatitic granite	—	—	—	—	—
	705.88	704.69 - 705.10	B	Granite-granodiorite	Granodiorite	Granodiorite	Grey	Foliation	—
	947.70	947.40 - 947.80	B	Granite-granodiorite	Monzogranite	Granodiorite	Grey	Foliation	—
	970.35	970.10 - 970.50	C	Granitoid	Monzogranite	Adamellite/Granite	Grey	—	—
	987.32●	—	—	Skarn-like rock	—	—	—	—	Quartz-dominated
KFM02A	*174.33 - 174.36*●	—	—	Episyenite	—	—	Red	—	Porous
	245.60 - 245.63●	—	—	Granite	—	—	Greyish red	—	—
	245.63	245.55 - 245.75	B	Granite	Monzogranite	Adamellite/Granite	Greyish red	—	—
	263.51 - 263.54	263.35 - 263.68	B	Quartz-bearing episyenite	Alkali feldspar granite	Adamellite	—	—	Slightly porous
	272.42●	—	—	Granite	—	—	—	—	—
	—	277.29 - 277.60	B	Episyenite	—	Adamellite	Red	—	Very porous
	278.19●	—	—	Episyenite	—	—	Red	—	Porous
	289.61●	—	—	Episyenite	—	—	Red	—	Porous
	290.03●	—	—	Amphibolite	—	—	—	—	Somewhat altered
	290.25 - 290.28●	—	—	Episyenite	—	—	Red	Foliation	Porous
	295.82 - 295.89●	—	—	Episyenite	—	—	Red	—	Very porous
	295.82 - 295.89	295.64 - 295.81	B	Episyenite	Alkali feldspar quartz syenite	Syenite	Red	—	Very porous
	—	316.85 - 317.05	B	Granite	—	Adamellite	Reddish grey	—	—
	317.26	317.05 - 317.45	B	Granite	Monzogranite	Adamellite	Reddish grey	—	—
	—	350.80 - 351.00	B	Granitoid	—	Granodiorite	Greyish red	Lineation	—
	351.57 - 351.59	351.45 - 351.85	B	Granitoid	Monzogranite	Adamellite/Granodiorite	Reddish grey	Lineation	—
	500.32 - 500.35	—	C?	Granitoid	Monzogranite	—	Greyish red	—	Slight retrograde alteration
	552.63 - 552.66	552.66 - 552.86	C?	Granitoid	Monzogranite	Adamellite	Reddish grey	—	—
	712.45 - 712.48	712.05 - 712.25	B	Granitoid	Monzogranite	Adamellite	Reddish grey	—	—
	916.83 - 916.85	916.85 - 917.05	C	Granitoid	Tonalite	Tonalite	Dark grey	Lineation	—
	917.70 - 917.75●	—	—	Granitoid	—	—	—	—	—
	949.87 - 949.90	949.90 - 950.10	B	Granitoid	Granodiorite	Tonalite	Grey	—	—
	953.45 - 953.48	953.25 - 953.45	B	Granitoid	Monzogranite/Granodiorite	Granodiorite	Reddish grey	—	—
KFM03B	62.32 - 62.36	62.09 - 62.28	D	Pegmatitic granite	Syenogranite	Granite	—	Massive	Equigranular
KFM03A	157.40 - 157.45	157.20 - 157.40	D?	Granite	Monzogranite	Granite	Red	Lineation	—
	165.90 - 165.95	165.70 - 165.90	B	Granite-granodiorite	Monzogranite	Adamellite	Greyish red	Lineation	—
	239.84 - 239.89	239.64 - 239.84	B	Tonalite-granodiorite	Tonalite	Quartz diorite	Grey	Lineation	—
	310.96 - 311.01	310.75 - 310.96	C	Tonalite-granodiorite	Tonalite	Quartz diorite	Dark grey	Lineation	—
	378.58 - 378.63●	—	—	Granitoid	—	—	Grey	—	Possible deformation zone
	433.27 - 433.32	433.07 - 433.27	B	Granite-granodiorite	Monzogranite	Granodiorite	Greyish red	Foliation	—
	504.40 - 504.45	504.20 - 504.40	B	Granite-granodiorite	Monzogranite	Adamellite	Reddish grey	Weak foliation	—
	510.95 - 511.05●	—	—	Granitoid	—	—	—	—	Possible deformation zone
	620.20 - 620.25	620.00 - 620.20	B	Granite-granodiorite	Monzogranite	Granodiorite	Light grey	—	—
	860.52 - 860.57	860.32 - 860.52	B	Granite-granodiorite	Monzogranite	Granodiorite	—	Weak fabric	Slight retrograde alteration
	957.60 - 957.65	957.40 - 957.60	B	Granite-granodiorite	Monzogranite	Adamellite	—	Weak fabric	Strong retrograde alteration

3 Equipment

3.1 Description of equipment

Optical microscopic investigations and modal analysis were carried out at the Geological Survey of Sweden (SGU) in Uppsala, at Ekström Mineral AB in Täby and at Earth Sciences Centre, Göteborg University, using standard polarizing microscopes with attached point counter equipment. Photomicrographs were taken using a polarizing microscope with digital photographic equipment at the SGU in Göteborg.

Core samples selected for whole-rock geochemical analysis and gamma-ray spectrometry were prepared for analysis by crushing and pulverizing by Swedish Geochem Services AB, Öjebyn. The samples were crushed using a Mn-steel crusher and pulverized using a LM5 mill. The powdered samples were subsequently analysed by gamma-ray spectrometry at the SGU in Uppsala and geochemically at the Acme Analytical Laboratories Ltd in Vancouver, Canada using the ICP (Inductively Coupled Plasma) technique. This laboratory was satisfactorily accredited under ISO 9002 during November 1996.

X-ray diffraction (XRD) work of fracture filling material was carried out at the mineralogical laboratory at the SGU in Uppsala using a Siemens D5000 (theta-theta) diffractometer operated by Sven Snäll. Chemical analyses of the fracture filling material were carried out at SGAB Analytica in Luleå using ICP-AES (ICP-Atomic emission spectroscopy) and ICP-QMS (ICP-Quadruple mass spectrometry).

Information regarding the instruments involved in the petrophysical analyses is given in the more extensive report of the borehole petrophysics by /Mattsson et al, 2004/.

4 Execution

The selection of samples for petrographical, modal, geochemical and petrophysical analysis was generally carried out after logging of each borehole had been completed. However, in order to provide an adequate petrographic basis for the bedrock mapping, eleven representative samples from borehole KFM01A were selected and analysed modally prior to the mapping activities.

The sample preparation, the analytical work and the data handling have followed the procedures recommended in the description of the methods for the analyses of bedrock samples (SKB MD 160.001; SKB internal controlling document).

Information regarding the methodology of petrophysical analyses is given in the more extensive report of the borehole petrophysics by /Mattsson et al, 2004/.

4.1 Perparatory work

Polished thin-sections from up to 4 cm wide core sections were prepared by Minoprep in Hunnebostrand. Samples selected for whole-rock geochemical analysis (20–40 cm, weighing 0.5–0.9 kg) were crushed and pulverized by Swedish Geochem Services AB. Crushing down to a size of < 10 mm in a Mn-steel crusher was followed by grinding to a powder with a size of < 200 mesh (90%) in a LM5 mill. The procedure is estimated to give rise to minor contamination of the elements Fe (~ 600 ppm), Mn (~ 9 ppm) and Cr (~ 1.5 ppm).

The fracture filling material was scraped of the fracture walls. The amount of material in the different samples was highly variable. The clay-rich samples were dispersed in distilled water, filtered and oriented according to /Drever, 1973/. In samples of small volumes the suspension was repeatedly put on glass and dried. Three XRD analyses were carried out on each of the fine fraction samples for clay mineral identification: (1) dried samples, (2) saturated with ethyleneglycol for two hours, and finally (3) after heating to 400°C in two hours. Coarser material was wet sieved and dried. The > 35 mm fraction was ground by hand in an agate mortar. The sample powder was randomly orientated in the sample holder (or on the glass, if very small sample volumes).

4.2 Analytical work

Modal analysis was done by determining the mineral composition at 500 evenly spaced points over each thin-section. Sven Lundqvist, Mary Ekström and Torbjörn Bergman, all at SGU, analyzed the thin-sections from KFM01A and KFM02A, whereas Jesper Petersson (SwedPower AB) analyzed those from KFM03A and KFM03B. In order to estimate the reproducibility of the modal data, both S Lundqvist and T Bergman analyzed a thin-section from 109.66 m depth of KFM01A. Most strikingly, the quartz content differs by 9 vol % between the two counting series (cf Table 5-1). This may, of course, be due to problems in the distinction between quartz and feldspars. However, also the biotite content differs

markedly by being 3.0 and 4.4 vol %, respectively. This suggests that the differences mainly can be ascribed to textural heterogeneities in the rock. Therefore, some samples of the dominant metagranite-granodiorite might have too coarse mineral domains to give reliable mineral modes by conventional point counting.

In addition to point counting, the grain-size, as well as the relevant textural and micro-structural characteristics of each sample were documented (Appendix 1). A qualitative analysis of the mineral composition and a general description of the thin-section were also completed for the remaining nine samples. Petrographic details regarding the 13 thin-sections from the upper 400 m of KFM02A are given by /Möller et al, 2003/.

Whole-rock geochemical analyses were carried out by Acme Analytical Laboratories Ltd in Vancouver, Canada. All major and minor oxides (SiO_2, Al_2O_3, Fe_2O_3, MgO, CaO, Na_2O, K_2O, TiO_2, P_2O_5, and MnO) and some trace element compositions (Sc, Cr, Ni and Ba) were analysed by ICP-AES, C and S by the Leco method and the trace elements V, Co, Cu, Zn, Ga, As, Rb, Sr, Y, Zr, Nb, Mo, Ag, Cd, Sn, Sb, Cs, Hf, Ta, W, Au, Hg, Tl, Pb, Bi, Th, U and the REE by ICP-MS. A more detailed description of the methodology is given by /Stephens et al, 2003/. Duplicate analysis of sample 317.05–317.45 from KFM02A showed that the reproducibility is better than about 60% for concentrations up to six times the detection limit, 25% for concentrations up to twelve times the detection limit, about 14% for concentrations up to 60 times the detection limit and better than 7% for higher concentrations. Selected trace elements of the five samples from the highly altered interval of KFM02A were analysed ICP-MS after aqua regia digestion of 15 g splits for enhanced solubility.

The radiation (CuK_α) in the XRD was generated at 40 kV and 40 mA, and the X-rays were focussed with a graphite monochromator. Scans were run from 2–65° (2-theta) or from 2–35° (samples with preferred crystal orientation) with step size 0.02° (2-theta) and counting time 1 s $step^{-1}$. The analyses were performed with a fixed 1° divergence and a 2 mm receiving slit. The XRD raw files were taken up in the Bruker/Siemens $DIFFRAC^{PLUS}$ software (version 2.2), and evaluated in the programme EVA. The minerals were identified by means of the /PDF, 1994/ computer database.

Chemical analyses of powdered fracture filling material were carried out at SGAB Analytica in Luleå. 0.125 g of sample material was melted together with 0.375 g $LiBO_2$ and dissolved in HNO_3. The sample volumes were to small to do LOI (Loss on ignition) measurements. The major elements and some of the trace elements (Ba, Be, Co, Cr, Cu, Ni, Sc, Sr, V, Y, Zn and Zr) were analysed using ICP-AES according to the EPA-method descriptions 200.7. Additional trace elements including REE and U, Th were analysed by ICP-QMS according to EPA-method 200.8. The inhomogeneity of the samples makes the results more dependent on the actual sample size than on the accuracy of the analyses.

4.3 Data handling

All numerical data, including modal and chemical analyses, were exported to the SKB database SICADA to be stored under Field note: Forsmark 61.

5 Results

5.1 Sampled rock types

Based on the field mapping of bedrock outcrops in the Forsmark area, /Stephens et al, 2003/ defined four major rock groups, designated A, B, C and D. This division rest more or less entirely on the temporal relationship between the lithologies, where group A includes the oldest, and D the youngest rocks. However, the relationship between groups C and D is not always obvious. The four groups include the following lithologies:

A. A stratigraphic sequence of various supracrustal rocks.

B. The majority of the plutonic rocks in the area.

C. Minor intrusives of fine-grained granitoids.

D. Ubiquitous, but yet subordinate intrusives of granites and pegmatites.

The use of these alphabetical designations throughout this report necessitates a more detailed definition of the major groups and the various rock types within each group. /Stephens et al, 2003/ have already done this, and the purpose here is not to replicate their discussion, but form a basis for the subsequent data presentation. Thus, only the lithologies sampled from the four drill-cores are described in more detail here.

Group A

The rocks within this group are limited to the peripheral parts of the Forsmark candidate area. None of them are, therefore, expected to be found in the four drill-cores sampled for this study. However, a few decimetre-wide occurrences of light greenish, skarn-like material are found in all three deep boreholes. They were all coded as ‘calc-silicate rocks’ (rock code 108019) during the Boremap mapping /Petersson and Wängnerud, 2003; Petersson et al, 2003, 2004/, which corresponds to subgroup A4 of /Stephens et al, 2003/.

Group B

This group includes by far the most common rocks in the boreholes, and displays a wide variety of compositions, ranging from ultramafic rocks to various granitoids. All of them have been variably affected by ductile deformation and recrystallization under amphibolite facies metamorphism. Based on the field appearance of these rocks, /Stephens et al, 2003/ divided them into ten subgroups. Only about one third of those occur in the boreholes. The predominant rock is a medium-grained, rather equigranular metagranite-granodiorite (B8; rock code 101057). A further subdivision into metagranite (B9) and metagranodiorite (B7) may be possible, but the fact that the feldspar colour is not always diagnostic renders separation difficult. The modal classification below shows, moreover, that several samples in this subgroup fall on, or close to, the boundary between the granite and granodiorite fields. Consequently, all these rocks are included in subgroup B8 (i.e. metagranite-granodiorite).

At 228–296 m depth borehole KFM03A intersects a probable subsurface equivalence of the metatonalite intrusion exposed south of Lillfjärden (rock code 101054). Texturally and structurally, this rock is more or less identical to the metagranite-granodiorite of subgroup B8. The subgroup to which this rock belongs is designated B5 by /Stephens et al, 2003/.

Another important subgroup, referred to as B4, includes amphibolites (rock code 102017). Those found in the boreholes, display a wide textural and compositional variability, though the majority are fine-grained, equigranular and with a rather high proportion of biotite.

Group C

The rocks within this group are found as a subordinate component in all four boreholes, where they form minor intrusives in the metagranite-granodiorite of subgroup B8. Compositionally, they range from granite to tonalite or quartz diorite (all represented by rock code 101051), with a bias towards more plagioclase-rich varieties. Group C rocks are distinguished from their host rock (subgroup B8) by being more fine-grained. However, there are still difficulties to separate granitic varieties of this group from the granites of group D. Based on field observations /Stephens et al, 2003/, inferred that they were emplaced after at least some deformation had affected the group B rock, but prior to the major regime of deformation and amphibolite-facies metamorphism in the area.

Group D

This group is divided into three subgroups. Samples from one, or possibly two, of these subgroups, representing pegmatitic granites (D2), and fine-grained, leucocratic granites (D1), are included this study. The leucocratic granites are inferred to be the youngest rocks in the area, and the majority are distinctly discordant to the deformational fabric in the host rock. Few occurrences of leucocratic granite exceed one meter in width. Subgroup D2 includes occurrences with highly variable and irregularly distributed grain-size, ranging from pegmatite to fine-grained, almost aplitic granite. Based on field relationships, /Stephens et al, 2003/ argued that the pegmatitic granite is coeval with, or post-dating the group C rocks.

5.2 Petrography including modal data

The petrographic account as follows for the various rock groups is a condensed version of the observations presented for individual thin-sections in Appendix 1. Petrographic details regarding the 13 thin-sections from the upper 400 m of KFM02A are given by /Möller et al, 2003/, and they are not discussed further in this section. Modal analyses of rock samples of all four drill-cores are listed in Table 5-1 to 5-3. Except from the two samples of albitised episyenite, all rocks analysed modally are quartz-rich metagranitoids, ranging from monzogranite to tonalite in a QAP classification diagram (Figure 5-1). To facilitate comparison of the proposed major rock groups in the area, corresponding data for surface bedrock samples from /Stephens et al, 2003/ are included. Altogether, these data reveal that Group B and C rocks are virtually indistinguishable in terms of their major constituents. However, the Group C rocks are typically somewhat less quartz-rich, with a compositional bias toward more granodioritic to tonalitic compositions. The Group D rocks, on the other hand, are more restricted in their composition and lie with one exception in the monzogranite field.

Table 5-1. Modal composition (vol %) of all samples from borehole KFM01A.

Length	109.66(1)	109.66(2)	242.44	317.79	355.33	433.03	477.30	521.27	705.88	947.70	970.35
Rock type	Metagranite-granodiorite	Metagranite-granodiorite	Meta-granodiorite	Metagranite-granodiorite	Amphibolite	Amphibolite	Metagranite-granodiorite	Metagrano-diorite-tonal	Metagranite-granodiorite	Metagranite-granodiorite	Metagranite
Rock code	101057	101057	101051	101057	102017	102017	101057	101051	101057	101057	101051
Rock group	B	B	C	B	B	B	B	C	B	B	C
Grain-size	0.1–2	0.1–2	0.1–2	0.5–2	0.5–2	0.1–2	0.05–1	0.05–1	0.05–1	0.05–1	0.1–2
Quartz	34.6	43.6	25.0	45.8	–	–	46.0	33.4	32.2	37.8	28.0
K-feldspar	22.8	19.2	8.0	12.8	–	–	12.6	5.6	13.2	23.2	32.4
Plagioclase[1]	37.6	33.8	49.0	34.4	45–50	~40	32.0	46.4	47.4	30.8	29.4
Biotite	4.4	3.0	9.0	5.4	1	10–20	8.8	9.4	4.2	7.2	8.4
Muscovite	–	–	–	–	–	–	–	–	+	+	+
Chlorite	+	+	–	–	–	–	0.4	–	+	+	0.2
Hornblende	–	–	5.0	0.4	45–50	~40	–	1.2	–	–	–
Epidote	0.6	0.2	3.0	0.2	2–3	2–3	+	3.8	1.0	0.6	1.2
Allanite	+	+	+	+	–	–	+	–	0.2	+	0.2
Prehnite	+	+	–	+	–	–	0.2	+	0.2	+	0.2
Sphene	+	+	0.4	+	2–3	2–3	–	+	0.4	+	–
Calcite	+	+	+	+	–	–	+	+	0.4	0.2	+
Apatite	+	+	0.4	0.6	–	–	+	+	+	+	+
Zircon	+	+	+	+	–	–	+	0.2	0.2	+	+
Opaque	+	0.2	0.2	0.4	–	–	+	+	0.6	+	+
Counted by	S Lundqvist	T Bergman	T Bergman	T Bergman	S Lundqvist	S Lundqvist	S Lundqvist	S Lundqvist	S Lundqvist	S Lundqvist	S Lundqvist

+ = trace amounts.

[1] Including sericitised plagioclase.

Table 5-2. Modal composition (vol %) of all samples from borehole KFM02A.

Length	245.63	263.51–263.54	295.82–295.89	317.26	351.57–351.59	500.32–500.35	552.63–552.66	712.45–712.48	916.83–916.85	949.87–949.90	953.45–953.48
Rock type	Metagranite	Resilicified episyenite	Very porous episyenite	Metagranite-granodiorite	Metagranite-granodiorite	Metagranite	Metagranite	Metagranite-granodiorite	Metatonalite	Metagranite-granodiorite	Metagranite-granodiorite
Rock code	101057	101057	101057	101057	101057	101051	101051	101057	101051	101057	101054
Rock group	B	B	B	B	B	C	C	B	C	B	B
Grain-size	0.2–3	0.1–2	0.2–1.5	0.2–2	0.1–2	0.2–1.5	0.1–2	0.2–2	0.1–1	0.2–2.5	0.2–2
Quartz	32.4	24.8	9.6	34.8	33.8	29.0	30.2	33.8	16.4	36.8	27.8
K-feldspar	34.6	28.2	20.0	23.6	21.2	38.0	30.0	35.0	–	9.4	24.4
Plagioclase	28.6	39.0[2]	42.8[2]	34.0	35.4	30.4	34.6	24.0	49.6	47.0	44.6
Biotite	3.6	–	–	6.2	5.8	1.8	3.0	7.0	7.2	6.2	1.8
Muscovite	0.4	+	+	+	+	0.2	+	–	–	–	+
Chlorite	+	+	2.4	+	1.2	0.2	+	+	0.2	+	0.2
Hornblende	–	–	–	–	–	–	–	–	25.2	–	–
Epidote	+	–	–	1.0	0.6	0.4	1.4	+	1.0	+	0.2
Allanite	+	–	–	–	0.6	+	0.4	0.2	–	+	+
Prehnite	+	–	–	–	0.2	+	+	+	+	–	+
Sphene	–	0.4[3]	+[3]	+	+	+	–	+	0.4	0.6	+
Calcite	0.2	–	–	+	0.2	+	+	+	–	+	0.2
Apatite	+	–	+	+	+	+	0.2	+	+	+	+
Zircon	0.2	+	+	0.2	0.2	+	+	+	+	+	+
Opaque	+	6.8	3.4	0.2	0.8	+	0.2	+	–	+	0.8
Vugs	–	0.8	21.8	–	–	–	–	–	–	–	–
Counted by	M Ekström	J Petersson	J Petersson	M Ekström	J Petersson	M Ekström	M Ekström	M Ekström	M Ekström	M Ekström	M Ekström

+ = trace amounts.

[1] Including sericitised plagioclase.

[2] Albite.

[3] Probably anatase.

Table 5-3. Modal composition (vol %) of all samples from borehole KFM03A and KFM03B.

Length	62.32–62.36	157.40–157.45	165.90–165.95	239.84–239.89	310.96–311.01	433.27–433.32	504.40–504.45	620.20–620.25	860.52–860.57	957.60–957.65
Rock type	Pegmatitic granite	Metagranite	Metagranite-granodiorite	Metatonalite	Metatonalite	Metagranite-granodiorite	Metagranite-granodiorite	Metagranite-granodiorite	Metagranite-granodiorite	Metagranite-granodiorite
Rock code	111058	111058?	101057	101054	101051	101057	101057	101057	101057	101057
Rock group	D	D?	B	B	C	B	B	B	B	B
Grain-size	0.5–5	0.1–2	0.2–2.5	0.1–2	0.1–1	0.1–2	0.1–2	0.1–2	0.1–4	0.1–3
Quartz	31.8	30.6	39.6	18.8	15.4	41.8	32.8	32.6	34.8	36.4
K-feldspar	45.0	31.4	21.6	1.2	–	22.2	29.2	29.6	29.4	21.4
Plagioclase[1]	20.6	33.2	32.8	52.4	50.8	28.8	32.0	31.2	27.0	35.0
Biotite	0.6	0.6	3.6	10.4	19.4	6.8	4.4	3.4	6.6	4.6
Muscovite	+	+	0.2	–	–	–	–	–	+	–
Chlorite	1.6	2.4	0.4	0.2	0.2	–	+	0.8	0.6	0.6
Hornblende	–	–	–	15.4	11.8	–	0.4	–	–	–
Epidote	0.2	0.8	1.2	0.6	0.6	0.2	+	1.6	0.2	0.2
Allanite	–	+	0.4	–	+	+	+	+	0.2	+
Prehnite	–	0.4	+	+	+	–	+	0.4	0.4	1.0
Sphene	–	–	+	0.6	1.4	+	+	0.2	+	+
Calcite	0.2	+	–	0.2	+	+	–	–	0.4	+
Apatite	+	–	+	0.2	+	+	+	+	0.2	0.2
Zircon	–	+	+	–	–	0.2	0.2	–	–	+
Opaque	+	0.6	0.2	+	0.2	+	0.6	0.2	+	0.6
Counted by	J Petersson	J Petersson	J Petersson	J Petersson	J Petersson	J Petersson	J Petersson	J Petersson	J Petersson	J Petersson

+ = trace amounts.

[1] Including sericitised plagioclase.

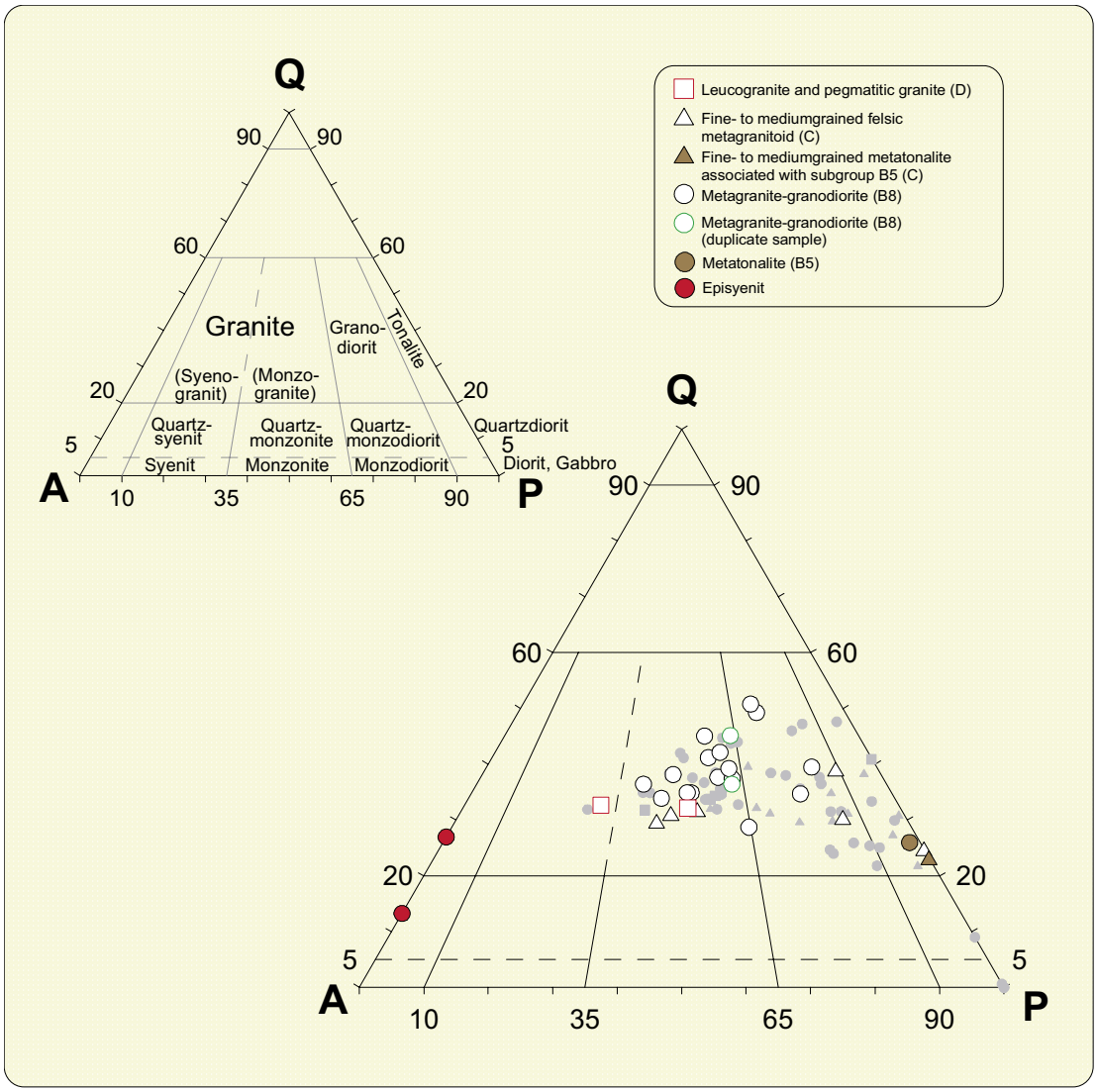

Figure 5-1. *Modal classification diagram after /Streckeisen, 1976/ for all rocks analysed in this study. Corresponding data for surface bedrock samples from /Stephens et al, 2003/ are included as shaded symbols for comparison.*

Possible calc-silicate rock (Subgroup A4; rock code 108019)

This sample is a fine-grained, granular rock, comprising strained quartz, sericitised plagioclase and about 8–10 vol % epidote with minor hornblende (Figure 5-2). A few polycrystalline quartz grains, showing sub-grain development and undulose extinction, reach up to 3 mm in length. Diopside, which predominates the skarn investigated by /Stephens et al, 2003/, is notably absent. In order of decreasing abundance, the accessory assemblage includes sphene, muscovite, allanite (< 0.2 mm; often euhedral and epidote-mantled), magnetite, pyrite, calcite, apatite and one single grain of chalcopyrite. The textural character of this rock, the seemingly igneous allanite and the absence of diopside, is not in accordance with the macroscopic interpretation. Instead, these features suggest an igneous origin.

Thin-sections – KFM01A: 987.32.

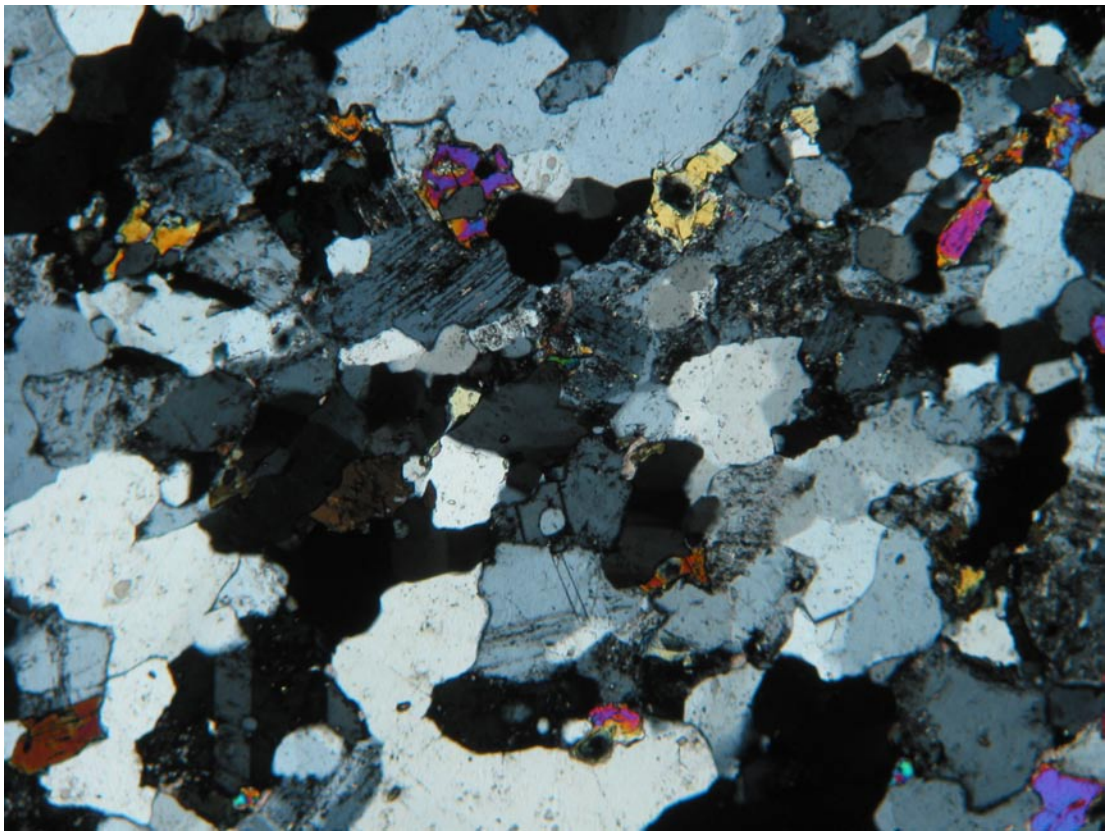

Figure 5-2. *Photomicrograph showing the texture of the skarn-like sample from 987.32 m depth of KFM01A. Field of view 2.8 x 2.1 mm; crossed polars.*

Amphibolites (Subgroup B4; rock code 102017)

The sampled amphibolites are fine-grained (< 1 mm) rocks with granular texture and rather weak, ductile deformational fabric. However, there are a few hornblende crystals that may reach up to 1.5 mm in length. The major constituents are hornblende, plagioclase (locally slightly sericitised) and, in one of the rocks, biotite. In addition, they contain 4–6 vol % epidote and sphene. Epidote displays often a very finely, almost submicroscopic, symplectite texture (Figure 5-3), whereas sphene occurs as isolated, subhedral to euhedral crystals, < 0.2 mm in diameter. Except of a single grain of pyrite in one of the rocks, opaque phases are notably abscent. The accessory minerals include calcite and stubby prisms of apatite (< 0.1 mm in diameter).

Thin-sections – KFM01A: 355.33, 433.03.

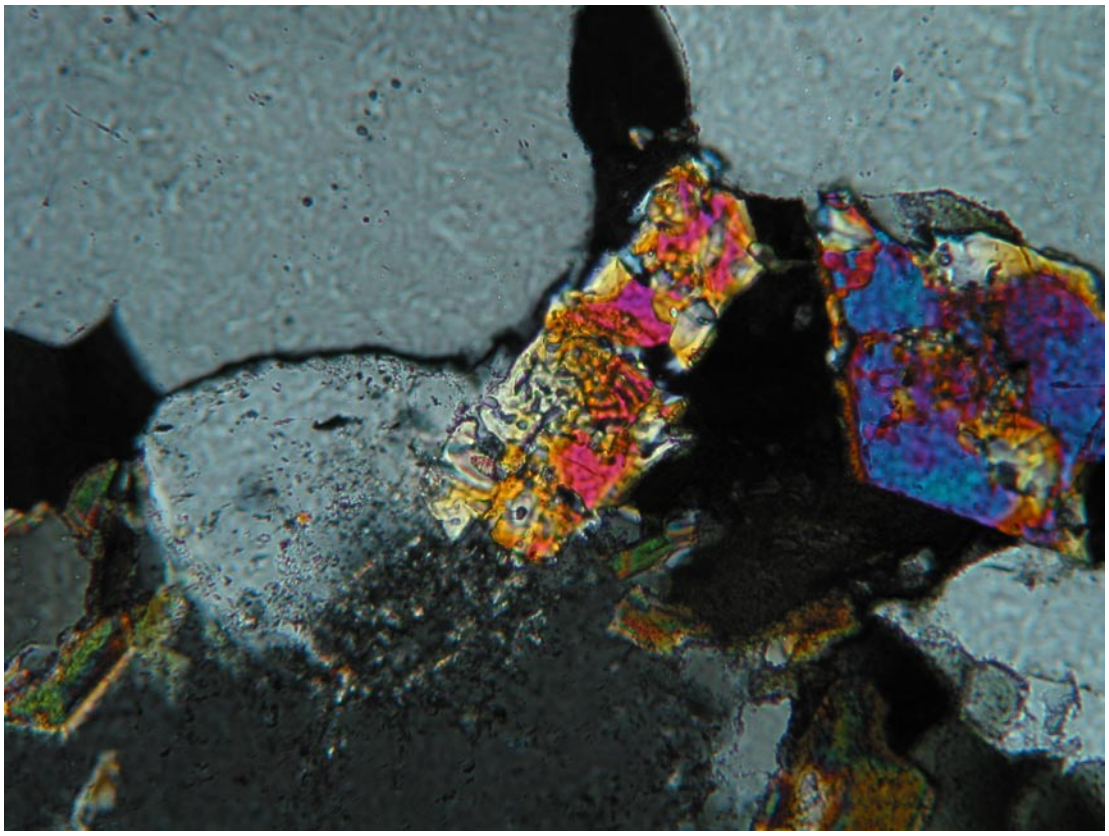

Figure 5-3. *Photomicrograph of epidote with very finely, almost sub-microscopic, symplectite texture. More or less well-developed varieties of this texture is typical for epidote from all rock groups found in the area. Sample from 521.27 m depth of KFM01A. Field of view 0.7 x 0.5 mm; crossed polars.*

Metatonalite (Subgroup B5; rock code 101054)

The only sample analysed petrographically in this subgroup is from the probable subsurface equivalence of the metatonalite intrusion exposed south of Lillfjärden. Texturally, the rock is granular with irregular, interlocking grain boundaries and a distinct ductile fabric, defined by elongated aggregates of hornblende and biotite (Figure 5-4). The grain-size ranges up to about 2 mm, which is less than expected from the macroscopic examination. This, together with the grain-shape fabric, suggests that the rock originally was medium-grained and that the grain-size reduction is a result of recrystallisation during amphibolite facies conditions. The major constituents are plagioclase (52.4 vol %), strained quartz (18.8 vol %), hornblende (15.4 vol %) and biotite (10.4 vol %), as well as some minor (1.2 vol %) K-feldspar. The retrogressive effects are limited to weak sericitisation of plagioclase and partial chloritisation, with associated prehnite formation in some of the biotite. The accessory assemblage includes epidote (< 0.5 mm; typically with a very finely symplectitic character), sphene (< 0.5 mm), calcite, apatite (rounded crystals < 0.1 mm) and a few tiny pyrite crystals.

Thin-section – KFM03A: 239.84–239.89.

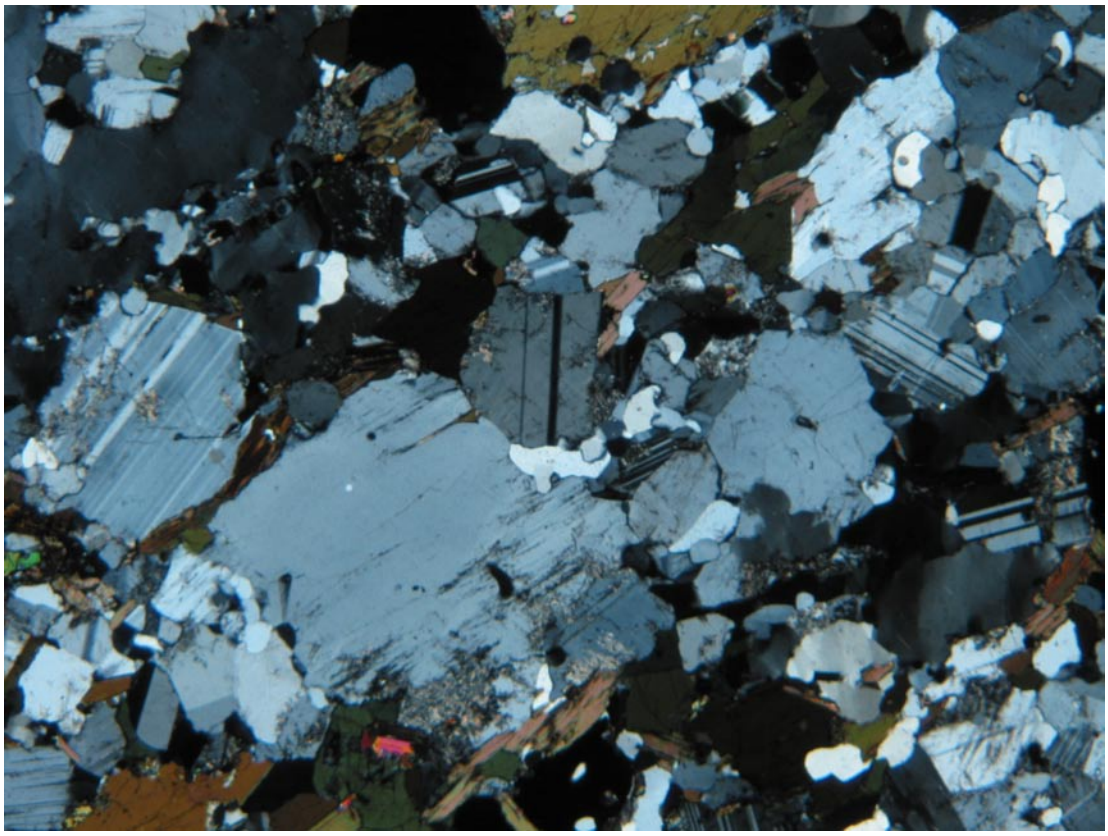

Figure 5-4. *Photomicrograph showing the texture of the metatonalite sample from 239.84–239.89 m depth of KFM03A. Field of view 5.6 x 4.2 mm; crossed polars.*

Metagranite-granodiorite (Subgroup B8; rock code 101057)

As the metagranite-granodiorite is by far the volumetrically most abundant rock type in the boreholes, half of the thin-sections belong to this subgroup. All samples have rather high quartz contents, varying from 27.8 to 46.0 vol %. In the QAP classification diagram these rocks fall unambiguously into the granite and granodiorite fields, and the fact that they tend to straddle the boundary between the two fields (cf Figure 5-1) render often macroscopic separation of granitic and granodioritic varieties impossible.

All these rocks have a granular texture with irregular, interlocking grain boundaries. The general grain-size is range typically up to 2 mm, with a few grains, often quartz and plagioclase, reaching up to 5 mm. This is less than expected from their macroscopic, medium-grained appearance, and suggests probable grain-size reduction in connection with the metamorphism. The majority of the rocks show a distinct ductile deformational fabric defined by linear or planar domains of strained quartz, alternating with feldspar-dominated domains and streaks of ferromagnesian minerals (Figure 5-5). Individual mineral grains within these domains display, however, relatively low strain, indicating development predominantly due to recrystallization rotation. Intracrystalline patterns of dynamic recrystallization are present only in quartz that shows subgrain development and strong undulose extinction.

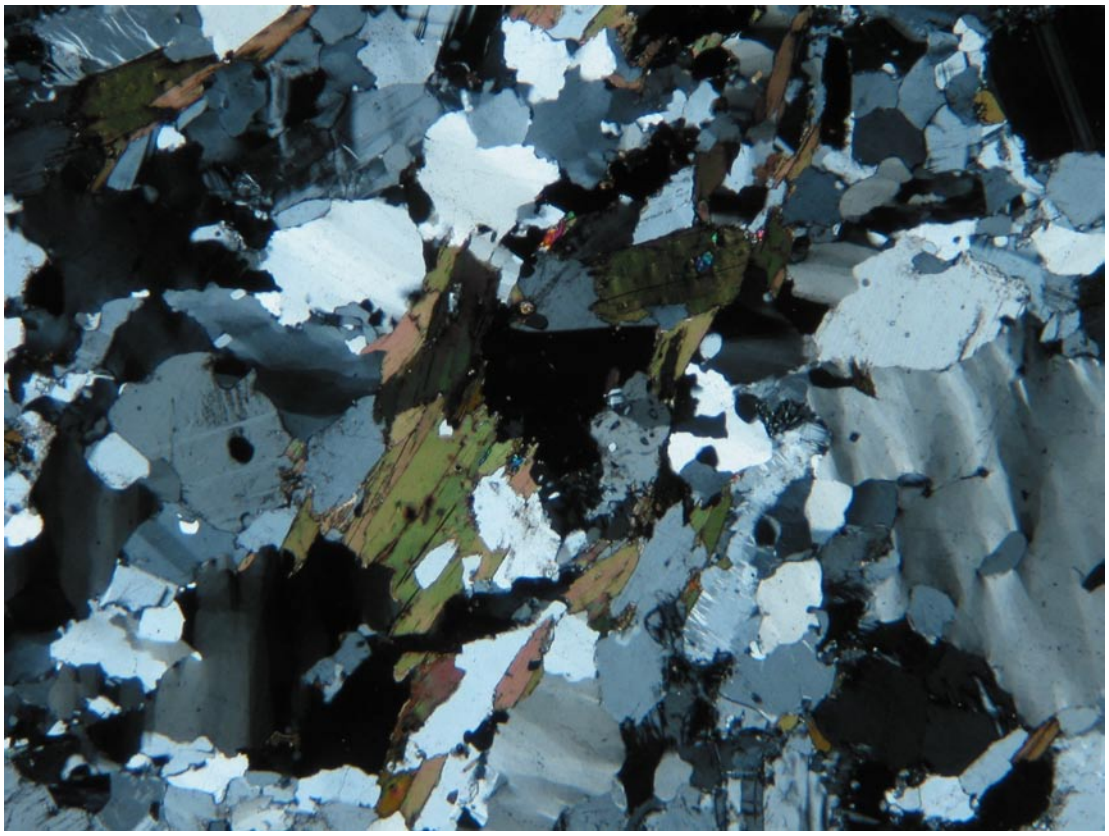

Figure 5-5. *Photomicrograph illustrating the textural features of a typical member of the metagranite-granodiorite subgroup. Sample from 504.40–504.45 m depth of KFM03A. Field of view 5.6 x 4.2 mm; crossed polars.*

Most plagioclase is twinned according to the albite law, whereas K-feldspar shows cross-hatched twinning and locally, perthitic lamellae or 'flames' of albite. The ubiquitous tartan structure bear witness to the fact that all K-feldspar is microcline. The primary ferromagnesian phase in this subgroup is biotite, comprising between 1.8 and 8.8 vol % of the mode. Other ferromagnesian silicates, including epidote, sphene, hornblende and allanite, are only found in accessory amounts. The occurrence of hornblende is limited to two of the 16 samples (477.30 from KFM01A and 504.40–504.45 from KFM03A), whereas epidote, sphene and allanite are found in almost all samples. Epidote occurs mostly as anhedral to subhedral grains, less than 0.3 mm in diameter, often with a finely symplectitic character (cf Figure 5-2). Allanite forms isolated, metamict crystals, averaging about 0.3 mm in length. Most allanite crystals are overgrown by epidote (Figure 5-6). Sphene occurs typically as subhedral crystals (< 0.5 mm) in close proximity to the other ferromagnesian phases or as overgrowths on magnetite, the major opaque mineral in these rocks. Magnetite is found in all but one grey coloured variety (620.20–620.25 from KFM03A), in which pyrite is the only opaque phase. A few pyrite crystals are also present in two other samples: 317.79 from KFM01A and 949.87–949.90 from KFM02A. Probable ilmenite, intimately intergrown with magnetite, was only distinguished in one sample: 953.45–953.48 from KFM02A. Other accessories found in virtually all samples are stubby prisms of apatitie (< 0.1 mm in diameter) and oscillary zoned zircons (< 0.1 mm).

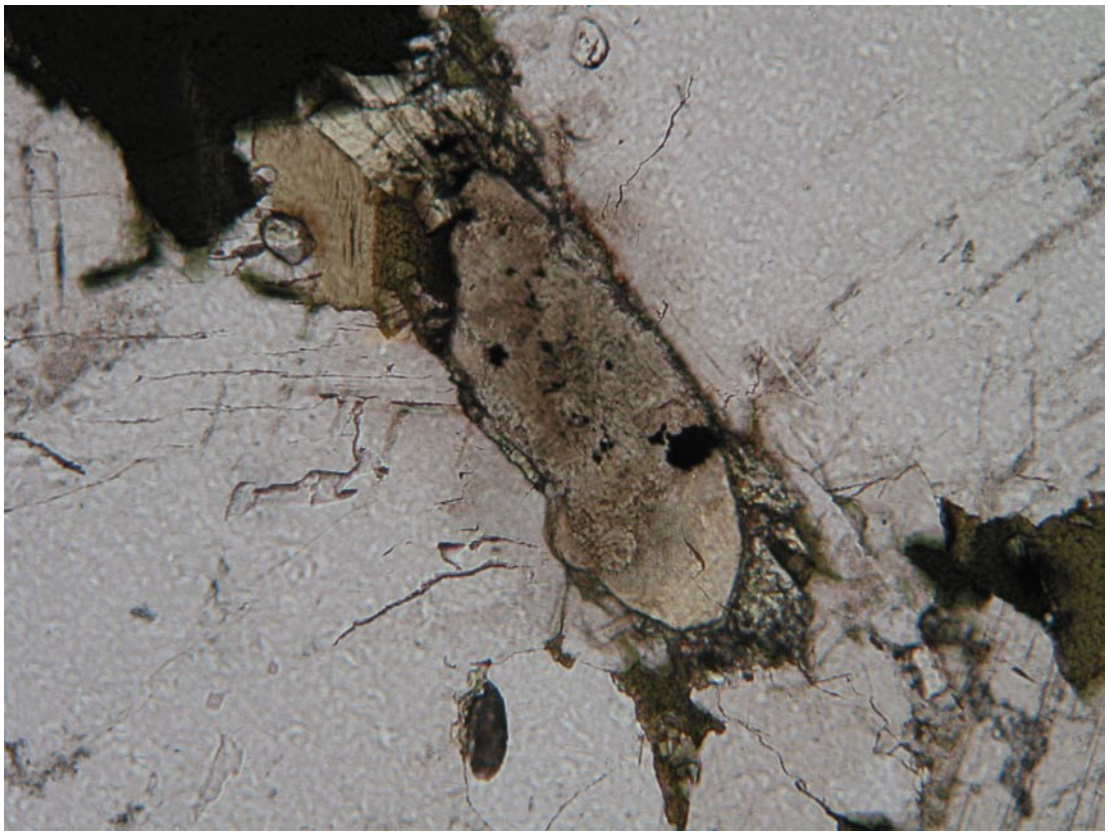

Figure 5-6. *Photomicrograph of an allanite crystal, 650 microns long and overgrown by epidote. Sample from 947.70 m depth of KFM01A. Field of view 1.5 x 1.1 mm; crossed polars.*

Plagioclase and biotite are to a highly variable extent affected by retrograde alteration, which includes sericitisation of plagioclase and conversion of biotite into chlorite and/or prehnite (Figure 5-7) or locally, what seems to be pumpellyite. The sericitised plagioclase contains typically also calcite, and locally minor sassurite. Pervasively sericitised plagioclase crystals appear whitish macroscopically. This is conspicuous in three of the samples, 379.90 from KFM01A and 860.52–860.57 and 957.60–957.65 from KFM03A, where the whitish grains give the rocks a speckled appearance.

Thin-sections – KFM01A: 109.66, 317.79, 379.90, 477.30, 705.88, 947.70; KFM02A: 712.45–712.48, 949.87–949.90, 953.45–953.45; KFM03A: 165.90–165.95, 433.27–433.32, 504.40–504.45, 620.20–620.25, 860.52–860.57, 957.60–957.65.

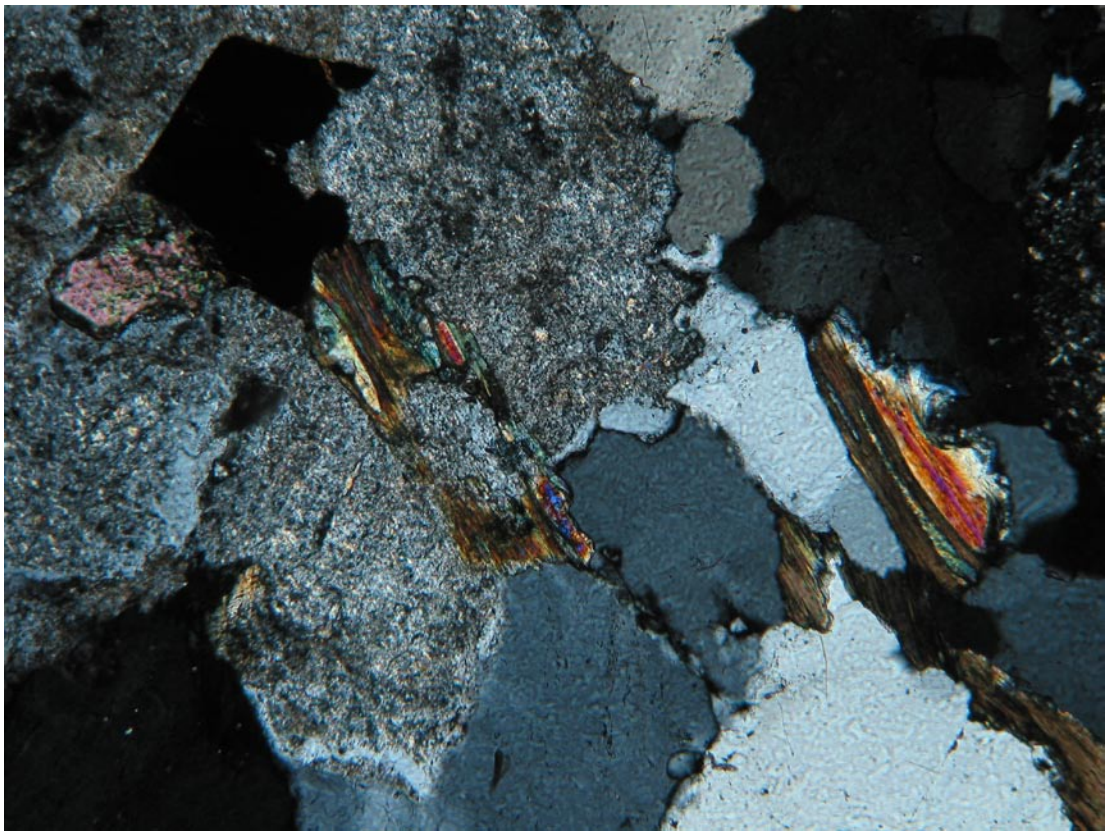

Figure 5-7. *Photomicrograph of a typical retrogressive assemble, including pervasively sericitised plagioclase and totally chloritised biotite with lenses of prehnite. Sample 957.60–957.65 from KFM03A. Field of view 1.5 x 1.1 mm; crossed polars.*

Fine- to medium-grained, felsic meta-intrusive rocks (Group C; rock code 101051)

This rock group displays a considerable compositional range, and includes monzogranites, granodiorites and tonalities, with a weighting towards the latter two varieties in the AQP-diagram (cf Figure 5-1). The hornblende content increases markedly with increasing plagioclase content, from complete absence in the three granitic samples, up to 11.8 and 25.2 vol % in the two metatonalites. Also the biotite content varies widely, between 1.8 vol % in one of the metagranites to 19.4 vol % in the metatonalite of KFM03A.

The most characteristic textural feature, which makes them easy to separate from group B rocks, is that the minerals are more evenly distributed in the rock volume (Figure 5-8). Thus, the monomineralic domains characterising the group B rocks is less well-developed here, and the ductile deformational fabric is, therefore, more or less limited to shape-preferred orientation of, for example, biotite. The macroscopic impression of this is that the strain seems to be less intense than in group B rocks. Further, their texture is granular with a general grain-size less than 1 mm, though there are often a few grains of more coarse plagioclase and/or quartz in each thin-section, reaching up to 2–3 mm in size. Judging from these features, it is plausible to assume that also these rocks originally were coarser and that their present texture resulted from dynamic grain-size reduction.

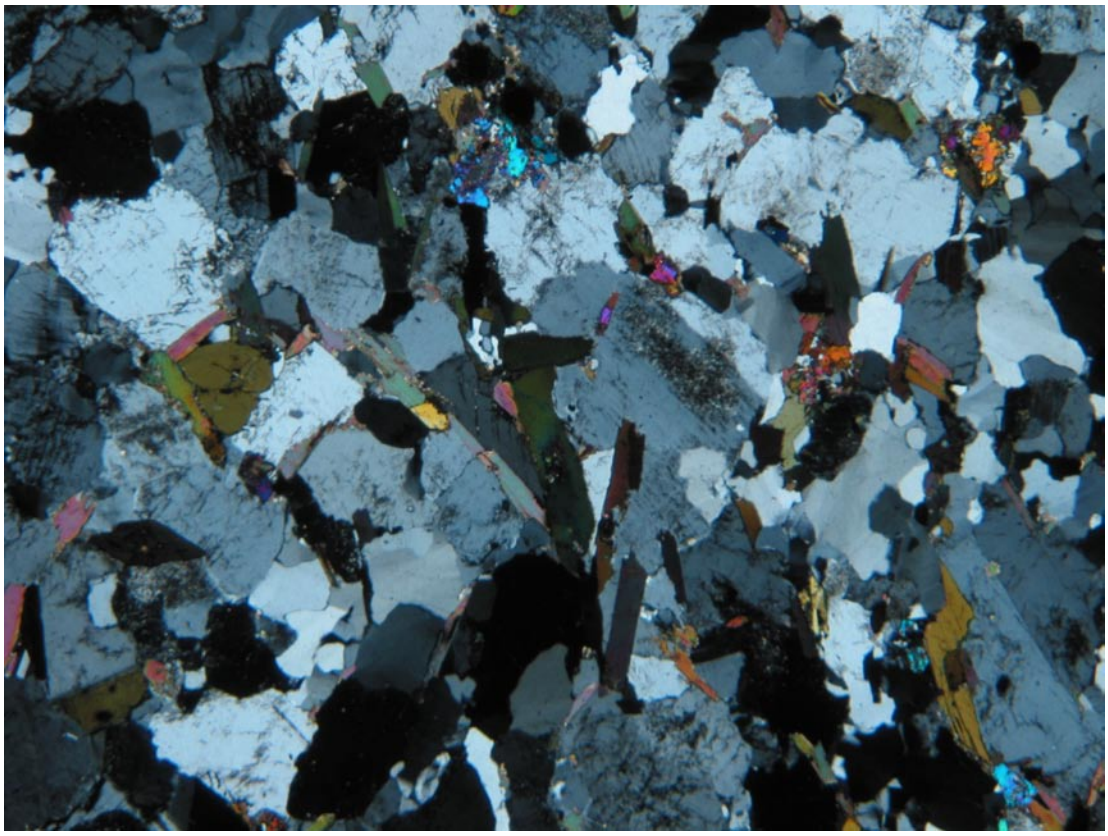

Figure 5-8. *Photomicrograph illustrating the textural features of a typical group C rock. Sample from 242.44 m depth of KFM01A. Field of view 5.6 x 4.2 mm; crossed polars.*

Similar to the group B rocks, K-feldspar displays tartan twinning and locally, lamellae- or flame-shaped exsolutions of perthitic albite, which both indicate microcline. In close proximity to the major ferromagnesian minerals (biotite and hornblende), there are minor amounts (0.4–3.8 vol %) of epidote, and an accessory assemblage identical to that of the group B rocks, with sphene, magnetite, allanite apatite, zircon and pyrite. Also chalcopyrite has been found in one sample (242.44 from KFM01A). Epidote occurs as anhedral to subhedral grains, up to 0.5 mm, often with the typical finely symplectite texture (cf Figure 5-3). Magnetite forms isolated, often rounded grains (< 0.7 mm). Sphene (< 0.5 mm) is found both as isolated grains and found as overgrowths on magnetite. Allanite occurs typically as metamict crystals (< 0.6 mm) overgrown by or enclosed within epidote. Apatite forms prisms with a length:width ratio of 3:1, whereas zircon crystals show oscillary zoning. Both apatite and zircon crystals are less than 0.1 mm in diameter. Minor pyrite crystals are only found in three of the more tonalitic varieties.

All samples are variably affected by retrograde alteration. However, only two of them are pervasively affected with strong sericitisation of plagioclase and total decomposition of biotite into chlorite with lenses of prehnite.

Thin-sections – KFM01A: 242.44, 521.27, 970.35; KFM02A: 500.32–500.35, 916.83–916.85, 917.70–917.75; KFM03A: 310.96–311.01.

Fine- to finely medium-grained, leucogranite (Subgroup D1; rock code 111058)

Based on its rather weak deformational fabric and low content of ferromagnesian phases, this rock is suggested to belong to subgroup D1. However, there is no textural or mineralogical feature on microscopic scale that clearly separates it from the granitic varieties of the group C rocks. It is, therefore, plausible that it actually belongs to the C group. The texture is granular and the fabric is primarily defined by elongated domains of strained quartz. Retrograde metamorphic evidence, such as sericitisation of plagioclase and chloritisation of biotite, are pervasively strong. The most strongly sericitised grains also contains minor amounts of muscovite, epidote and calcite, whereas the secondary chlorite often encloses lenses of prehnite/pumpellyite. K-feldspar is apparently unaffected by this alteration and displays cross-hatched twinning and locally, perthitic lamellae of albite. Accessory assemblage includes epidote (often somewhat finely symplectitic), rounded grains of magnetite (< 0.5 mm), metamict allanite (< 0.4 mm) and oscillary zone zircon (< 150 microns).

Thin-section – KFM03A: 157.40–157.45.

Pegmatitic granite (Subgroup D2; rock code 101061)

Macroscopically, these two samples seem to be massive, rather equigranular and coarsely medium-grained rocks. However, the thin-sections reveal that they actually are inequigranular with rounded porphyroclasts of strained quartz and feldspars (< 6 mm in diameter) in a matrix of grain-size reduced material. Plagioclase has been subjected to a variable degree of seicitisation, and in the sample from KFM03B it is locally myrmecitic. K-feldspar displays typically tartan twinning or perthitic intergrowths of albite, indicating the presence of microcline. The ferromagnesian assemblage is limited to about 2–3 vol % of lobate and mostly chloritised biotite together with minor amounts of epidote (with finely symplectitic texture), prehnite sphene and allanite. The latter two are only found in the sample from KFM01A. Other accessory minerals found are apatite, pyrite, hematite, zircon, calcite and a single grain of chalcopyrite.

Thin-sections – KFM01A: 528.66; KFM03B: 62.32–62.36.

Suspected ductile deformation zones

Two samples of fine-grained felsic material, which seem to have undergone more intense grain-size reduction than the surrounding metagranite-granodiorite (subgroup B8 rocks). Both intervals adjoin minor amphibolite occurrences towards depth, whereas the upper contacts are gradual toward the metagranite-granodiorite. The grain-size is less than 1 mm and the deformational fabric is defined both by grain-shape orientation and distinct streaks of ferromagnesian phases. However, the rocks are rather equigranular, and the expected mylonitic texture with alternating domains of variable grain-size, indicating anisotropic response to the stress, can only be distinguished in one of the samples (510.95–511.05).

The mineralogy is more or less identical to that of the subgroup B8 rocks, with strained quartz, slightly sericitised plagioclase and tartan twinned K-feldspar as the major constituents. The ferromagnesian phases consists mainly of biotite with some minor epidote. Also hornblende is found in the sample from 378.58–378.63 m depth. Epidote and some of the biotite display somewhat finely symplectitic margins. Sphene and magnetite are notably abscent. The accessories include apatite, and in the sample from 378.58–378.63 m depth, pyrite and possible allanite.

Thin-section – KFM03A: 378.58–378.63, 510.95–511.05.

5.3 Geochemistry

Major and trace element compositions of the samples from the four boreholes are presented in Appendix 2. The data are, moreover, plotted in a series of figures together with corresponding data for surface bedrock samples from /Stephens et al, 2003/ to illustrate the key geochemical characteristics of the major igneous rock groups in the area.

5.3.1 Major elements

The majority of the granitoids from the rock groups B, C and D, and particularly those of subgroup B8 (metagranite-granodiorite), have high and rather similar silica contents, reaching 76 wt % in some of the most K-feldspar deficient varieties. In the P-Q diagram of /Debon and LeFort, 1983/ (Figure 5-9), these high-silica varieties form a gently dipping trend towards increasing P-values. Compared with the modal classification, several rocks shift into the granodioritic, tonalitic and even quartz dioritic fields of the P-Q diagram. /Stephens et al, 2003/ suggested that this shift has been caused by secondary alteration processes that have affected the alkali proportions of the rocks. However, the shift is typically highest for those rocks with high contents of ferromagnesian minerals, such as some of the group C rocks. A plausible interpretation is, therefore, that the shift is due to alkali concentration in other minerals than K-feldspar and plagioclase.

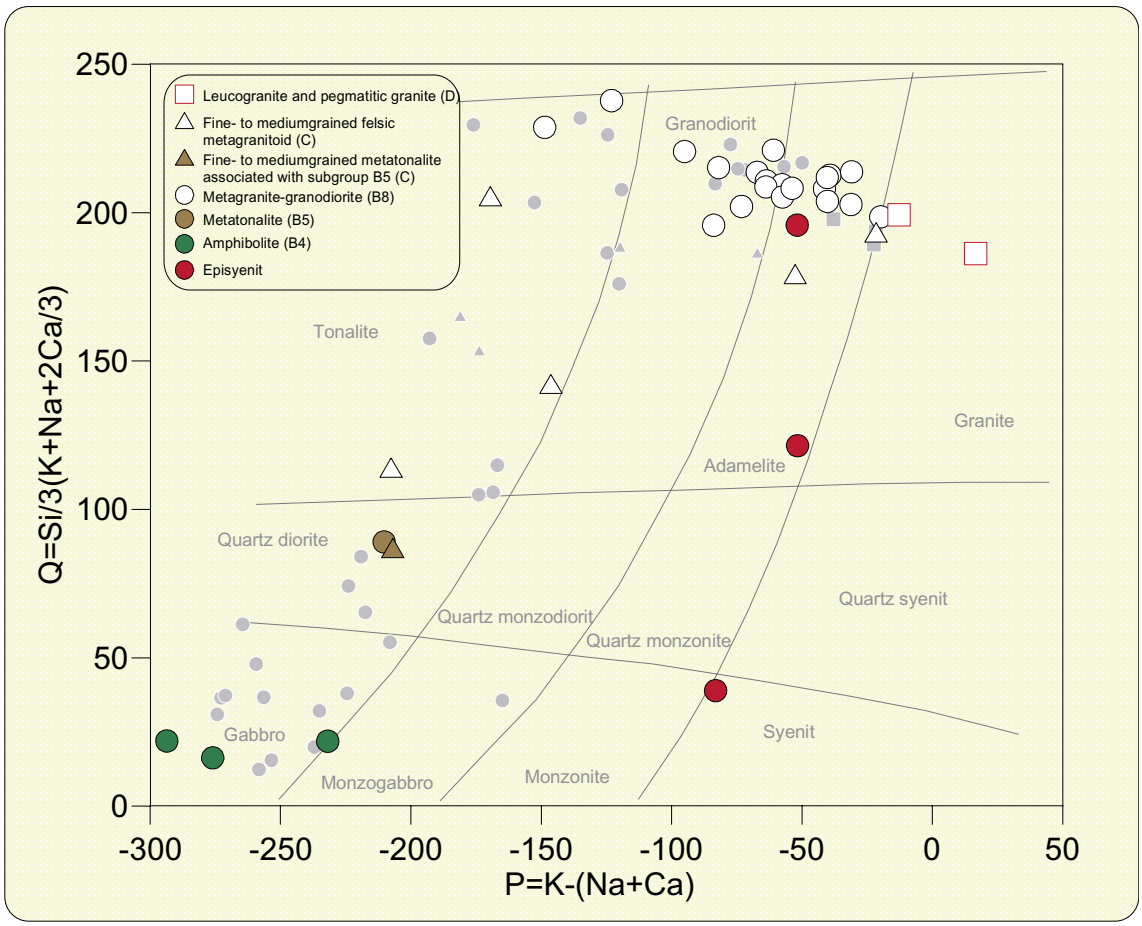

Figure 5-9. *Q-P diagram /after Debon and LeFort, 1983/ illustrating the compositional characteristics for all rocks analysed in this study. Corresponding data for surface bedrock samples from /Stephens et al, 2003/ are included as shaded symbols for comparison.*

Excepting the three amphibolite samples, the analyzed rocks range from mildly metaluminous to mildly peraluminous, with aluminium saturation indices (ASI) between 0.93 and 1.18 (Figure 5-10). Generally, the ASI increases with decreasing content of K-feldspar, with lowest indices for the two group D rocks and highest for hornblende-deficient granodioritic-tonalitic varieties of groups B and C (e.g. samples 477.10–477.50 and 521.10–521.40 from KFM01A and 949.90–950.10 from KFM02A). The three episyenite samples are distinguished from the apparently unaltered rocks, by their slightly higher agpaitic indices.

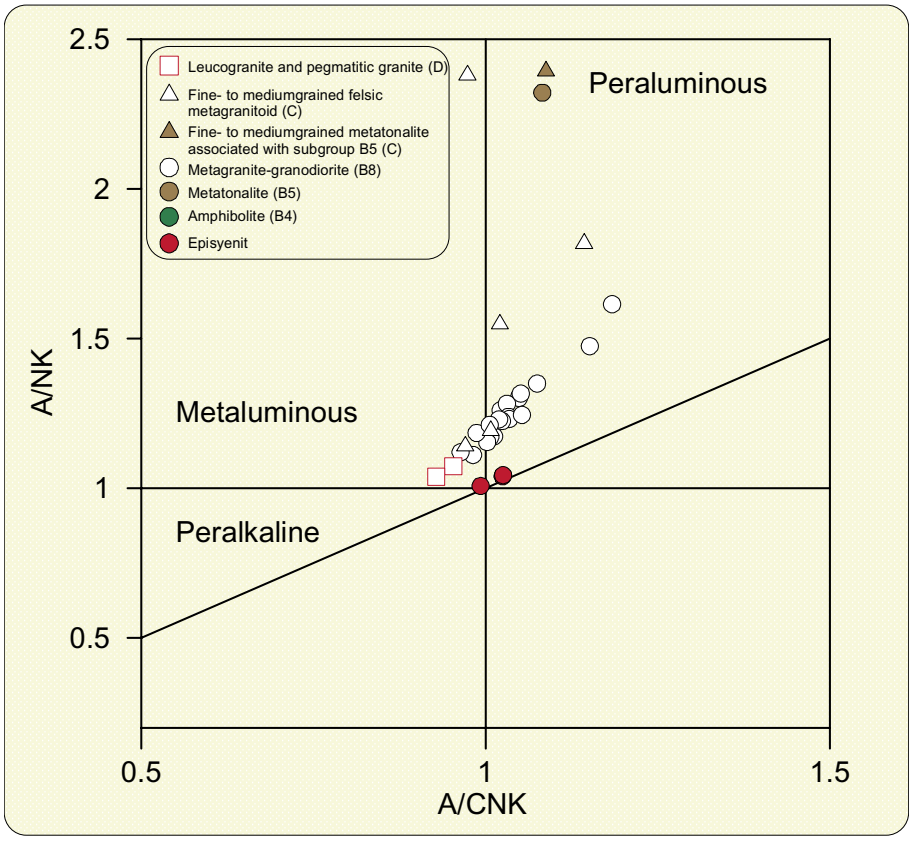

Figure 5-10. *Inverse agpaitic index (Al_2O_3/Na_2O+K_2O; A/NK) versus Al saturation index ($Al_2O_3/CaO+Na_2O+K_2O$; A/CNK) plot for all granitoids analysed in this study. Boundaries according to /Maniar and Piccoli, 1989/.*

5.3.2 Trace elements

As typical granitoids, all rock sampled display a general enrichment of large ion lithophile (LIL) relative to high field strength (HFS) elements (Figure 5-11). A similar pattern is shown by corresponding data for the surface bedrock samples. The trace element variability within the dominant metagranite-granodiorite rock (subgroup B8) of the boreholes is generally rather limited. There are, however, a few elements, such as Rb, Ba and some of the REE, which show a spread outranging the overall variation within virtually all sampled rock groups. The total variability within the rock groups, from the amphibolites to the leuco-granite and pegmatitic granite of group D, is, however, more consistent, and characterised by increasing Rb, Zr, Th and U, and decreasing P and Ti with increasing degree of differentiation as gauged by increasing Si content. Most other trace elements, as for example Sr, Nb, Ba and Ta, do not display such systematic compositional trends. These patterns appear also within a spidergram (Figure 5-11). A notable feature, as revealed by the trace element composition, is the similarity between the medium-grained and the more fine-grained metatonalite samples from 239.64–239.84 and 310.75–310.96 m depth of borehole KFM03A (Figure 5-11). Based on this, the petrography and their spatial association, it seems reasonable to conclude that they are co-genetic, and that the more fine-grained variety might represent a peripheral phase. Another conspicuous group in Figure 5-11 is the episyenites, which show a strong depletion of Sr relative to the apparently unaltered metagranite-granodiorite. The most obvious reason for this is the complete albitisation of plagioclase within these samples.

Most samples show a chondrite-normalised rare earth element (REE) pattern, which is typical for granitic rocks with enrichment in light REE relative to heavy REE (Figure 5-12). Apart from the amphibolites and two of the group C rocks, all samples have small to moderate negative Eu anomalies. The patterns within each group/subgroup are mostly sub-parallel, though there are exptions. Some of the rocks within subgroup B8 and groups C and D show a concave-up spectrum for the heavy REE. Such patterns are commonly explained by fractional crystallisation of hornblende, or alternatively, partial melting of an amphibolite, eclogite or garnet amphibolite source /Cullers and Graf, 1984/. In addition, both amphibole and granet are presumed to produce slightly positive Eu anomalies, as shown by sample 521.27 from KFM01A. Under reducing conditions, most of the Eu would be in the 2+ oxidation state, and anomalies may be explained by models involving plagioclase fractionation /Cullers and Graf, 1984/. Returning to the samples of medium-grained and the more fine-grained metatonalite, as discussed above, it is evident that also the REE patterns are closely similar (Figure 5-12). This further supports a genetic relationship. Two of the episyenite samples, on the other hand, show a remarkable depletion in the light REE spectrum, whereas the third, ‘resilicifed’ sample has a pattern, which is indistinguishable from the apparently unaltered metagranites-granodiorites of subgroup B8. The light REE in subgroup B8 is most certainly concentrated in allanite, and the depletion in two of the episyenites is probably a result of the break down of the latter. The fate of allanite during the alteration is unknown, but /Möller et al, 2003/ do not mention allanite in their description of the episyenite samples, and we did not found any allanite during the point counting sessions of the two samples.

The concentrations of heat-producing elements, including K, Th and U, display a systematic enrichment with increasing differentiation in the group. Thus, the highest concentrations are found in the pegmatitic granite and the more evolved members of group C and subgroup 8B. The average contents of K_2O, Th and U in the predominant metagranite-granodiorite are about 3.5%, 15.5 ppm and 4.9 ppm, respectively, which is slightly higher than averages for continental crust /cf Taylor and McLennan, 1985/. The maximum for all rocks analysed are 5.86%, 32.8 ppm (sample 62.09–62.28 from KFM03B) and 15.6 ppm (sample 949.90–950.10 from KFM02A), respectively.

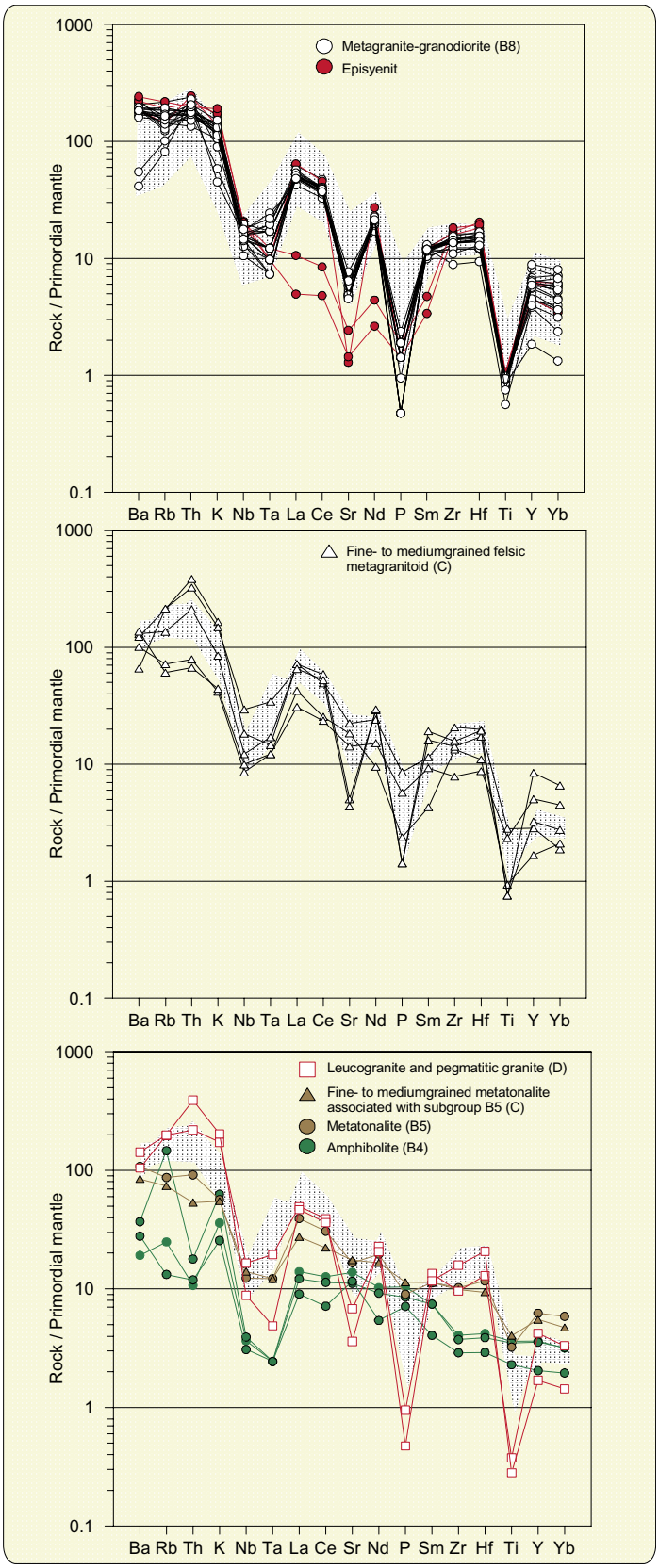

Figure 5-11. *Trace element variation diagrams showing the relationships between large ion lithophile (LILE) and high field strength (HFSE) elements for all rocks analysed in this study. Primordial mantle values of 92.000 for P /Sun, 1980/ and 0.481 for Yb; all other after /McDonough et al, 1992/. Shaded areas are the compositional span of surface bedrock samples from /Stephens et al, 2003/.*

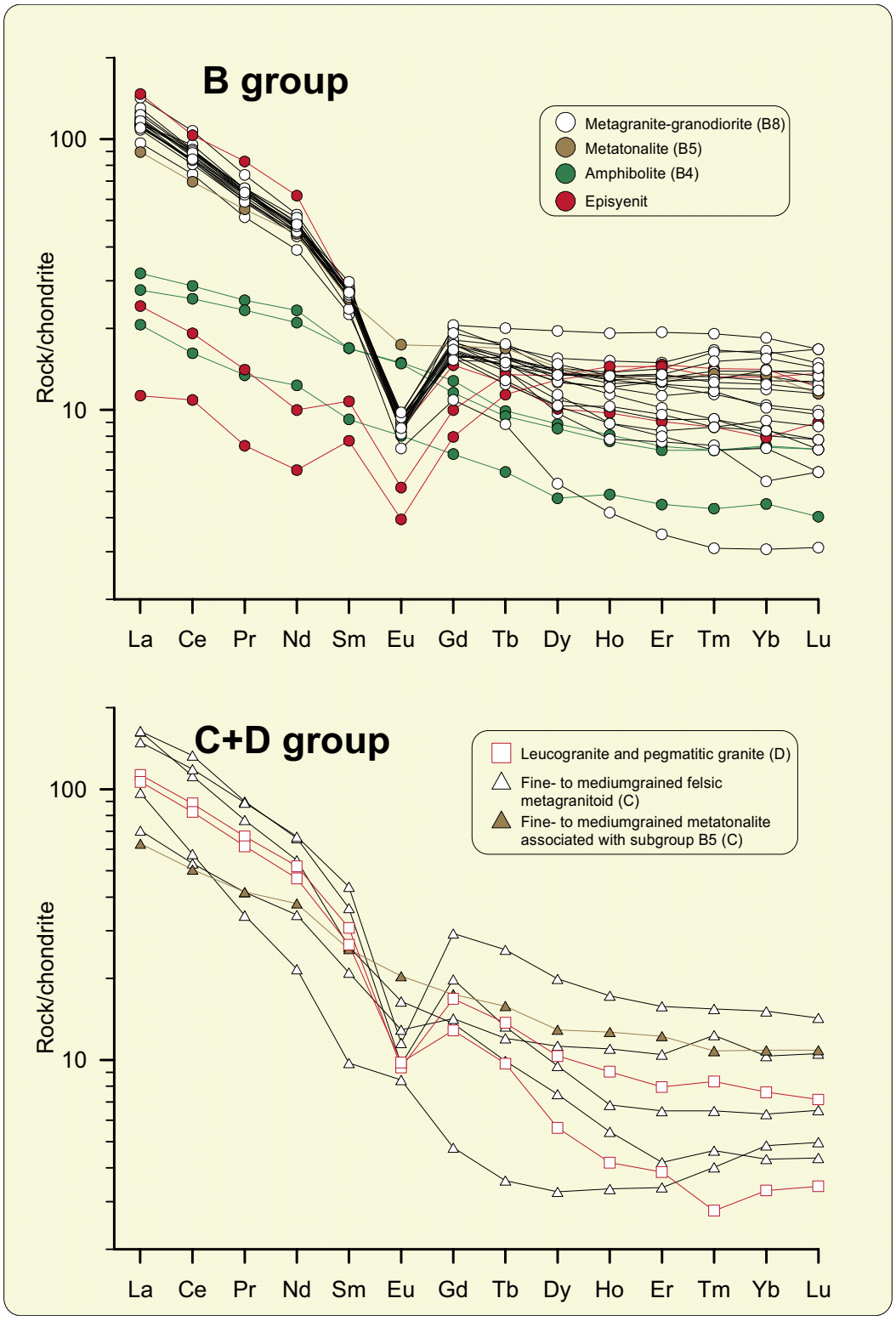

Figure 5-12. *Chondrite-normalized REE patterns for all rocks analysed in this study. Normalization factors from /Boynton, 1984/.*

5.3.3 Selected trace elements for the episyenite occurrence in KFM02A

The highly altered interval of KFM02A bears all the characteristics of a so-called episyenite; a rock formed by hydrothermal processes involving the selective removal of quartz /cf IUGS recommendations; Le Maitre, 2002/. As episyenites are known from the literature to be the host rocks for various mineralizations, including U, Sn–W and Au, it was judged necessary to analyse its ore potential. The results of these trace element analyses are presented in Appendix 3. A brief discussion of the data is given by /Lindroos et al, 2004, p 46/, and a replicate of the essentials follows below:

'There are no visible sulphide minerals in the examined drill cores. Nor are there any large quartz-filled fractures or any minerals that could be related to a gold mineralization. The proposed test sampling is therefore aimed at a number of representative samples of the drill cores.'

'The analyzed samples contain very low concentrations of gold. The concentration of other trace elements is normal for granitic rocks. The absence of sulphide minerals is underscored by a very low sulphide content, on average about 0.04% S for the five samples. There is nothing to suggest that the alteration zone in borehole KFM02A has any ore potential.'

5.4 Fracture mineralogy

5.4.1 Identified fracture minerals

The following fracture coatings have been identified in the randomly orientated grain samples of fracture coating from borehole KFM01A, KFM02A and KFM03A (Appendix 4):

Quartz: (SiO_2) has been identified in many of the analysed samples, often as very small and hematite stained idiomorphic crystals covering the fracture walls and often showing light brownish colour and sugary appearance (Figure 5-13).

Albite (Na-Plagioclase): ($NaAl\ Si_3O_8$) is often found in fillings together with hydrothermal K-feldspar (Adularia). The fillings can be brick red due to hematite staining.

K-feldspar: ($KAlSi_3O_8$) is in the Forsmark fracture samples usually adularia (the low-temperature form) but is also present showing typical microcline twinnings. Similar to albite the colour can be brick red.

Epidote: ($Ca_2Al_2Fe(SiO_4)(Si_2O_7)(O,OH)_2$) is relatively rare in KFM01, KFM02 and KFM03 especially in the open fractures.

Prehnite: ($Ca_2Al_2Si_3O_{10}(OH)_2$). Light greyish green to gray, hydrothermal mineral, but also typical for burial metamorphism (prehnite-pumpellyite facies). In the Formark samples it is often inmixed with quartz or calcite and in some cases with analcime.

Laumontite: ($CaAl_2Si_4O_{12}x4H_2O$) is a very common zeolite mineral in the Forsmark area. It shows a prismatic shape and is brittle. The mineral is white but is mostly coloured red by micrograins of hematite (Figure 5-14), although white varieties are observed as well.

Figure 5-13. *Photography of fracture surface at 267.0 m depth of KFM01A, showing quartz coating with euhedral pyrite and calcite crystals.*

Figure 5-14. *Photography of laumontite sealed breecia at approximately 128.4 m depth of KFM01A.*

Analcime: ($Na(Si_2Al)O_6xH2O$) has colourless, usually trapetzohedral crystals (like garnet). This is considered as one of the highest temperature zeolites but has a large range of formation temperatures.

Apophyllite: ($(K,Na)Ca_4Si_8O_{20}Fx8H_2O$) is a hydrothermal sheet silicate with white to silvery surface. Detected in some fractures at Forsmark.

Pyrite: (FeS_2) is found in many fractures as small idiomorphic cubic crystals grown on open fracture surfaces (Figure 5-13).

Hematite: (Fe_2O_3) is common in the Formark fractures but the amount is relatively low (does not so often turn up in the diffractograms), instead micrograins of hematite cause intense red-staining of many fracture coatings.

Chlorite: ($((Mg,Fe)_6(Si,Al)_4O_{10}(OH)_8$). Dark green mineral found in several associations. XRD identifies the chlorite as clinochlore but large variations in Mg/Fe ratios are indicated from microscopy.

Calcite: ($CaCO_3$) is like chlorite very common and occurs in different assemblages and with different crystal shapes.

Fluorite: (CaF_2). Violet fluorite is found in a few fractures.

Quartz together with albite ± K-feldspar is present in many of the samples. It can be suspected that these minerals belong to the fracture wall rock but microscopy as well as macroscopic observations support that quartz, and secondary, low temperature feldspars are common fracture fillings, especially in the fracture zones intersected by borehole KFM03A. Chlorite and calcite are very common and present in many different associations and occur in several generations. Prehnite occurs in some fillings together with analcime and only in one case together with laumontite.

Despite the large variation in colour and appearance of the fracture coatings the XRD results show a fairly limited number of minerals in the samples. It should, however, be kept in mind that very small portions of a mineral can not be spotted by the diffractometry (< 5–10%). On the other hand the more analyses carried out the better the chances to find also minor constituents.

The following clay minerals have been identified within oriented grain samples of fracture coating from borehole KFM01A, KFM02A and KFM03A (Appendix 4):

Mixed-Layer clays: Mixed layer clay with layers of illite and smectite has been identified in some fractures. The ratio is 3:2 where it has been possible to determine. This is a swelling type of clay as are also corrensite and saponite below.

Corrensite: ($((Mg,Fe)_9(Si,Al)_8O_{20}(OH)_{10}xH_2O$) is a chlorite-like mixed layer clay with layers of chlorite and smecitite/vermiculite, usually with ratio of 1:1. Some of the corrensite samples identified from Forsmark show irregular ordering in the layering; indicating either that they have not reached to perfect corrensite crystallinity or that they are altered. Corrensite is the clay mineral most frequently found.

Illite: ($KAlSi_3O_8$). Occur as micro- to cryptocrystalline, micaceous flakes, and is in the Forsmark samples usually light grey in colour.

Saponite: ($Mg_3(Si_4O_{10})(OH)_2xnH_2O$), This is a variety of swelling smectite. It is identified in some fractures, most of which are in borehole KFM03A.

Corrensite is the most frequent clay mineral but also illite and mixed layer clay (illite/smectite) occurs. Smectite (recorded as saponite in the XRD analyses) have been found mainly in the fracture zones in borehole KFM03A (139 m, 380–389 m and 944 m core lengths).

It is probable that clayish and soft material originally present in the fractures have been lost during drilling, therefore the amounts of clay minerals recorded in the core mapping and in the XRD analyses are too low. From the BIPS pictures it is obvious that many of the fracture zones (e.g. at KFM03B 65 m core length and probably KFM03A:388 m) are filled with gouge material including altered rock fragments and clay minerals. Unfortunately, it has so far not been possible to reveal the composition of the gouge material or to determine the maximum clay mineral contents in these zones, mainly due to disturbances/flushing during the drilling.

5.4.2 Chemical composition

Samples from 12 fracture coatings (7 from KFM01A and 5 from KFM02A) have been analysed for chemical composition including main and trace elements (Appendix 4). The samples are mixtures of different fracture minerals which were scraped from the fracture surfaces. X-ray diffraction analyses have been carried out on the same samples. When possible both chemical and XRD analyses were carried out. The mineral composition of the sample is indicated in Appendix 5.

These chemical analyses can be seen as a first documentation of main and trace element compositions of the fracture coatings. The sample set is too small to make any extensive interpretations but some indications are noted below:

All the fracture samples analysed except for the apophyllite sample (KFM02A: 893.45 m) are rich in **Fe** (from 2.03 to 14.2 wt % given as Fe_2O_3). There is a positive correlation between Fe and **Mg** in most of the samples, indicating that chlorite and clay minerals are important hosts for the Fe. Fe(II) in fracture coatings constitutes an important redox buffer along the water flow paths, and Fe(II)/Fe(III) ratios in chlorite and clay minerals are of importance but have not yet been analysed. Some samples, e.g. KFM01: 127.40 m and 179.35 m, show excess Fe indicating presence of other Fe minerals. In the case of 179.35 m this mineral is probably hematite and in KFM01: 127.40 it is more likely pyrite.

Manganese is another redox sensitive element which may be enriched in fracture coatings. However, in the samples analysed the amounts are low.

Strontium is usually correlated with Ca or Na, and in fresh rocks most of the Sr is hosted in plagioclase. In the fracture coatings the Sr/Na as well as Ca/Sr is equal, or lower than in the host rock. The two samples having the highest Sr content (359 and 338 ppm) are a calcite rich sample and a laumontite rich sample respectively.

Cesium and in some cases **Rb** are higher in the fracture samples that in the host rock. It seems to be a positive correlation between Cs and Rb in samples containing illite and mixed layer clays, whereas samples containing analcime seem to be selectively enriched in Cs.

The **Th** values are generally low (max 12 ppm Th) and lower than in the host rock, whereas the **U** values are higher (the maximum U content is 40 ppm). Ten of the analysed samples have U/Th values that are larger than 1.

The chondrite normalised **REE** curves for the fracture samples are shown Figure 5-15. Most of the samples have REE contents in the same range as the host rock. The La/Yb ratios are in the range 8 to 20 and most samples have pronounced Eu-anomalies.

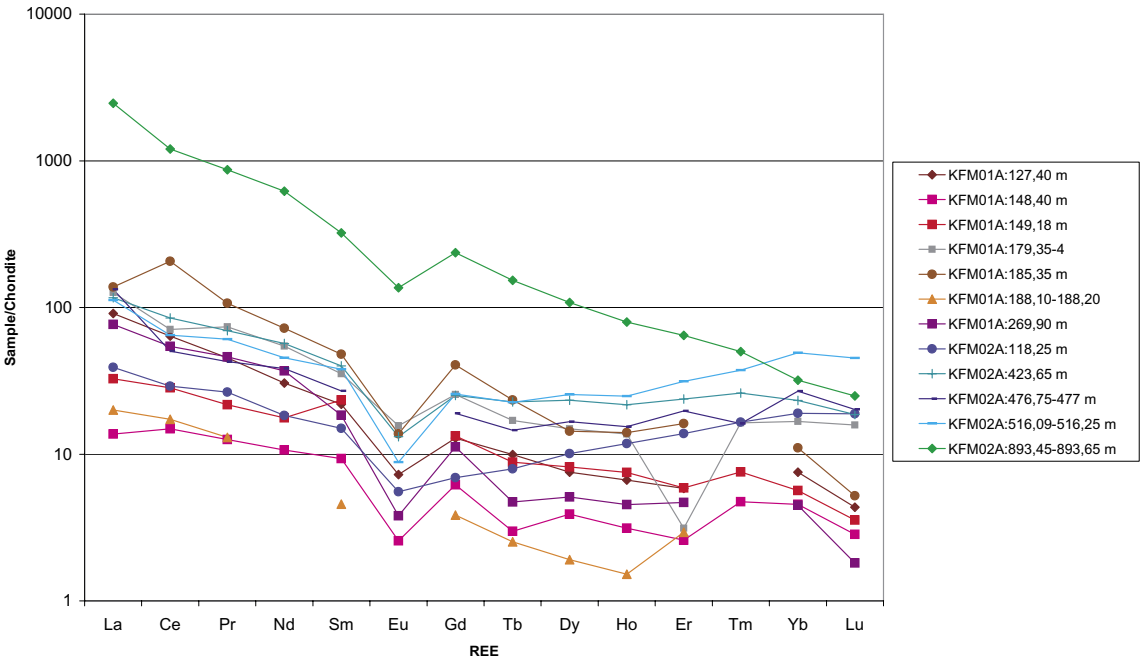

Figure 5-15. *Chondrite-normalised REE patterns for 12 fracture coating samples from KFM01A and KFM02A.*

The apophyllite sample (KFM02A: 893.45 m) in contrast, shows significantly higher content of REEs andalso the highest La/Yb ratio (128). Very low La/Yb ratios (3-4) are obtained in some samples, e.g. the illite rich sample KFM02A:118.25 m. Sample KFM01A: 185.35 m (prehnite, illite and hematite) shows a small but significant positive Ce-anomaly, indicating oxidation of Ce (III) to Ce(IV), probably in connection with hematite formation.

5.4.3 Conclusions

The most common fracture minerals have been identified. The order of crystallisation is roughly from higher to lower temperatures; i.e. from epidote, prehnite, analcime, apophyllite, laumontite, low temperature K-feldspar, albite to quartz. In addition chlorite, calcite and clay minerals are found in association with many of the above mentioned minerals.

Pyrite and hematite have been identified. The former is usually grown as idiomorphic crystals in open space and on fracture surfaces, the latter is found as pigments and small grains usually on laumontite, feldspar, and clay mineral surfaces.

Amongst the clay minerals the swelling, mixed layer clay, corrensite (chlorite/smectite or chlorite/vermiculite) is the most common mineral found, but illite, smectite and mixed layer illite/smectite has also been identified. It is assumed that the amounts of clay minerals are underrepresented in the core logging due to 1) loss of material during drilling and 2) the problem with distinguishing corrensite from chlorite, which is almost impossible without XRD analyses.

5.5 Petrophysical data

5.5.1 Density and magnetic properties

KFM01A

Four of the metagranite to granodiorite samples cluster tightly close to the granite curve in the density-susceptibility rock classification diagrams in Figure 5-16. Their average density is 2661 ± 2 kg/m^3. The outlying sample (depth c 476 m) has a significantly lower magnetic susceptibility but a slightly higher density than the other samples of this group. The two amphibolites have a fairly low magnetic susceptibility, which is the normal for this rock type, and densities of 2989 kg/m^3 and 3048 kg/m^3. The group C metagranite sample has a density of 2642 kg/m^3, the lowest value of all samples in the borehole, whereas the two other samples have densities that indicate a mineral composition corresponding to granodiorite.

The low susceptibility metagranite to granodiorite sample at depth c 476 m also have lower remanent magnetization intensity then the other samples of the group, but its Q-value of 1.01 is slightly higher than the group average. The two amphibolite samples have very low Q-values (average of Q = 0.002) and the three group C samples have Q-values in the same range as the metagranite to granodiorite samples of group B8.

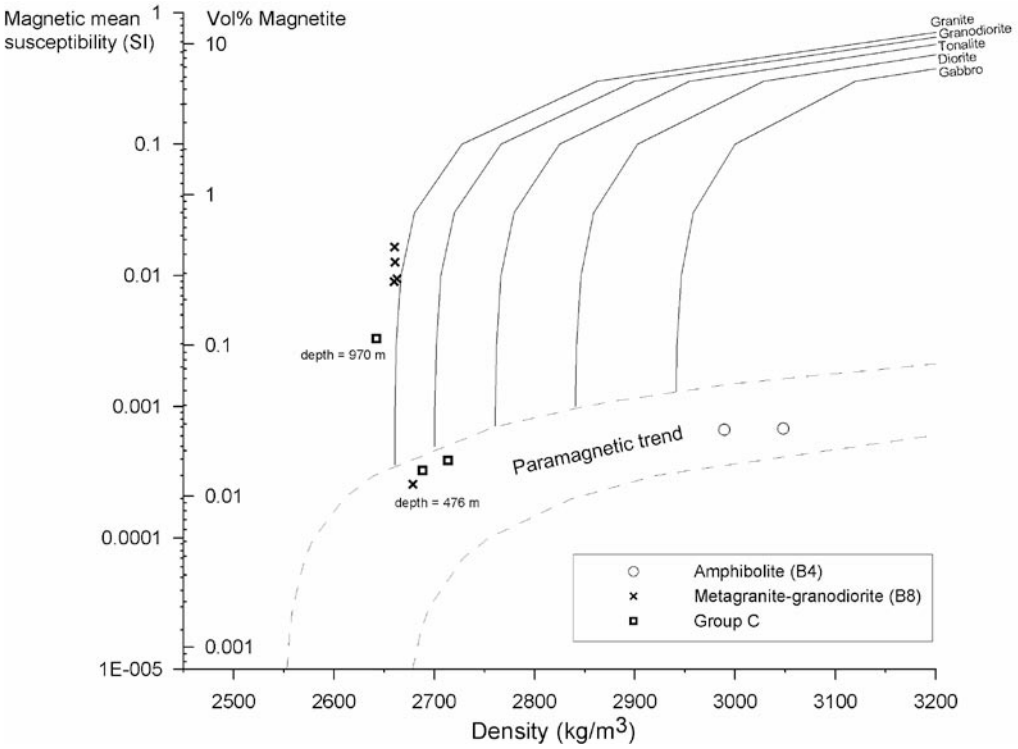

Figure 5-16. *Density-susceptibility rock classification diagram for the rocks of KFM01A. See the text for explanation.*

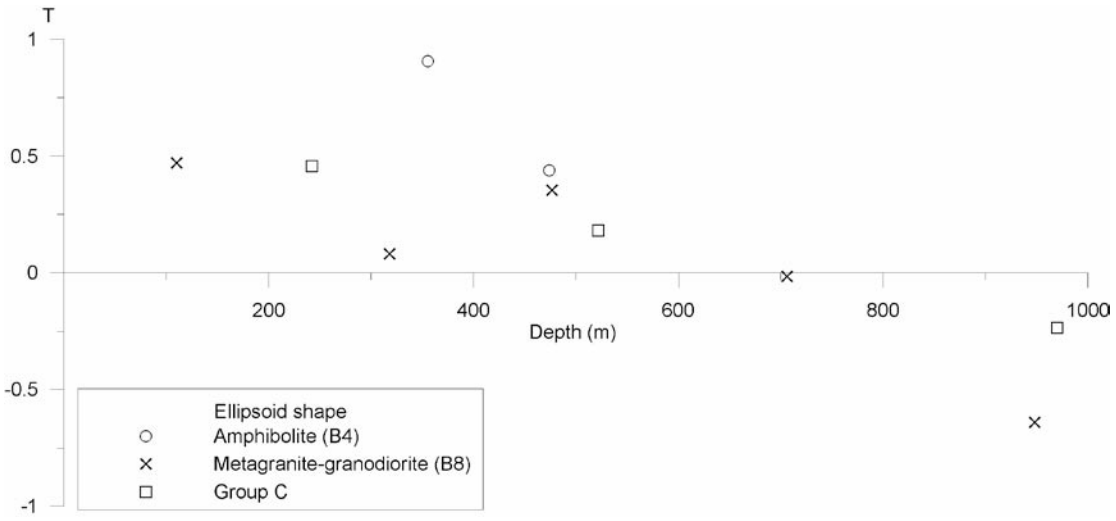

Figure 5-17. *Shape of the magnetic anisotropy ellipsoid with reference to the borehole depth of KFM01A (T > 0 indicates S-tectonite, T < 0 indicates L-tectonite).*

The shape of the anisotropy ellipsoid (Figure 5-17) indicates dominant S-tectonites in the uppermost 600 m of the borehole (T > 0). There is a tendency (with respect to the few data points) that the metagranite to granodiorite rock fabric changes in shape with depth, going from dominant S-tectonite to dominant L-tectonite (T < 0). This may indicate a depth dependent variation of the type of deformation of the rocks in the vicinity of the borehole. The magnetic foliation planes dip steeply throughout the entire borehole whereas the magnetic lineations mainly dip moderately.

KFM02A

The metagranite to granodiorite (B8) and metagranite (B9) samples have a narrow density distribution with an average of 2651 ± 6 kg/m^3 (Figure 5-18). Two samples (depth co-ordinates 244 m and 712 m) have significantly lower magnetic susceptibilities than the rest of the group. The group C metatonalite (depth 916 m) has a density that indicates a mineral composition corresponding to diorite rock whereas the group C metagranite has a density well in accordance with the group B8 and B9 rock samples. The porous rocks have very low densities, ranging from 2064 kg/m^3 to 2568 kg/m^3, and also very low magnetic susceptibilities averaging at c 0.0002 SI.

The porous rock samples have Q-values of 0.57, 1.24 and 2.06. The group B8 and B9 rocks have Q-values between 0.13 and 0.58. The two low-susceptibility samples (depth co-ordinates 244 m and 712 m) also have a low remanence intensity, which clearly indicates that these rock samples have a significantly lower content of magnetite than the other samples of this group.

The shape of the magnetic anisotropy ellipsoid (Figure 5-19) indicates dominant L-tectonites in the uppermost c 400 m of the borehole. There is a tendency (with respect to the few data points) of a change in shape with depth, moving towards a neutral ellipsoid in the deeper parts of the borehole. The magnetic foliation planes dip moderate close to the altered section at about 300 m depth, and show mainly steep dips in the rest of the borehole. The dip of the magnetic lineation is moderate throughout the entire borehole.

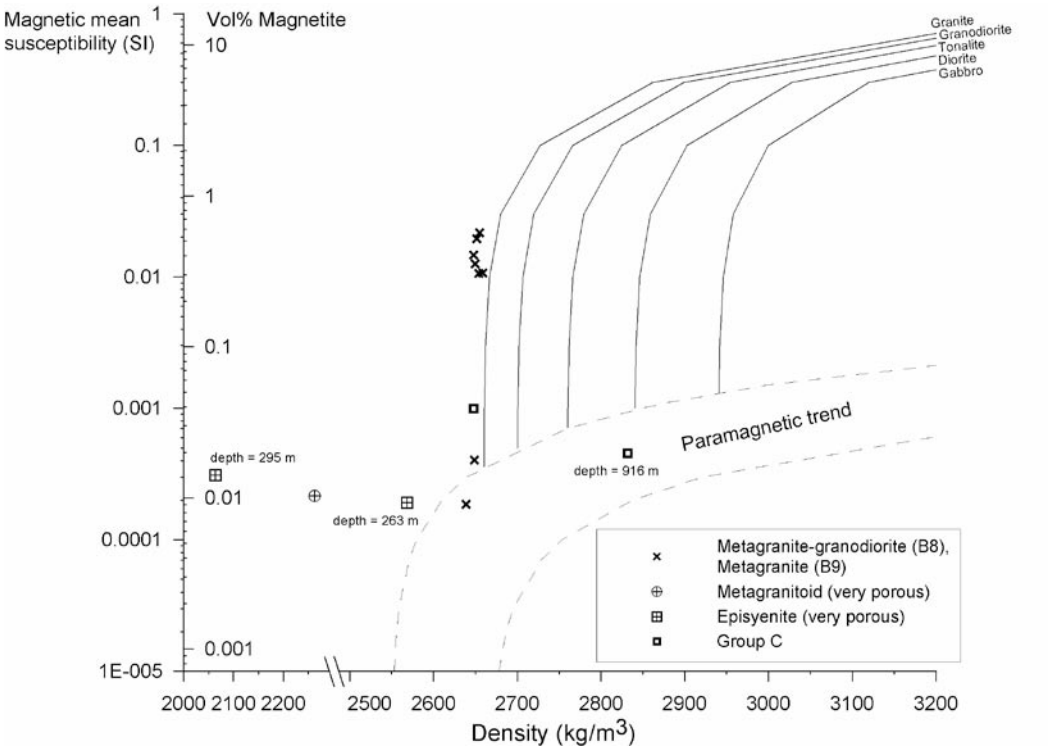

Figure 5-18. *Density-susceptibility rock classification diagram for the rocks of KFM02A. See the text for explanation.*

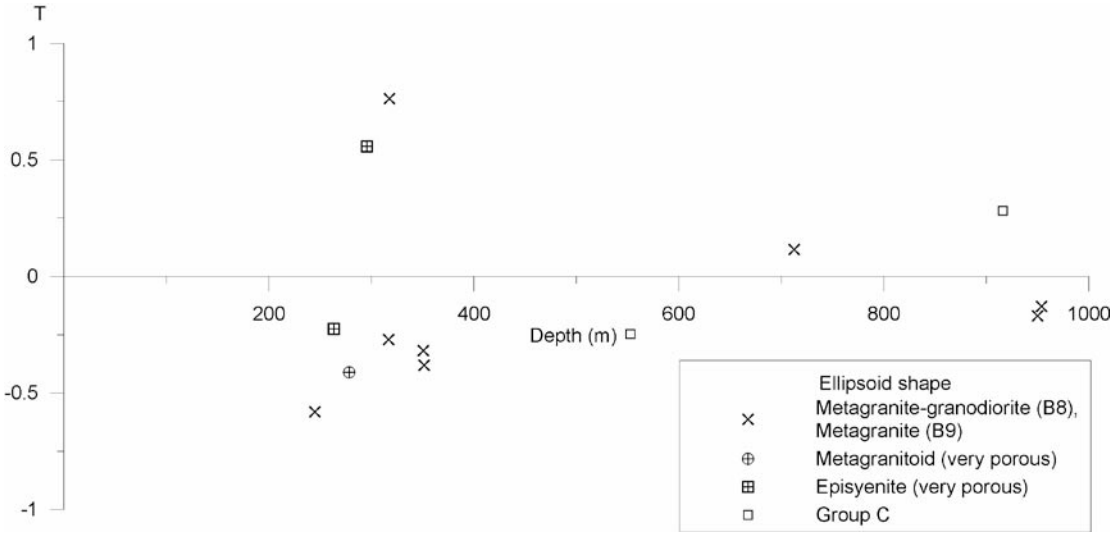

Figure 5-19. *Shape of the magnetic anisotropy ellipsoid with reference to the borehole depth of KFM02A (T > 0 indicates S-tectonite, T < 0 indicates L-tectonite).*

KFM03A and KFM03B

Five of the metagranite to granodiorite samples cluster tightly close to the granite curve in the density-susceptibility rock classification diagrams in Figure 5-20. The outlying sample (depth c 619 m) has a significantly lower magnetic susceptibility but the density is corresponds well to the rest of the group. The average density of all six samples is 2653 ± 2 kg/m^3. The two metatonalite samples (group B5 and group C) plot between the tonalite and diorite rock type curves, thus indicating a mineral composition that corresponds to tonalite to diorite rock. The metagranite of group D has a low density of 2627 kg/m^3 and the pegmatitic granite of KFM03B is only slightly denser but has a significantly lower content of magnetic minerals.

The anomalous metagranite to granodiorite sample (depth c 619 m) has a relatively high Q-value of 1.41 whereas the other group B8 samples and the metatonalite (group C) have Q-values between 0.1 and 1.0. The rest of the samples have Q-values below 0.1.

The shape of the anisotropy ellipsoid (Figure 5-21) indicates dominant weak S-tectonites throughout the entire borehole. The magnetic foliation planes mainly show shallow to moderate dips, and it is the same also for the dip of the magnetic lineation. These shallow dips are anomalous in comparison to the other two boreholes and also to the surface data.

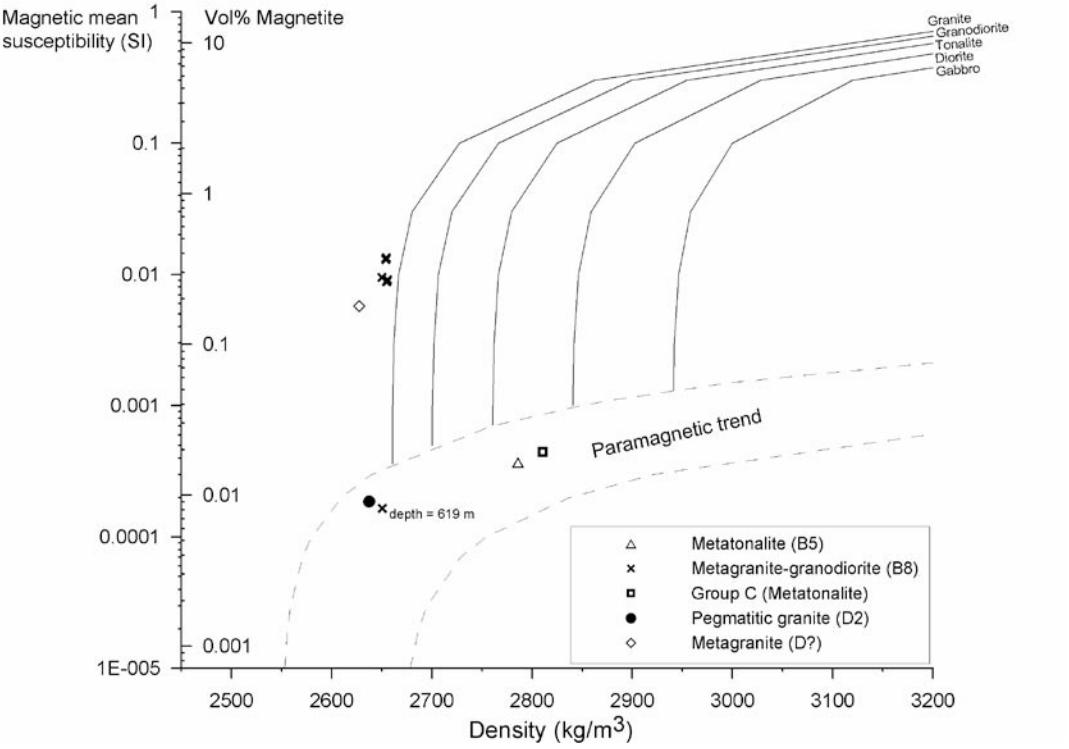

Figure 5-20. *Density-susceptibility rock classification diagram for the rocks of KFM03A and KFM03B. See the text for explanation.*

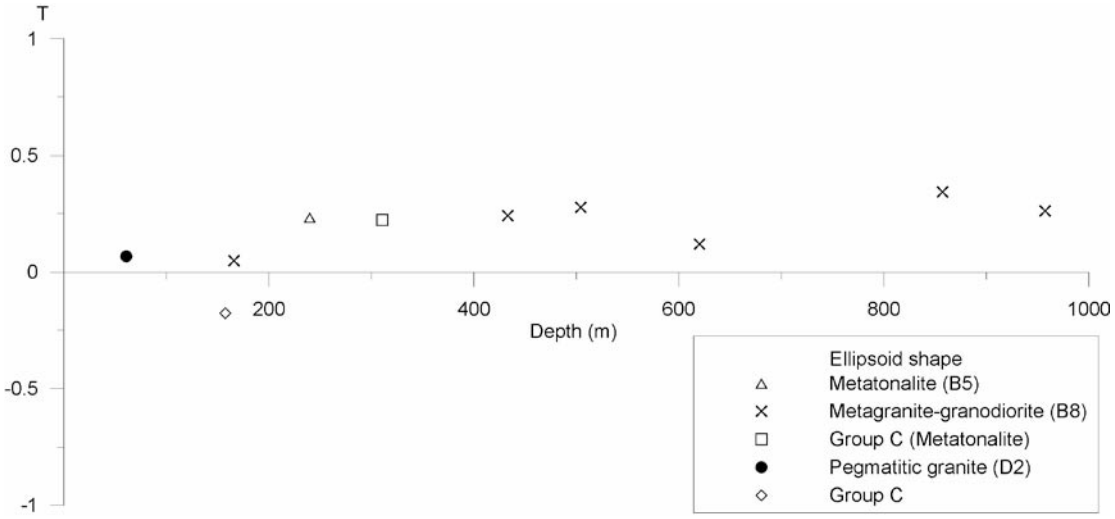

Figure 5-21. *Shape of the magnetic anisotropy ellipsoid with reference to the borehole depth of KFM03A and 3B (T > 0 indicates S-tectonite, T < 0 indicates L-tectonite).*

5.5.2 Electrical properties and porosity

The porosity and resistivity measured in salt water (2.5% NaCl) can be seen in Figure 5-22. The vuggy granite/episyenite samples from KFM02A have anomalously high porosity ranging from ca 2% up to 13%. The other samples form a cluster in the graph with porosities ranging from 0.25 to 0.75% (Table 5-6). Excluding the vuggy granite/episyenite samples, type D rocks seem to have slightly higher porosity than other rock types. Among the type B8 rocks the highest porosities are seen for KFM03A (median 0.46%) and the lowest for KFM01A (median 0.29%) whereas KFM02A show intermediate values (median 0.37%).

The resistivity is low for the vuggy granite/episyenite samples due to their high porosity. The other samples take resistivity values ranging from 340 to 3300 Ωm. No significant differences can be seen between different rock types. In spite of the differences in porosity, no significant difference in resistivity can be seen among the B8 rock samples for the different boreholes.

No correlation between resistivity and porosity can be seen in Figure 5-22 if the vuggy granite/episyenite samples are excluded. Archie's law is often used to model such a relation for rocks with higher porosity:

$\sigma = a \cdot \sigma_w \cdot \phi^m$

where

σ = electric conductivity (S/m, inverse of resistivity)
σ_w = conductivity of pore water (S/m)
ϕ = porosity
a, m = empirical constants.

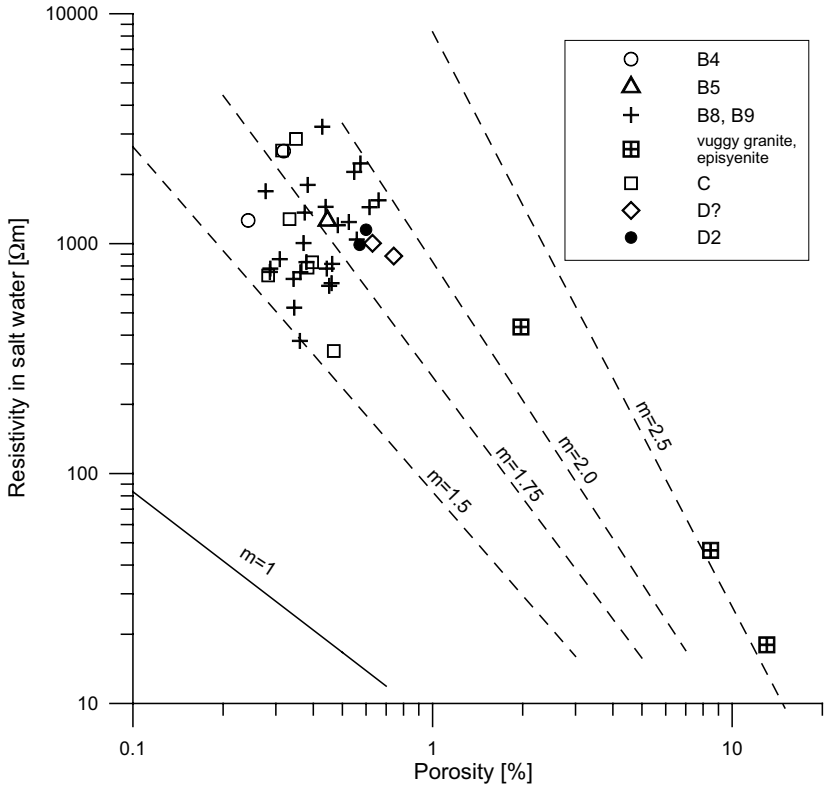

Figure 5-22. *Resistivity in salt water (2.5% NaCl) vs porosity for samples from KFM01A, KFM02A and KFM03A,B. Straight lines corresponding to Archie's law (see text) and a = 3.0 and different values of m are also plotted.*

The factor *a* can be used to account for surface conductivity whereas *m* accounts for pore space geometry. Apparent values of *m* can be estimated from Figure 5-22 since the effect of surface conductivity becomes small in saline water. Straight lines corresponding to Archie's law and a reasonable value for *a* (a = 5) and different values for *m* can be seen in Figure 5-22. The vuggy granite/episyenite samples get high apparent values of m indicating presence of vugs, constrictions, dead-end pores and/or crocked path-ways. The other samples take apparent values of m ranging from 1.5 to 2.0 which can be regarded as normal values. Among the B8 samples higher apparent m-values are found for KFM03A (median 1.89) than for KFM01A (median 1.65) and KFM02A (median 1.74).

The resistivity in fresh water as a function of porosity can be seen in Figure 5-23. The vuggy granite/episyenite samples have fairly low resistivity. The resistivity for the other samples are in the interval 4300 to 55000 Ωm, which can be regarded as normal values for crystalline rocks. No correlation can be seen between porosity and resistivity. Apparent values for the factor *a* in Archie's law can be calculated using the apparent *m*-values from the salt water measurements. Such apparent *a*-values fall in the interval 25 to 340 (excluding vuggy granite/episyenite samples), with the highest values for B5 and high density type C rocks. The high apparent *a*-values indicate that the resistivity in fresh water is strongly dependent upon surface conductivity. Pore space contact surface is thus of much greater importance than pore space volume. Comparisons with thin-section analysis are not fully conclusive but samples with high apparent *a*-values usually have 'locally strongly sericitised plagioclase' and 'partly chloritised biotite' and 'lenses of prehnite'. Presence of fine grained phyllosilicates thus seems to have a major impact on electrical properties in fresh water. Median apparent *a*-values for type B8 rocks are 56.2 (KFM01A), 92.2 (KFM02A) and 91.6 (KFM03A).

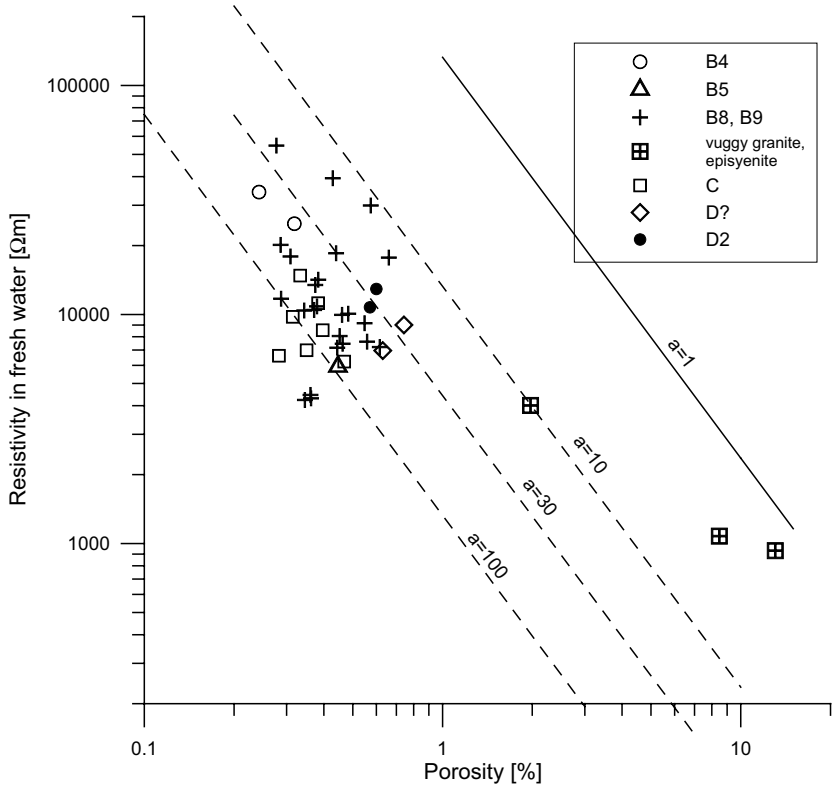

Figure 5-23. *Resistivity in fresh water (42 Ωm) vs porosity for samples from KFM01A, KFM02A and KFM03A,B. Straight lines corresponding to Archie's law (see text) and m = 1.75 and different values of the factor a are also plotted. Note that the choice of m = 1.75 is not valid for some of the samples.*

5.5.3 Gamma-ray spectrometry

KFM01A

In KFM01A (Appendix 6), the amphibolite rock (B4) shows gamma ray characteristics common for this rock type, that is, a low potassium, uranium and thorium content, 1% K, 2 ppm U and 3 ppm Th respectively.

The metagranite-granodiorite (B8) is within normal levels for potassium and uranium, however, a sample at 477.3 m shows very low potassium, 1.2% (Appendix 6). In general, the thorium levels, 15–23 ppm, are slightly higher than normal granite.

The rocks within group C are of various compositions. The metagranodiorite and the metagranodiorite-tonalite show normal values. However, a metagranite at 970.3 m shows very high thorium content, 42 ppm, and increased potassium content 4%, which in total also gives a high natural exposure rate, 23 micro-R/h.

KFM02A

In KFM02A (Appendix 6), the metagranite-granodiorite (B8) is in general within normal levels for potassium, uranium and thorium. The potassium and thorium enrichment in the sample close to the episyenite samples (see below) possibly indicate a similar (incipient?) alteration. This sample, at 245.65 m, also shows a low uranium concentration. A sample at 950.00 m shows a high uranium level, 19 ppm, coincident with very low potassium content, 1.0%.

The episyenite, which is an altered metagranite-granodiorite, shows anomalous levels for both potassium and thorium, up to 4.6% K and 23 ppm Th respectively. The uranium level is normal, 5 ppm. Hence, the natural exposure rate is higher than normal; up to 18 micro-R/h. Notably is that the most porous samples show the highest relative concentrations.

Of the two rock samples within group C, the metagranite at 552.76 m shows high thorium content, 29 ppm, and slight enrichment in uranium and potassium (Appendix 6). The metatonalite shows normal values.

KFM03A+B

In KFM03A+B (Appendix 6), the metatonalite (B5) shows normal values.

The metagranite-granodiorite (B8) is within normal levels for potassium, uranium and thorium. However, a sample at 860.42 m shows very low uranium, 0.8 ppm. The sample at 957.50 m is slightly enriched in uranium and thorium.

The group C metatonalite sample shows normal values.

The leucogranite and pegmatitic granite of group D shows typically high content of potassium, uranium and thorium (Appendix 6): 4.2 and 4.9% K, 8 and 12 ppm U, 22 and 38 ppm Th respectively. Hence, the natural exposure rate is high, 18 and 26 micro-R/h. However, the relative distribution of the elements falls within normal granite.

5.5.4 Compilation of petrophysical parameters

A brief summary of selected petrophysical parameters (averages) for the rock groups that have sufficient amount of data (> 10 samples, only groups B8 and B9) to form the basis of a statistical conclusion, is presented in Table 5-4. The resistivity mean is calculated as a geometrical mean whereas arithmetical means have been calculated for the other parameters.

Table 5-4. Compilation of petrophysical parameters for B8/B9 Metagranodiorite to metagranite/Metagranite (B8/B9).

Rock group	Volume susceptibility	Q-value	Density	Porosity	Resistivity, fresh water	IP**, fresh water	K*	U*	Th*	Natural exposure*
Unit	SI	SI	kg/m^3	%	Ωm	mrad	%	ppm	ppm	µR/h
B8/B9	0.010	0.36	2655	0.41	10980	5.6	2.9	5.3	17.4	13.1

* based on 19 gamma-ray spectrometry samples, not spatially coincident with the petrophysical parameter samples.

** as phase angle at 0.1 Hz.

A compilation of some petrophysical parameters measured on the core samples from KFM01A, KFM02A and KFM03A and B are presented in the Tables 5-5, 5-6 and 5-7 below.

Table 5-5. Some petrophysical parameters of KFM01A.

Sec up (m)	Sec low (m)	Wet density (kg/m³)	Porosity (%)	Kmean (SI)	Remanence intensity (A/m)	Q-value (SI)	Resistivity (Ohm-m)	Petrophysical rock classification
110.06	110.26	2663	0.28	0.00946	0.09199	0.237	33154	granite
241.90	242.10	2713	0.40	0.00039	0.00780	0.487	8293	granodiorite
317.80	318.00	2660	0.29	0.00896	0.08905	0.243	19866	granite
355.10	355.30	2989	0.24	0.00067	0.00007	0.003	36693	mafic volcanite
474.00	474.20	3048	0.32	0.00069	0.00005	0.002	18864	mafic volcanite
476.60	476.80	2678	0.34	0.00026	0.01070	1.014	9710	granite-granodiorite
521.40	521.60	2688	0.28	0.00033	0.02155	1.603	6473	granite-granodiorite
706.00	706.20	2661	0.29	0.01647	0.08265	0.122	10768	granite
947.80	948.00	2661	0.36	0.01262	0.21877	0.423	3876	granite
969.90	970.10	2642	0.47	0.00330	0.01401	0.104	6049	granite

Table 5-6. Some petrophysical parameters of KFM02A.

Sec up (m)	Sec low (m)	Wet density (kg/m³)	Porosity (%)	Kmean (SI)	Remanence intensity (A/m)	Q-value (SI)	Resistivity (Ohm-m)	Petrophysical rock classification
244.40	244.60	2639	0.66	0.00019	0.00130	0.171	19569	granite
263.15	263.35	2568	1.97	0.00019	0.00450	0.572	3610	no classification
277.90	278.10	2263	8.47	0.00022	0.01095	1.238	1278	no classification
295.45	295.64	2064	13.06	0.00031	0.02626	2.060	1055	no classification
316.63	316.83	2648	0.53	0.01466	0.14230	0.237	11861	granite
317.45	317.65	2650	0.46	0.01260	0.06524	0.126	10235	granite
350.60	350.80	2654	0.44	0.01057	0.06548	0.151	16595	granite
351.00	351.20	2659	0.31	0.01067	0.06076	0.139	16584	granite
552.43	552.63	2648	0.38	0.00100	0.00477	0.117	11356	granite
712.25	712.45	2649	0.37	0.00040	0.00195	0.118	10252	granite
915.90	916.10	2832	0.33	0.00046	0.00454	0.243	11055	diorite
949.67	949.87	2655	0.35	0.02157	0.49025	0.555	4369	granite
953.48	953.68	2652	0.36	0.01948	0.46113	0.578	4326	granite

Table 5-7. Some petrophysical parameters of KFM03A and KFM03B.

Sec up (m)	Sec low (m)	Wet density (kg/m³)	Porosity (%)	Kmean (SI)	Remanence intensity (A/m)	Q-value (SI)	Resistivity (Ohm-m)	Petrophysical rock classification
60.46	60.66	2637	0.59	0.00019	0.00046	0.061	11789	granite
157.00	157.20	2627	0.69	0.00573	0.00733	0.031	7921	granite
165.50	165.70	2656	0.38	0.00908	0.04101	0.110	13822	granite
239.44	239.64	2786	0.45	0.00037	0.00087	0.058	7501	tonalite-diorite
310.49	310.75	2810	0.33	0.00045	0.00232	0.127	6985	tonalite-diorite
432.75	432.95	2654	0.43	0.01295	0.43080	0.812	10458	granite
504.00	504.20	2655	0.45	0.00878	0.07020	0.195	7592	granite
619.80	620.00	2651	0.58	0.00017	0.00961	1.414	8130	granite
856.82	857.02	2654	0.51	0.01337	0.06058	0.111	7538	granite
957.20	957.40	2650	0.50	0.00952	0.04029	0.103	34325	granite

Some evident anomalies in the results from the petrophysical investigation are commented below:

- Vuggy granite/episyenite samples have high porosity, low density, low magnetic susceptibility and low resistivity.
- Vuggy granite/episyenite samples have a relation between resistivity and porosity that indicates presence of vugs, constrictions, dead-end pores and/or crocked path-ways.
- Resistivity of samples measured in fresh water is strongly dependent upon surface conductivity. Samples with fine-grained phyllosilicates seem to have the lowest resistivities, vuggy granite/episyenite samples excluded.
- The median porosity is highest in KFM03A and lowest in KFM01A.
- The magnetic fabric orientation of KFM03 clearly deviates from the fabric orientations of KFM01 and KFM02.
- A metagranite sample of KFM01A (depth c 476 m) has a significantly lower magnetic susceptibility but a slightly higher density than the other metagranite samples in this borehole.
- Some metagranite samples belonging to group C show high thorium levels, 29 and 42 ppm.
- The episyenite samples and a metagranite-granodiorite sample close to the episyenite, in the upper part of KFM02A, show a relative enrichment in potassium and thorium, 4.2–4.6% K and 19–23 ppm Th, respectively.
- A leucogranite and a pegmatite granite sample in KFM03 show typically high content of potassium, uranium and thorium.

6 References

Boynton W V, 1984. Geochemistry of the rare earth elements: metiorite studies. In Henderson P (editor), Rare earth element geochemistry. Elsevier, pp 63–114.

Cullers R L, Graf J L, 1984. Rare earth elements in igneous rocks of the continental crust: intermediate and silicic rocks – ore petrogenesis. In Henderson P (editor), Rare earth element geochemistry. Elsevier, pp 275–316.

Debon F, LeFort P, 1983. A chemical-mineralogical classification of common plutonic rocks and associations. Transactions of the Royal Society of Edinburgh, Earth Sciences 73, 135–149.

Drever S I, 1973. The preparation of oriented clay mineral specimens for X-ray diffraction analysis by a filter-membrane peel technique. American Mineralogist 58, 553–554.

Le Maitre R W (ed), 2002. Igneous rocks: A classification and glossary of terms. Recommendations of the International Union of Geological Sciences Subcommision on the Systematics of Igneous rocks. Cambridge University Press, 240 pp.

Lindroos H, Isaksson H, Thunehed H, 2004. The potential for ore and industrial minerals in the Forsmark area. SKB R-04-18. Svensk Kärnbränslehantering AB, 51 pp.

Maniar P D, Piccoli P M, 1989. Tectonic discrimination of granitoids. Geological Society of America Bulletin 101, 635–643.

Mattsson H, Thunehed H, Isaksson H, 2004. Interpretation of petrophysical data from from the cored boreholes KFM01A, KFM02A, KFM03A and KFM03B. SKB P-04-107. Svensk Kärnbränslehantering AB.

McDonough W F, Sun S, Ringwood A E, Jagoutz E, Hofmann A W, 1992. K, Rb and Cs in the earth and moon and the evolution of the earth's mantle. Geochimica et Cosmochimica Acta, Ross Taylor Symposium volume.

Möller C, Snäll S, Stephens M B, 2003. Dissolution of quartz, vug formation and new grain growth associated with post-metamorphic hydrothermal alteration in KFM02A. SKB P-03-77. Svensk Kärnbränslehantering AB, 56 pp.

PDF, 1994. Powder diffraction file computer data base. Set 1–43. International Centre for Diffraction Data, Park Lane, Swartmore, PA, USA.

Petersson J, Wängnerud A, 2003. Boremap mapping of telescopic drilled borehole KFM01A. SKB P-03-23. Svensk Kärnbränslehantering AB, 97 pp.

Petersson J, Wängnerud A, Stråhle A, 2003. Boremap mapping of telescopic drilled borehole KFM02A. SKB P-03-98. Svensk Kärnbränslehantering AB, 111 pp.

Petersson J, Wängnerud A, Danielsson P, Stråhle A, 2004. Boremap mapping of telescopic drilled borehole KFM03A and core drilled borehole KFM03B. SKB P-0-03-116. Svensk Kärnbränslehantering AB, 55 pp.

Stephens M B, Lundqvist S, Ekström M, Bergman T, Andersson J, 2003. Bedrock mapping – Rock types, their petrographic and geochemical characteristics, and a structural analysis of the bedrock based on stage 1 (2002) surface data. SKB P-03-75. Svensk Kärnbränslehantering AB, 50 pp.

Streckeisen A, 1976. To each plutonic rock its proper name. Earth Science Reviews 12, 1–33.

Stråhle A, 2003. Introduktion för Boremapkartering. Svensk Kärnbränslehantering AB, 58 pp.

Sun S S, 1980. Lead isotopic study of young volcanic rocks from mid-ocean ridges, ocean islands and island arcs. Philosophical Transactions of the Royal Society A297, 409–445.

Taylor S R, McLennan S M, 1985. The continental crust; its composition and evolution. Blackwell, Oxford, 312 pp.

Appendix 1

Description of thin-sections

KFM01A

109.66 m. *Metagranite-granodiorite (101057).*

The rock exhibits an anhedral, rather equant texture and only a few grains exceed 1 mm in size. The major phases include quartz, plagioclase, microcline and minor amounts (c. 3–4 vol.%) of biotite. The tectonic fabric is primarily defined by oriented biotite and elongated quartz grains. Quartz domains display a typical pattern of dynamic recrystallisation with undulose extinction and irregular subgrains of variable size and shape. Plagioclase is occasionally slightly sericitisied and some of the affected grains contain also minor calcite. Most microcline grains show a cross-hatched twin texture with a very low proportion of exsolved perthitic albite. Biotite occurs as subhedral grains, with a width up to about 0.2 mm. Accessory minerals, typically associated with biotite, are epidote, magnetite, sphene, chlorite, allanite, apatite and zircon. Magnetite forms separate grains, up to 0.3 mm in diameter. Some of them are overgrown by a thin, discontinuous rim of sphene or epidote. Allanite occurs as euhedral, rather metamict crystals, overgrown by epidote.

242.44 m. *Metagranodiorite (101051).*

This rock has a general grain-size of about 0.5–1.5 mm, and displays a granular texture, similar to that in the preceding thin-section (109.66). However, there are a few grains of coarser plagioclase, reaching up to 2–3 mm in size. All microcline grains, on the other hand, are less than 0.6 mm in size. Quartz has developed subgrains with sutured boundaries and undulose extinction, whereas microcline typically displays cross-hatched twinning. Plagioclase is to a variable extent sericitised and may include both calcite and epidote.

The major mafic components of the rock are biotite (9 vol.%), hornblende (5 vol.%) and epidote (3 vol.%). The rather weak deformational fabric of the rock is primarily defined by the biotite, which forms subhedral grains, 0.1–0.2 mm in width. Hornblende forms anhedral grains, less than 1 mm in size. Epidote is less than a few tenths of a millimeter in size, and shows typically a very fine-scaled, symplectitic texture. The accessory minerals, including titanite, apatite, allanite, zircon, pyrite, chalcopyrite and magnetite, occur as separate grains, but most are intimately associated with biotite and hornblende. Sphene forms subhedral to euhedral grains up to 0.6 mm in size. Apatite forms stubby prisms with a length:width ratio of 3:1 and a diameter of 0.1–0.2 mm. Allanite crystals are all metamict and 0.15–0.3 mm in length, except for one grain, which reach up to 0.6 mm in length.

317.79 m. *Metagranite-granodiorite (101057).*

The grain-size of this rock is generally less than 0.6 mm, with some grains reaching up to 1 mm. The mineralogy and textural features are typical for the metagranite-granodiorite samples from the three deep boreholes, with strained quartz, slightly sericitised plagioclase and tartan twinned K-feldspar, except for the fact that this rock is hornblende-bearing (0.4 vol.%). The hornblende is normally intimately associated with biotite. The deformational fabric is primarily defined by biotite and elongated quartz–feldspar aggregates. The opaque minerals consist of pyrite and magnetite in approximately equal proportions.

355.33 m. *Amphibolite (102017).*

A fine-grained amphibolite with a general grain-size of 0.3–1.0 mm and a few hornblende crystals up to 1.5 mm in length. The texture is granular with a faint mineral fabric defined by hornblende. Besides hornblende and plagioclase, comprising more than 90 vol.% of the mode, the rock contains minor amount of sphene, epidote and biotite, as well as accessory amounts of calcite, apatite and pyrite (a single grain). Except for this single grain of pyrite, opaque phases are notably absent. Epidote displays a very fine-scaled, symplectitic texture, whereas sphene forms subhedral grains less than 0.1 mm in size. Apatite occurs as stubby prisms, 50–100 microns in diameter. Plagioclase is to a variable extent sericitised, especially along an about 2 mm wide zone surrounding a fracture or shear plane which runs across the thin-section. In addition, this zone is characterised by an increased content of epidote and, to some extent, calcite, relative to the wall rock.

379.90 m. *Metagranite-granodiorite (101057) speckled by whitish plagioclase.*

Also this rock shows the typical granular texture with a grain-size of 0.5–1.5 mm. The mineralogy and textural features are more or less identical with those of the other metagranite-granodiorite samples from the three deep boreholes, with strained quartz, tartan twinned K-feldspar and less than 5 vol.% biotite. However, the intensity of the retrograde alteration is higher in this thin-section, and the macroscopically distinctive whitish plagioclase is typically crowded by sericite ± calcite and submicroscopic grains of hematite. In addition, biotite shows signs of retrograde alteration by local conversion to chlorite with thin lenses of pumpellyite/prehnite. Also some muscovite, with isolated grains of epidote, is associated with the biotite, but whether its origin is purely replacive is unclear. Other accessory phases include sphene, magnetite, allanite and zircon.

433.03 m. *Biotite-rich amphibolite (102017).*

This is a fine-grained amphibolite with an estimated biotite content of about 10–20 vol.%. The general grain-size range between 0.4 and 1.0 mm, with a few hornblende crystals up to 1.5 mm in length. Also the typical granular texture is identical, though the mineral fabric is more distinctly defined by the more abundant biotite. Besides the main components hornblende, plagioclase and biotite, the rock contains some 5 vol.% of epidote and sphene. Epidote shows a very fine-scaled, symplectitic texture, whereas sphene occurs as isolated, sub- to euhedral grains up to 0.2 mm in length. Plagioclase is locally slightly sericitised. Trace amounts of calcite and a single stubby apatite prism, about 50 microns in diameter, were also found in this thin-section.

477.30 m. *Metagranite-granodiorite (101057).*

This rock has a granular texture with a distinct tectonic fabric defined by biotite and elongated quartz. The general grain-size ranges up to about 1 mm with a few quartz grains reaching 4 mm in length. Quartz has undergone recrystallisation into sub-grains with undulose extinction and sutured, irregular boundaries. Plagioclase tends to be fresh and virtually unaffected by sericitisation. K-feldspar displays typically a cross-hatched twin texture and a very low proportion (<<1 vol.%) of exsolved perthitic albite. Few K-feldspar grains exceed 0.5 mm in diameter. Except for some accessory phases, the only ferromagnesian mineral is biotite, comprising 8.8 vol.% of the mode. Individual grains form well-developed booklets, less than about 0.2 x 0.8 mm in size. Some minor grains are almost totally chloritised. The accessory minerals include: anhedral epidote, often with a very fine-scaled, symplectitic character; prehnite, generally in close proximity to

biotite (or chlorite); stubby prisms of apatite; oscillary zoned zircon crystals (<80 microns); and one, about 0.5 mm long, allanite crystal rimmed by epidote.

521.27 m. *Metagranodiorite-tonalite (101051).*

A fine-grained rock (up to about 1.0 mm in grain-size) with granular texture and weakly defined tectonic fabric. Although more equigranular and fine-grained than other metagranite-granodiorite samples from the three boreholes, the rock shows almost identical textural features with strained quartz, sparsely sericitised plagioclase and tartan twinned K-feldspar; the latter less than 0.5 mm in diameter. Biotite occurs primarily as scattered booklet-shaped crystals (less than about 0.1 x 0.7 mm in size) together with minor amounts of epidote and hornblende. Epidote typically forms anhedral crystals, up to 0.5 mm in size, with a very fine-scaled symplectitic character. A few anhedral crystals of sphene (<0.1 mm) also occur in close proximity to the other ferromagnesian minerals. Apatite is found as minor prisms, about 60–80 microns in diameter.

528.66 m. *Pegmatitic granite (101061).*

This rock consists of rounded plagioclase and quartz porphyroclasts (1–6 mm in diameter), in a matrix of grain-size reduced quartz–feldspar material. All quartz is strained and plagioclase has been subjected to a slight, but in some grains strong, sericitisation. The more intensely sericitised parts may also contain muscovite and calcite. K-feldspar is the least frequent of the major phases, and typically found within the grain-sized reduced material. The microtexture of K-feldspar include tartan twinning, and locally, perthitic lamellae of albite. Biotite forms lobate clusters, together with minor epidote (<0.4 mm) and turgid lenses of prehnite. Locally, biotite is partially to totally chloritised. Other accessory minerals include apatite (<0.1 mm), allanite (metamict, euhedral, epidote rimmed crystals 0.4–0.7 mm in length), pyrite, zircon, sphene and a single crystal of chalcopyrite about 0.1 mm in diameter.

705.88 m. *Metagranite-granodiorit (101057).*

A rock characterised by granular texture and distinct tectonic fabric defined by thin streaks of biotite and polycrystalline domains of strained quartz, with some sub-grains reaching up to 7 mm in length. However, the feldspars rarely exceed 1.5 mm in grain-size. K-feldspar exhibits cross-hatched twin texture. Plagioclase is frequently slightly sericitised, and locally, also saussuritised. The prime ferromagnesian mineral in the rock is biotite comprising 4.2 vol.% of the mode. Minor grains of biotite are locally replaced by chlorite. The majority of the accessory minerals, including epidote, magnetite, sphene, zircon, allanite, prehnite and apatite, occur preferentially in or in close proximity to the biotite. Epidote forms anhedral grains (<0.2 mm), with very fine-scaled, symplectitic texture. Magnetite is rounded, up to 0.7 mm in diameter, and rarely, slightly matitised along fractures. Sphene occurs as isolated, subhedral to anhedral crystals (<0.5 mm), or as overgrowths on magnetite. Allanite is more or less metamict and intimately associated with epidote. Apatite occurs as stubby prisms, less than 0.1 mm in diameter.

947.70 m. *Metagranite-granodiorite (101057).*

The thin-section reveals a granular texture with a distinct tectonic fabric marked by streaks of biotite and strained quartz. Grain sizes are variable up to about 1.2 mm, with a few K-feldspar and quartz grains reaching up to 2 mm in length. The mineralogy and textural relations are more or less identical to that of the other metagranite-granodiorite samples from the three boreholes, and includes strained quartz, locally slightly

sericitised plagioclase and tartan twinned K-feldspar devoid of perthitic exsolutions. Biotite is the prime ferromagnesian mineral in the rock with a mode of 7.2 vol.%. Associated with the biotite are trace amounts of retrogressive chlorite, prehnite and hematite. Other accessory minerals found in close proximity to biotite is epidote, allanite, sphene, oscillary zoned zircon, and stubby prisms of apatite. Allanite is normally metamict and occurs both as euhedral and irregular grains, from about 0.3 to 1 mm in diameter, and the majority is mantled by epidote.

970.35 m. *Metagranite (101051).*

This rock is texturally very similar to that of thin-section 521.27 (KFM01A), with an almost massive, granular texture. The grain-size range up to about 2 mm. Quartz displays strain-induced sub-grains, with sutured boundaries and undulose extinction. Plagioclase is often slightly, and some grains strongly, sericitised. K-feldspar shows cross-hatched twinning and some grains contain numerous perthitic albite lamellae. Biotite forms booklet-shaped crystals (less than 0.2 x 0.6 mm in size), which are scattered throughout the thin-section. Epidote is found as sub- to anhedral crystals, often associated with biotite. The accessory assemblage includes prehnite, rounded crystals of magnetite (<0.5 mm), metamict and epidote-mantled allanite, oscillary zoned zircon and apatite (<40 microns).

987.32 m. *Quartz-dominated, skarn-like rock (108019).*

A fine-grained (0.1–1.0 mm) rock composed of quartz, sericitised plagioclase and about 8–10 vol.% epidote with minor hornblende. Its texture is rather granular with a few polycrystalline quartz grains reaching up to about 3 mm in size. Individual sub-grains show undulose extinction and sutured boundaries. In order of decreasing abundance, the accessory assemblage includes euhedral sphene (<0.1 mm), muscovite, allanite (<0.2 mm; typically euhedral and epidote-mantled), magnetite, pyrite, calcite, apatite and a single grain of chalcopyrite.

KFM02A

500.32–500.35 m. *Metagranite (101051?).*

A fine-grained rock with a rather massive, granular texture. The most conspicuous feature is that the rock has been subjected to pervasive retrograde alteration, resulting in more or less strong sericitisation of plagioclase and complete chloritisation of biotite. Also secondary calcite, epidote and a sub-microscopic staining of hematite are found in the most strongly sericitised plagioclase grains. Quartz displays a typical strain-induced texture with irregular sub-grains, undulose extinction and sutured grain boundaries. K-feldspar shows tartan twinning and often perthitic intergrowths comprising lamellae or ‘flames’ of albite. The content of ferromagnesian phases is less than about 2.5 vol.% and limited to some scattered grains of chloritised biotite, together with trace amounts of epidote, prehnite/pumpellyit, metamict allanite and titanite. Additional accessory minerals found are zircon and some stubby prisms of apatite, less than 50 microns in diameter.

552.63–552.63 m. *Metagranite (101051?).*

This rock shows a granular texture with a grain-size ranging up to 2 mm and a rather weak tectonic fabric primarily defined by strained quartz. The latter forms sub-grains with sutured boundaries and undulose extinction. Plagioclase is locally strongly sericitised with scattered grains of calcite, chlorite, epidote, and muscovite. Most K-

feldspar displays cross-hatched twinning, and locally perthitic lamellae or 'flames' of exsolved albite. The ferromagnesian assemblage consists essentially of biotite (3.0 vol.%) and spatially associated epidote (1.4 vol.%). Minor grains of biotite is frequently replaced by chlorite and lenses of pumpellyite and/or prehnite. Epidote occurs as anhedral to subhedral grains (<0.4 mm), locally with a very fine-scaled symplectitic character. Allanite forms metamict, up to almost 1.3 mm in length. Other accessories are oscillary zoned zircons and stubby prisms of apatite.

712.45–712.48 m. *Metagranite-granodiorite (101057).*

This rock is characterised by a more fine-grained, granular texture, than expected from the macroscopic investigation, as well as a distinct tectonic fabric defined by elongated domains of strained quartz, alternating with elongated, feldspar-dominated domains and thin streaks of biotite. Plagioclase is locally slightly sericitised. K-feldspar, on the other hand, typically displays cross-hatched twinning and locally, perthitic lamellae or 'flames' of albite. Except for some accessories, biotite is the only ferromagnesian mineral, constituting 7.0 vol.% of the mode. A few minor biotite grains have been chloritsed, and thin lenses of prehnite are found in some grains. Other accessory minerals include anhedral epidote (often with a very fine-scaled symplectite texture), allanite (rounded, metamict grains, 0.2–0.6 mm, locally with overgrowths of epidote), anhedral sphene, stubby prisms of apatite and euhedral zircons (oscillary zoned and often included in biotite).

916.83–916.85 m. *Metatonalite (101051).*

This rock displays a weak, but rather distinct tectonic fabric and a granular texture with rounded grains, up to 1 mm in size, composed of plagioclase, hornblende, strained quartz and minor amounts (7.2 vol.%) of biotite. Plagioclase is locally faintly sericitised, though the majority is apparently unaffected by retrograde alteration. The accessory minerals include epidote, sphene, chlorite, prehnite, apatite, zircon and possibly allanite. Epidote forms anhedral to subhedral grains, averaging about 0.1 mm, with a few grains reaching up to 0.5 mm in size. Some grains displays a very fine-scaled symplectitic character. Sphene is found as anhedral crystals up to 0.2 mm in diameter. Apatite occurs as stubby prisms about 50 microns in diameter and a length:width ratio of 3:1. Possibly allanite is rounded, highly metamict and found enclosed by epidote.

917.70–917.75 m. *Metatonalite (101051).*

An amphibolite-like rock with estimated quartz content of about 20 vol.%. The texture is granular with a weak deformational fabric and a general grain-size ranging between 0.1 and 0.8 mm. With a total plagioclase-hornblende content of about 70–75 vol.%, the rock is closely similar to that described above (thin-section 916.83–916.85). However, this rock has undergone a rather pervasive retrograde alteration with strong but variable sericitisation of plagioclase and total decomposition of biotite into chlorite with abundant lenses of prehnite. Chloritised biotite and epidote occupy about 5–10 vol.% of the rock. The latter occurs as an- to subhedral grains up to 0.5 mm, often with the characteristic very fine-scaled, symplectitic texture. The accessory minerals include anhedral sphene (<0.5 mm), rounded grains of apatite and a few crystals of pyrite. In addition, there is a set of submicroscopic fractures, which runs more or less parallel to the longitudinal direction of the thin-section. The actual sealing is too thin to make mineralogical identification accurately.

949.87–949.90 m. *Metagranite-granodiorite (101057).*

A rock, which is texturally similar to that of the other metagranite-granodiorite samples from the three deep boreholes, with a rather well-defined tectonic fabric. The general grain-size is about 0.2–1.5 with a few grains of plagioclase and strained quartz reaching up to 3–4 mm. However, K-feldspar rarely exceeds 0.5 mm. A few plagioclase grains have undergone a slight sericitisation. K-feldspar typically shows cross-hatched twinning and are virtually free from perthitic albite. Biotite is the only ferromagnesian phase, not found in accessory amounts. In the order of decreasing abundance, the accessory minerals include epidote, magnetite, sphene, apatite, zircon, allanite and pyrite. Epidote occurs as somewhat very fine-scaled symplectitic, anhedral to subhedral grains, up to 0.2 mm in size. Magnetite forms isolated, rounded grains, up to about 1 mm in diameter. Sphene is anhedral to subhedral, whereas apatite forms up to 150 microns wide prisms with a length:width ratio up to 4:1. Zircon is found as rounded, oscillary zoned crystals (<0.1 mm).

953.45–953.48 m. *Metagranite-granodiorite (101057).*

This rock displays a granular texture, closely similar to that of the other metagranite-granodiorite samples from the three deep boreholes, with irregular grain boundaries and a distinct deformational fabric defined by alternating domains of strained quartz, feldspars and streaks of biotite. The general grain-size is 0.2–2 mm, with a few plagioclase grains reach 2.5 mm. Plagioclase is generally slightly and locally, strongly sericitised. K-feldspar shows tartan twinning and a few grains carry trace amounts of perthitic albite. The prime ferromagnesian phases is biotite and magnetite, which together only constitute 2.6 vol.% of the rock. Some minor biotite grains have been replaced by chlorite and thin lenses of prehnite. Magnetite occurs as isolated anhedral grains, locally intergrown with what probably is ilmenite. Other accessory minerals found are epidote, sphene (typically as overgrowths on magnetite), muscovite, allanite (about 0.6–0.7 mm + one 1.5 mm long grain), apatite (about 150 microns in diameter), oscillary zoned zircon (<0.1 mm) and pyrite.

KFM03B

62.32–62.36 m. *Medium-grained part of pegmatitic granite (101061).*

An inequigranular, rather massive rock with porphyroclasts of K-feldspar and quartz (3–5 mm) in a more finely grained matrix (<3 mm) dominated by more or less strongly sericitsed plagioclase. One K-feldspar crystal is almost 1 cm in length. Plagioclase is locally myrmekitic. K-feldspar often displays perthitic intergrowths comprising lamellae or ‘flames’ of albite, whereas other parts show tartan twinning. Quartz forms irregular sub-grains with undulose extinction and sutured boundaries. The content of ferromagnesian minerals is limited to some small, lobate and mostly chloritised grains of biotite (2.2 vol.%), locally associated with minor hematite. In addition, there are a few anhedral grains of epidote, with a very fine-scaled, symplectite texture. Also apatite and calcite have been distinguished as accessories.

157.40–157.45 m. *Metagranite (111058?).*

A rock with granular texture and a rather weak tectonic fabric, primarily defined by elongated domains of strained quartz. The latter consists of irregular sub-grains with strongly undulose extinction and sutured contacts. The retrograde effects, including sericitisation of plagioclase and chloritisation of biotite, is strongly pervasive. The most strongly sericitsed parts carry scattered grains of muscovite, epidote and calcite,

whereas the secondary chlorite is intimately associated with prehnite/pumpellyite and submicroscopic grains of what probably is be hematite. K-feldspar is apparently unaffected by the alteration and displays cross-hatched twinning and locally, perthitic lamellae of albite. The accessory phases found are epidote (often with a very fine-scaled symplectite texture), rounded grains of magnetite (<0.5 mm), metamict allanite (<0.4 mm) and oscillary zoned zircon (<150 microns).

165.90–165.95 m. *Metagranite-granodiorite (101057).*

A rock which both mineralogically and texturally strongly resembles typical metagranite-granodiorite samples from the three deep boreholes. The texture is granular with a distinct tectonic fabric marked by elongated domains of feldspar alternated by domains of strained quartz and streaks of ferromagnesian minerals. Quartz forms sub-grains with sutured contacts and undulose extinction; individual grains may reach up to about 3 mm in length. K-feldspar displays tartan twinning and locally, perthitic lamellae of albite. Plagioclase is to a variable extent sericitised. The prime mafic phases are biotite and epidote, which together with accessory amounts of magnetite, allanite, sphene, zircon and apatite forms elongated aggregates. Minor grains of biotite are frequently replaced by chlorite with lenses of prehnite and possibly also pumpellyite. Epidote occurs as anhedral grains (<0.3 mm), with very fine-scaled, symplectite texture. Magnetite forms rounded grains, locally with overgrowths of sphene. Allanite occurs as subhedral to euhedral, more or less metamict crystals (<0.4 mm), overgrown by epidote. Zircon is found enclosed in magnetite. Apatite forms stubby prisms about 50 microns in diameter.

239.84–239.89 m. *Metatonalite (101054).*

This rock displays a granular texture with irregular grain-boundaries and a distinct deformational fabric defined by elongated aggregates of hornblende and biotite, which together occupy 25.8 vol.% of the rock. Other major components are slightly sericitised plagioclase and strained quartz, as well as some minor (1.2 vol.%) K-feldspar. Hornblende is irregularly anhedral with a variable grain-size up to 2 mm. A few biotite grains are partially chloitised, and lenses of prehnite are rather frequent. Both sphene and epidote occur in accessory amounts and form anhedral grains up to 0.5 mm; the epidote crystals generally have a very fine-scaled, symplectitic character. Other accessory minerals are calcite, apatite (rounded crystals <0.1 mm) and a few tiny pyrite crystals.

310.96–311.01 m. *Metatonalite (101051).*

This rock seems to be a more fine-grained variety of the metatonalite described above (thin-section 239.84–239.89). However, the ferromagnesian phases are more dispersed in this rock, and the modal content of biotite is, moreover, considerably higher (19.4 vol.%). The rock displays a granular texture in which coarser feldspars are typically rounded. Plagioclase is faintly (locally strongly) sericiticed, whereas quartz is strained and shows undulose extinction. The distinct deformational fabric of the rock is primarily defined by booklet-shaped crystals of biotite and irregularly anhedral grains of hornblende. Intimately associated with the major mafic phases are minor amounts of titanite and epidote. Both form anhedral grains up to 0.3 mm in size, and epidote shows mostly a very fine-scaled symplectite texture. The accessory minerals include chlorite (after biotite), prehnite (as lenses in biotite/chlorite), allanite (enclosed in epidote), calcite (associated with the sericitisation), apatite and pyrite.

378.58–378.63 m. *Suspected ductile deformation zone rock adjacent to amphibolite.*

This rock displays a granular texture with a general grain-size less than 1 mm and distinct streaks of ferromagnesian phases. Based on a rough estimation of the feldspar proportions, the rock corresponds to a granodiorite. The texture is similar to that of the other granitoids sampled in KFM03A, with strained quartz, slightly sericitised plagioclase and tartan twinned K-feldspar. The ferromagnesian phases consist mainly of biotite, hornblende and epidote. Sphene and magnetite are notably absent. Epidote and some of the biotite display very fine-scaled, symplectitic margins. The accessory assemblage includes stubby prisms of apatite (<50 microns in diameter), pyrite (<0.3 mm), and a few metamict grains of possible allanite.

433.27–433.32 m. *Metagranite-granodiorite (101057).*

This rock is mineralogically and texturally almost identical with the other metagranite-granodiorite samples from the three deep boreholes. The texture is granular with irregular grain boundaries and a general grain-size ranging up to about 2 mm. There are, however, a few grains of strained quartz reaching up to 3 mm in length. Locally, plagioclase has been subjected to a weak sericitisation. K-feldspar displays cross-hatched twinning, and some grains are rich in coarse perthitic lamellae of albite. The ferromagnesian assemblage is limited to biotite (6.8 vol.%), associated with accessory amounts of epidote (<0.1 mm and with very fine-scaled, symplectitic character), sphene (<0.1 mm), magnetite (<0.1 mm) and allanite (rounded, often epidote mantled grains, <250 microns). Other accessories are apatite (stubby prisms, <50 microns in diameter) and calcite (intergrown with sericite).

504.40–504.45 m. *Metagranite-granodiorite (101057).*

Mineralogically and texturally similar to the other metagranites-granodiorite samples from the three deep boreholes. The general grain-size ranges up to 2 mm, with a few grains of elongated quartz reach up to almost 6 mm. Quartz displays a typical pattern of tectonic recrystallisation with sub-grains and strong undulose extinction. Plagioclase is to a variable extent sericitised. K-feldspar shows generally tartan twinning, and perthitic lamellae and ‘flames’ of exsolved albite are common. The ferromagnesian phases include biotite (4.4 vol.%), with accessory amounts of hornblende, magnetite, epidote, titanite and allanite. Biotite occurs either as isolated grains or in elongated aggregates; a few grains are partially replaced by chlorite. Sphene forms anhedral to subhedral grains (<0.5 mm), spatially associated with biotite or as thin overgrowths on magnetite. Epidote (<0.3 mm) tends to show a very fine-scaled, symplectite texture. The occurrence of allanite is limited to a few isolated, subhedral to anhedral grains, up to 0.8 mm in length. Magnetite is found as rounded grains, up to 0.5 mm in diameter. Apatite forms rounded prisms, less than 150 microns in diameter, whereas oscillary zoned zircons (<50 microns) mainly occur as inclusions in some of the mafic minerals.

510.95–511.05 m. *Suspected ductile deformation zone adjacent to amphibolite.*

The sampled section consists of a fine-grained, felsic and rather equigranular rock, in the lower half with elongated domains or streaks of amphibolitic material. Both the preferential orientation of individual grains and streaks of ferromagnesian minerals define the deformational fabric. Alternating domains of slightly variable grain-size further emphasizes the picture.

The felsic variety displays a granodioritic composition, with strained quartz, slightly sericitsed plagioclase and, subordinately, K-feldspar with tartan twinning and perthitic

lamellae. The only ferromagnesian phases are biotite and accessory amounts of epidote. The amphibolite domains, on the other hand, consist predominantly of hornblende, up to 2 mm in diameter, and minor amounts of plagioclase, biotite and epidote, and less than 1 vol.% apatite and calcite.

620.20–620.25 m. *Grey variety of the metagranite-granodiorite (101057).*

This rock shows a granular texture with a well-defined deformational fabric marked by thin streaks of biotite and alternating domains of recrystallized feldspar and strained quartz. The general grain-size ranges up to about 2 mm, with a few quartz grains reaching up to about 4 mm. Plagioclase is to a variable degree, and locally strongly sericitised. K-feldspar shows commonly tartan twinning and locally pertithic lamellae of albite. The most abundant ferromagnesian phases are biotite, locally chloritised, and epidote (<0.3 mm, typically with a very fine-scaled, symplectitic character), which together comprise 5.8 vol.% of the mode. Most biotite encloses turgid lenses of prehnite. Other accessory phases are sphene (<0.3 mm), pyrite and apatite (<30 microns). In addition, there is an anhedral and metamict grain of allanite about 0.5 mm in diameter.

860.52–860.57 m. *Metagranite-granodiorite (101057) speckled by whitish plagioclase.*

A rather massive rock with a highly variable grain-size ranging up to almost 5 mm. Most feldspars are somewhat rounded, whereas quartz have recrystallised into sub-grains with sutured boundaries and strong undulose extinction. Plagioclase is slightly, and locally strongly sericitised. Accessory amounts of calcite are commonly found together with the sericite. K-feldspar displays cross-hatched twinning and locally perthitic lamellae of albite. The prime ferromagnesian mineral is biotite which occupy 6.6 vol.% of the rock. Locally, biotite is partially chloritised, and lenses of prehnite occur frequently. Other ferromagnesian phases, found in accessory amounts in close proximity to biotite, are epidote (anhedral, <250 microns, and with a very fine-grained, symplectitic character), allanite (sub- to anhedral, <0.4 mm, and often with overgrowths of epidote), magnetite (irregularly rounded, <0.5 mm; one grain reaching up to 1.3 mm in size), sphene (as overgrowths on magnetite) and pyrite (ca. 0.1 mm). In addition, there are a few scattered apatite crystals, rounded and less than about 150 microns in diameter.

957.60–957.65 m. *Metagranite-granodiorite (101057) speckled by whitish plagioclase.*

Texturally almost identical with the rock described above from 860.52–860.57 m depth, but with slightly more intense retrogressive alteration. However, this rock displays a weak deformational fabric. Plagioclase typically shows a strong sericitisation, which gives the grains a whitish appearance macroscopically. Biotite is to a varying extent chloritised, and the majority of the affected grains are also rich in prehnite. The accessory assemblage includes magnetite (<0.5 mm), epidote, sphene (<0.1 mm), apatite (rounded stubby prisms, <0.1 mm in diameter) and a few zircons (<0.1 mm, with oscillary zoning).

Appendix 2

Whole-rock geochemical analyses

	KFM01A										
Length	109.60–110.06	242.25–242.55	315.85–316.25	355.30–355.50	432.96–433.15	473.53–473.71	477.10–477.50	521.10–521.40	704.69–705.10	947.40–947.80	970.10–970.50
Rock type	Metagranite-granodiorite	Meta-granodiorite	Metagranite-granodiorite	Amphibolite	Amphibolite	Amphibolite	Metagranite-granodiorite	Metagrano-diorite-tonal	Metagranite-granodiorite	Metagranite-granodiorite	Metagranite
Rock code	101057	101051	101057	102017	102017	102017	101057	101051	101057	101057	101051
Rock group	**B**	**C**	**B**	**B**	**B**	**B**	**B**	**C**	**B**	**B**	**C**
SiO_2 (wt%)	74.92	66.78	75.18	49.68	50.32	49.18	76.13	73.14	75.03	74.48	73.63
TiO_2	0.19	0.60	0.19	0.77	0.75	0.49	0.18	0.20	0.19	0.22	0.16
Al_2O_3	12.48	14.90	12.41	16.32	16.06	15.64	12.13	14.08	12.75	12.72	13.34
Fe_2O_3	2.76	4.48	2.7	11.00	11.11	10.46	2.53	2.65	2.67	3.04	2.38
MnO	0.04	0.05	0.04	0.20	0.24	0.19	0.03	0.04	0.03	0.04	0.04
MgO	0.63	1.37	0.34	5.66	5.78	6.92	0.81	0.63	0.30	0.35	0.32
CaO	1.75	3.72	1.70	10.24	8.73	12.48	1.71	3.41	1.75	1.79	1.58
Na_2O	3.69	4.09	3.20	3.58	3.56	2.69	3.98	4.16	3.58	3.31	2.94
K_2O	2.60	2.45	3.42	1.04	1.82	0.74	1.69	1.20	3.05	3.37	4.78
P_2O_5	0.03	0.18	<0.01	0.22	0.18	0.15	0.01	0.05	0.03	0.03	0.03
LOI	0.6	1.0	0.5	1.0	1.1	0.8	0.7	0.3	0.3	0.3	0.5
TOT/C	0.02	0.04	<0.01	0.03	0.03	0.02	0.05	0.04	0.02	0.01	0.02
TOT/S	<0.01	0.06	0.01	<0.01	0.01	<0.01	0.04	0.03	0.01	0.02	0.02
SUM	99.69	99.62	99.680	99.71	99.65	99.74	99.90	99.86	99.68	99.65	99.70
Sc (ppm)	5	7	5	39	40	42	5	2	5	6	6
V	10	60	9	267	271	252	10	10	7	9	8
Cr	21	7	<7	41	41	116	<7	<7	<7	<7	<7
Co	3.5	9.2	2.6	36.4	36.2	43.3	3.0	3.1	2.5	2.9	2.0
Ni	10.9	7.4	3	11	14.5	8.7	1.6	3.5	2.2	1.5	2.2
Cu	8.2	21.1	9.6	2.1	2.0	2.0	17.0	6.7	6.2	1.2	5.9
Zn	26	76	26	44	64	25	24	27	21	28	48
Ga	15.7	22.2	15.2	18.5	18.4	15.4	15.6	15.5	15.0	15.3	15.8
As	<0.5	0.5	<0.5	<0.5	<0.5	<0.5	<0.5	<0.5	<0.5	<0.5	<0.5
Se	<0.5	<0.5	<0.5	<0.5	<0.5	<0.5	<0.5	<0.5	<0.5	<0.5	<0.5
Rb	78.3	86.3	99.3	15.8	93.2	8.4	64.1	45.6	91.1	105.1	135.0
Sr	124.7	471.8	114.4	291.3	234.8	244.5	161.6	387.2	124.2	126.2	106.2
Y	27.9	12.9	28.4	16.5	16.1	9.3	37.4	7.6	31.1	20.3	14.7
Zr	150.9	231.5	157.5	45.5	41.9	32.4	166.6	149.6	149.3	181.1	158.1
Nb	11.1	8.7	10.9	2.6	2.8	2.2	12.0	6.1	12.3	9.4	13
Mo	0.6	0.4	0.5	0.4	0.7	0.6	2.4	0.2	1.2	12.8	0.7
Ag	<0.1	<0.1	<0.1	<0.1	<0.1	<0.1	<0.1	<0.1	<0.1	<0.1	<0.1
Cd	<0.1	<0.1	<0.1	<0.1	<0.1	<0.1	<0.1	<0.1	<0.1	<0.1	<0.1
Sn	2	2	2	2	4	2	3	2	3	2	3
Sb	0.1	0.1	0.1	<0.1	<0.1	<0.1	<0.1	<0.1	0.1	0.1	0.1
Cs	0.9	0.7	0.4	0.2	1.0	0.1	0.6	0.5	0.6	0.7	0.8
Ba	1307	909	1263	134	258	195	385	701	1587	1488	861
Hf	4.3	6.1	4.9	1.3	1.2	0.9	4.9	3.4	4.5	5.0	5.3
Ta	0.7	0.7	0.4	0.1	0.1	0.1	0.7	0.5	1.0	0.3	0.6
W	0.1	0.2	<0.1	1.3	0.2	17.0	0.5	0.7	0.3	0.4	0.3
Hg	0.01	<0.01	0.01	0.01	0.01	<0.01	<0.01	<0.01	0.01	<0.01	<0.01
Tl	0.2	0.3	0.2	<0.1	0.2	<0.1	0.3	0.2	0.2	0.3	0.4
Pb	4.9	5.0	4.4	1.0	0.9	1.2	3.4	2.5	4.0	3.6	11.4
Bi	0.1	<0.1	<0.1	0.1	0.1	0.1	<0.1	<0.1	<0.1	0.2	<0.1
Th	18.9	17.7	16.0	0.9	1.5	1.0	15.3	6.6	11.3	14.1	32.3
U	5.8	3.0	4.8	1.1	1.3	0.7	4.8	2.5	5.5	2.1	6.5
La	34.4	50.6	39.0	9.9	8.6	6.4	34.8	30.0	30.0	44.1	50.8
Ce	67.1	90.3	73.4	23.2	20.8	13.1	68.0	46.6	60.0	86.7	107.6
Pr	7.13	9.39	7.85	3.10	2.85	1.64	7.33	4.17	6.29	9.01	10.98
Nd	26.4	32.8	28.5	14.0	12.6	7.4	26.9	13.0	23.4	31.6	39.6
Sm	5.4	5.1	5.4	3.3	3.3	1.8	5.4	1.8	4.4	5.5	7.1
Eu	0.68	1.21	0.65	1.10	1.09	0.59	0.71	0.62	0.64	0.67	0.71
Gd	4.61	3.53	4.59	3.32	3.00	1.78	5.22	1.23	4.18	4.28	5.14
Tb	0.73	0.47	0.75	0.47	0.45	0.28	0.81	0.17	0.69	0.66	0.63
Dy	4.32	2.41	4.43	2.86	2.75	1.52	5.00	1.05	4.59	3.51	3.06
Ho	0.98	0.39	0.95	0.58	0.55	0.35	1.09	0.24	0.99	0.72	0.49
Er	2.61	0.88	2.81	1.54	1.49	0.94	3.14	0.71	2.98	1.93	1.36
Tm	0.39	0.15	0.43	0.23	0.23	0.14	0.54	0.13	0.53	0.30	0.21
Yb	2.49	0.90	2.68	1.52	1.54	0.94	3.38	1.01	3.46	1.68	1.32
Lu	0.37	0.14	0.41	0.23	0.23	0.13	0.54	0.16	0.48	0.25	0.21
Au (ppb)	1.5	0.8	0.9	<0.5	0.8	<0.5	1.0	<0.5	1.2	15.3	0.7

KFM02A														
Length	245.55–245.75	263.35–263.68	277.29–277.60	295.64–295.81	316.85–317.05	317.05–317.45	317.05–317.45	350.80–351.00	351.45–351.85	552.66–552.86	712.05–712.25	916.85–917.05	949.90–950.10	953.25–953.45
Rock type	Metagranite granodiorite	Resilicified episyenite	Episyenite	Episyenite	Metagranite granodiorite	Metagranite granodiorite	Metagranite granodiorite	Metagranite granodiorite	Metagranite granodiorite	Metagranite	Metagranite granodiorite	Metatonal.	Metagranite granodiorite	Metagranite granodiorite
Rock code	101057	101057	101057	101057	101057	101057	101057	101057	101057	101051	101057	101051	101057	101057
Rock group	**B**	**B**	**B**	**B**	**B**	**B**	**B**	**B**	**B**	**C?**	**B**	**C**	**B**	**B**
SiO_2 (wt%)	74.56	74.57	69.43	63.89	74.74	74.33	74.52	74.77	74.43	72.78	74.56	60.11	75.67	74.67
TiO_2	0.12	0.21	0.22	0.23	0.19	0.20	0.20	0.19	0.19	0.16	0.17	0.50	0.18	0.19
Al_2O_3	13.13	12.41	15.23	17.29	12.57	12.64	12.69	12.82	12.84	14.00	12.88	15.90	12.95	12.78
Fe_2O_3	1.91	3.14	3.02	4.35	3.09	2.85	2.82	2.78	2.99	2.38	2.48	8.05	2.56	2.95
MnO	0.04	0.02	0.03	0.03	0.04	0.04	0.04	0.04	0.04	0.05	0.03	0.15	0.04	0.04
MgO	0.33	0.41	0.90	1.03	0.39	0.45	0.44	0.28	0.30	0.28	0.50	2.69	0.54	0.27
CaO	1.15	0.13	0.19	0.19	1.26	1.30	1.30	1.52	1.47	1.66	1.25	7.16	2.16	1.51
Na_2O	3.11	4.12	4.80	6.09	3.16	3.21	3.15	3.45	3.37	3.53	3.30	3.32	4.27	3.48
K_2O	4.76	3.93	5.02	5.50	4.01	4.02	3.98	3.52	3.64	4.28	4.17	1.28	1.30	3.55
P_2O_5	0.04	0.03	0.03	0.04	0.02	0.03	0.05	0.01	0.03	0.03	0.03	0.12	0.04	0.03
LOI	0.5	0.7	0.8	1.0	0.2	0.6	0.5	0.3	0.4	0.6	0.3	0.4	0.1	0.2
TOT/C	0.05	<0.01	0.04	0.02	0.03	0.06	0.04	<0.01	0.02	0.03	<0.01	0.02	0.02	0.04
TOT/S	0.01	0.01	0.01	0.02	0.02	0.04	0.04	0.01	0.01	0.01	0.01	0.07	0.32	0.08
SUM	99.65	99.67	99.67	99.64	99.67	99.67	99.69	99.68	99.70	99.75	99.67	99.68	99.81	99.67
Sc (ppm)	4	5	5	6	5	5	5	5	4	7	5	23	5	4
V	<5	9	8	7	7	6	7	7	7	9	6	139	5	7
Cr	<7	<7	<7	7	<7	<7	<7	<7	<7	<7	<7	7	<7	<7
Co	1.7	1.9	3.0	4.2	3.4	2.9	3.1	2.5	2.5	2.0	2.1	19.0	3.7	2.5
Ni	2.5	2.8	3.0	2.4	2.5	2.8	2.3	2.6	2.7	2.6	2.5	1.9	2.2	2.1
Cu	8.6	12.3	13.7	12.3	35.8	55.6	51.5	9.0	9.2	9.7	8.3	14.9	43.5	15.7
Zn	30	20	39	43	28	30	28	31	26	47	23	46	26	25
Ga	13.7	12.8	16.7	20.5	15.0	15.1	15.9	15.5	15.7	18.3	14.9	17.7	15.2	15.0
As	1.5	0.6	<0.5	<0.5	<0.5	0.6	<0.5	<0.5	<0.5	0.5	<0.5	<0.5	<0.5	<0.5
Se	<0.5	<0.5	<0.5	<0.5	<0.5	<0.5	<0.5	<0.5	<0.5	<0.5	<0.5	<0.5	<0.5	<0.5
Rb	137.6	90.4	122.2	138.4	117.3	117.7	123.2	102.3	105.4	135.6	122.8	38.5	51.8	89.7
Sr	104.0	27.2	30.4	51.1	99.2	103.7	107.6	102.2	100.5	92.0	96.5	299.2	123.1	107.7
Y	17.3	20.7	28.5	27.7	26.7	22.9	23.6	19.5	20.5	38.3	29.6	22.9	40.2	28.0
Zr	99.3	187.2	178.9	204.1	150.4	160.0	161.0	163.1	155.0	176.7	134.1	87.7	151.1	165.6
Nb	9.0	13.4	14.8	14.5	14.0	11.6	11.6	10.4	11.0	20.9	11.0	7.1	11.4	10.1
Mo	0.6	0.6	0.5	0.4	1.0	1.2	0.9	0.7	0.8	0.7	1.0	0.2	0.7	1.1
Ag	<0.1	<0.1	<0.1	<0.1	<0.1	<0.1	<0.1	<0.1	<0.1	<0.1	<0.1	<0.1	<0.1	<0.1
Cd	<0.1	<0.1	<0.1	<0.1	<0.1	<0.1	<0.1	<0.1	<0.1	<0.1	<0.1	<0.1	<0.1	<0.1
Sn	2	3	3	4	3	2	3	4	4	3	2	3	4	2
Sb	0.2	0.2	0.1	0.1	0.1	0.1	0.1	0.1	0.1	0.1	0.1	<0.1	0.1	0.1
Cs	1.2	0.6	0.2	0.6	0.8	0.8	0.8	0.6	0.6	0.9	1.0	0.8	0.6	0.5
Ba	1449	1296	1549	1688	1310	1352	1364	1242	1172	459	1336	955	290	1290
Hf	2.9	6.3	5.6	6.0	4.3	4.6	4.9	4.7	4.3	6.0	3.7	2.7	4.5	4.7
Ta	0.4	0.4	0.4	0.5	0.7	0.5	0.5	0.5	0.5	1.4	0.8	0.5	0.7	0.5
W	0.8	1.5	0.7	1.9	1.3	0.5	0.2	0.4	0.3	0.3	0.8	0.4	0.2	0.3
Pb	4.5	2.9	1.9	3.0	5.4	5.9	5.1	5.2	5.2	8.8	5.3	1.9	4.8	3.9
Hg	0.01	<0.01	0.01	<0.01	<0.01	0.01	0.01	<0.01	<0.01	0.01	<0.01	<0.01	<0.01	<0.01
Tl	0.1	<0.1	0.1	<0.1	0.2	0.2	0.2	0.2	0.2	0.2	0.3	0.2	0.3	0.1
Bi	<0.1	<0.1	<0.1	0.1	<0.1	<0.1	<0.1	<0.1	<0.1	<0.1	<0.1	0.2	<0.1	<0.1
Th	20.1	20.6	17.8	16.6	15.3	15.2	15.8	14.9	16.0	27.3	14.7	5.6	19.3	13.5
U	2.6	2.4	5.0	4.5	4.8	4.1	3.9	4.2	5.5	8.5	6.6	2.9	15.6	4.7
La	35.1	45.5	3.5	7.5	35.8	35.2	37.7	36.5	34.4	46.2	40.4	21.8	36.8	35.0
Ce	77.0	83.6	8.8	15.5	73.9	73.0	75.9	71.6	67.6	95.9	74.0	43.0	69.6	66.6
Pr	7.98	10.09	0.90	1.72	7.78	7.64	8.04	7.79	7.47	10.87	7.96	5.08	7.61	7.30
Nd	29.6	37.1	3.6	6.0	28.5	27.9	29.2	28.3	27.5	40.1	28.1	20.6	28.9	26.3
Sm	5.4	5.3	1.5	2.1	5.6	5.4	5.7	5.0	5.0	8.5	5.1	4.1	5.8	5.3
Eu	0.69	0.63	0.29	0.38	0.68	0.68	0.73	0.63	0.61	0.85	0.66	0.95	0.60	0.67
Gd	4.55	3.79	2.06	2.59	4.70	4.50	4.62	4.03	4.15	7.60	4.06	3.68	5.33	4.09
Tb	0.67	0.60	0.54	0.64	0.82	0.74	0.74	0.59	0.61	1.21	0.74	0.57	0.95	0.74
Dy	3.13	3.25	4.17	4.31	4.42	4.20	4.29	3.32	3.34	6.42	4.56	3.63	6.31	4.44
Ho	0.56	0.70	0.99	1.04	0.93	0.82	0.82	0.64	0.74	1.24	0.93	0.79	1.38	0.9
Er	1.6	1.90	3.09	3.04	2.59	2.14	2.23	1.76	2.02	3.31	2.75	2.20	4.07	2.66
Tm	0.24	0.28	0.46	0.43	0.37	0.30	0.29	0.28	0.28	0.50	0.45	0.40	0.62	0.44
Yb	1.14	1.65	2.95	2.76	2.18	1.77	1.86	1.91	1.75	3.16	2.9	2.16	3.86	2.79
Lu	0.19	0.29	0.39	0.44	0.32	0.23	0.24	0.28	0.25	0.46	0.45	0.34	0.54	0.40
Au (ppb)	2.9	2.4	2.5	2.4	1.8	2.7	2.4	1.0	2.0	1.9	2.1	<0.5	0.9	0.6

	KFM03A & KFM03B										Standard	
Length	62.09-62.28	157.20-157.40	165.70-165.90	239.64-239.84	310.75-310.96	433.07-433.27	504.20-504.40	620.00-620.20	860.32-860.52	957.40-957.60	SO-17/CSB	
Rock type	Pegmatitic granite	Leucogran.	Metagranite granodiorite	Metatonal.	Metatonal.	Metagranite granodiorite	Metagranite granodiorite	Metagranite granodiorite	Metagranite granodiorite	Metagranite granodiorite		
Rock code	101061	111058	101057	101054	101051	101057	101057	101057	101057	101057		
Rock group	**D**	**D?**	**B**	**B**	**C**	**B**	**B**	**B**	**B**	**B**		
SiO_2 (wt%)	74.19	75.14	74.79	59.26	57.83	73.82	74.4	73.37	74.67	74.32	62.13	61.76
TiO_2	0.06	0.08	0.18	0.69	0.86	0.21	0.20	0.20	0.20	0.16	0.59	0.59
Al_2O_3	13.48	12.97	12.62	18.52	18.37	13.01	13.04	13.55	12.82	12.59	13.70	13.73
Fe_2O_3	1.35	2.04	2.81	6.99	8.03	2.93	2.72	2.57	2.90	2.85	5.82	5.82
MnO	0.02	0.04	0.03	0.10	0.12	0.04	0.04	0.03	0.04	0.04	0.54	0.53
MgO	0.18	0.14	0.28	1.08	1.48	0.52	0.30	0.33	0.30	0.26	2.37	2.38
CaO	1.14	1.13	1.58	6.76	6.84	1.41	1.62	1.92	1.60	1.35	4.70	4.69
Na_2O	2.71	3.05	2.87	3.86	3.68	3.70	3.36	3.69	3.29	3.11	4.07	4.16
K_2O	5.86	4.98	4.23	1.64	1.59	3.36	3.76	3.27	3.81	4.39	1.42	1.42
P_2O_5	<0.01	0.02	0.04	0.19	0.24	0.04	0.05	0.04	0.01	<0.01	1.01	0.97
LOI	0.7	0.3	0.4	0.7	0.7	0.6	0.2	0.7	0.1	0.6	3.4	3.4
TOT/C	0.05	0.03	0.02	0.02	0.07	<0.01	0.02	0.07	0.03	0.04	2.39	2.40
TOT/S	0.01	0.01	0.02	0.02	0.02	0.02	0.01	0.43	0.06	0.02	5.27	5.28
SUM oxid	99.69	99.89	99.83	99.79	99.74	99.64	99.69	99.67	99.74	99.67	99.75	99.45
Sc (ppm)	1	4	3	14	23	6	5	5	4	3	24	23
V	7	< 5	7	64	24	8	7	9	13	13	125	135
Cr	14	<7	<7	<7	<7	<7	<7	<7	<7	<7	3018	2984
Co	1.3	0.9	2.4	10.3	12.4	2.5	2.6	3.4	2.7	2.0	18.3	18.6
Ni	1.8	2.3	2.2	1.0	1.0	2.3	2.1	2.5	2.2	2.3	22.9	23.9
Cu	7.5	9.9	8.3	6.3	8.8	10.4	6.3	90.3	26.4	7.6	137.4	136.0
Zn	18	31	35	65	71	25	37	18	28	23	141	136
Ga	12.9	15.5	13.6	21.4	19.6	15.2	14.8	15.5	14.9	14.4	19.4	19.2
As	<0.5	0.7	<0.5	<0.5	<0.5	<0.5	<0.5	<0.5	0.7	0.7	18.6	19.8
Se	<0.5	<0.5	<0.5	<0.5	<0.5	<0.5	<0.5	0.6	<0.5	<0.5	4.8	4.7
Rb	125.9	125.2	98.3	55.2	46.8	81.0	108.3	89.4	96.8	104.7	22.9	22.7
Sr	143.1	75.9	121.9	351.4	368.7	100.5	103.2	135.1	102.3	95.3	307.3	309.3
Y	7.7	19.2	8.4	28.4	25.1	25.1	25.7	28.6	18.0	26.9	27.7	27.4
Zr	177.7	107.3	137.5	114.6	110.6	172.5	154.0	160.9	152.5	122.7	366.9	364.9
Nb	6.3	11.8	7.5	8.8	10.0	11.1	11.1	11.6	10.4	12.6	26.5	26.4
Mo	0.7	0.7	0.6	0.5	0.4	0.8	0.5	1.1	2.3	0.6	12.1	12.3
Ag	<0.1	<0.1	<0.1	<0.1	<0.1	<0.1	<0.1	0.1	0.1	<0.1	0.3	0.3
Sn	2	3	1	2	2	2	2	2	2	2	11	11
Cd	<0.1	0.1	<0.1	<0.1	<0.1	<0.1	<0.1	<0.1	<0.1	<0.1	5.5	5.6
Sb	0.1	0.1	0.1	0.1	<0.1	0.1	0.1	0.1	0.1	0.1	3.5	3.4
Cs	0.8	0.4	0.3	0.7	1.0	0.5	0.7	0.8	0.5	0.6	3.7	3.8
Ba	996	730	1278	754	592	1370	1276	1265	1123	1281	402	420
Hf	6.4	3.9	3.8	3.6	2.9	5.2	4.5	4.8	4.3	4.0	11.6	11.7
Ta	0.2	0.8	0.3	0.5	0.5	0.4	0.4	0.8	0.3	0.9	4.2	4.3
W	0.1	0.3	0.1	0.5	0.4	0.2	0.2	0.7	0.7	0.2	10.8	10.2
Hg	<0.01	<0.01	<0.01	<0.01	<0.01	<0.01	<0.01	<0.01	<0.01	<0.01	0.16	0.17
Tl	<0.1	<0.1	0.2	0.2	0.2	0.2	0.2	0.2	0.2	0.1	1	1
Pb	8.4	11.9	5.8	3.2	2.5	3.4	4.9	4.5	5.3	6.2	25.5	25.4
Bi	<0.1	<0.1	<0.1	<0.1	<0.1	<0.1	<0.1	0.1	<0.1	0.1	6.0	6.2
Th	32.8	18.4	12.7	7.6	4.5	14.6	14.3	14.9	16.5	17.3	11.6	12.5
U	10.8	6.1	1.6	2.2	2.3	4.1	3.3	4.9	2.6	6.8	11.1	11.7
La	33.0	35.0	37.3	27.8	19.5	33.6	35.8	38.1	36.2	34.1	10.7	10.3
Ce	66.6	71.6	70.4	56.3	40.8	65.3	67.5	72.9	71.9	68.2	23.2	23.3
Pr	7.51	8.16	7.68	6.72	5.09	7.16	7.61	8.02	8.04	7.75	3.02	3.00
Nd	28.1	31.2	27.2	26.8	22.7	27.3	28.6	29.7	30.8	29.1	13.2	13.3
Sm	5.2	5.9	4.6	5.0	5.0	5.1	5.3	5.2	5.2	5.3	3.3	3.5
Eu	0.72	0.69	0.53	1.28	1.5	0.64	0.63	0.70	0.69	0.72	1.08	1.13
Gd	3.33	4.36	2.82	4.45	4.53	4.50	4.27	4.33	3.96	4.98	3.73	3.92
Tb	0.46	0.65	0.42	0.80	0.75	0.71	0.69	0.69	0.71	0.83	0.64	0.69
Dy	1.81	3.33	1.72	4.63	4.16	4.07	4.10	4.34	3.67	4.76	4.31	4.25
Ho	0.30	0.65	0.30	0.95	0.91	0.87	0.87	0.96	0.64	0.96	0.90	0.90
Er	0.81	1.67	0.73	2.72	2.57	2.37	2.68	2.84	1.68	2.84	2.72	2.72
Tm	0.09	0.27	0.10	0.44	0.35	0.38	0.42	0.49	0.23	0.41	0.44	0.41
Yb	0.69	1.59	0.64	2.82	2.27	2.13	2.93	3.24	1.51	2.60	2.82	2.88
Lu	0.11	0.23	0.10	0.37	0.35	0.31	0.43	0.46	0.19	0.38	0.43	0.45
Au (ppb)	1.8	4.0	1.2	0.5	<0.5	3.7	1.0	0.8	1.4	0.9	42	39.5

Appendix 3

Selected trace element analyses for the episyenite occurrence in KFM02A

	KFM02A					Standard
Length	249.17–249.36	258.04–258.20	291.87–292.00	292.00–292.20	307.00–307.15	DS5
Rock type	Pegmatite	Pegmatite	Pegmatite/ Granite	Altered granite	Unaltered granite	
Rock code	101061	101061	101057	101057	101057	
Rock group	**D**	**D**	**D/B**	**B**	**B**	
Special reason	Abundant hematite and chlorite	Granulated feldspars with fracture hematite	Contact with chlorite and quartz	Type sample	Type sample	
Ti (wt%)*	0.019	0.003	0.019	0.021	0.04	0.095
Al (wt%)*	0.65	0.19	0.58	0.87	0.52	2.08
Fe (wt%)*	1.61	0.62	1.16	1.5	1.44	2.98
Mn (ppm)*	179	44	145	209	195	778
Mg (wt%)*	0.32	0.03	0.31	0.44	0.17	0.66
Ca (wt%)*	0.22	0.05	0.05	0.26	0.13	0.72
Na (wt%)*	0.025	0.047	0.056	0.092	0.05	0.033
K (wt%)*	0.16	0.09	0.11	0.11	0.23	0.13
P (wt%)*	0.028	0.001	0.013	0.02	0.013	0.093
S (wt%)*	0.03	0.02	0.07	0.07	0.03	0.05
B (ppm)*	1	<1	1	1	2	18
Sc (ppm)*	1.8	0.6	1.9	1.8	2.2	3.3
V (ppm)*	9	2	4	6	6	59
Cr (ppm)*	7.4	6.4	7.2	9.1	7.5	189.7
Co (ppm)	2.3	0.4	2.6	3.8	2.4	12.5
Ni (ppm)*	1.5	1	1.6	1.9	1.2	25.4
Cu (ppm)	5.8	6.32	10.7	13.17	27.74	143.79
Zn (ppm)	26.7	2.6	20.8	29.6	19.1	137.2
Ga (ppm)	5.3	0.8	3.8	5.3	3.2	6.5
As (ppm)	0.1	0.2	0.1	0.1	<0.1	18.3
Se (ppm)	0.1	<0.1	0.1	0.1	0.1	4.6
Sr (ppm)*	3.9	2	3.4	5.1	5.1	46.8
Mo (ppm)	0.65	0.44	0.44	0.51	0.49	12.42
Ag (ppb)	17	9	36	36	45	275
Cd (ppm)	0.01	<0.01	0.02	0.02	0.01	5.61
Sb (ppm)	0.03	0.04	0.02	0.02	0.02	3.59
Te (ppm)	<0.02	<0.02	<0.02	<0.02	0.05	0.86
Ba (ppm)*	53.9	13.3	39.4	44.3	53.1	135.9
La (ppm)*	31.8	6.5	6.5	7.1	34.3	12
W (ppm)*	1.7	1.4	1.2	1.2	1.2	4.5
Au (ppb)	0.7	0.5	<0.2	<0.2	0.3	40.5
Hg (ppb)	<5	7	<5	<5	18	173
Tl (ppm)	0.06	0.02	0.05	0.06	0.14	1.04
Pb (ppm)	3.11	1.27	1.62	1.72	2.19	23.87
Bi (ppm)	0.05	0.05	0.02	0.02	0.05	6.3
Th (ppm)*	14.1	4.5	11.3	15.4	15.5	2.6
U (ppm)*	1.8	4.5	1.8	2.1	6.4	6.1

* Alkaline and refractory metals with partial solubility in dilute aqua regia. Fusion attack is necessary to obtain their total content.

Appendix 4

XRD results of fracture coatings

Randomly oriented grain samples														
KFM01	**Ca**	**Qz**	**Alb**	**Kfsp**	**Pre**	**Lau**	**Ana**	**Apo**	**Chl/Corr**	**Py**	**Hm**	**Ill**	**Ep**	**Fl**
105.3	X	XX	XX						X2			X		
122.88		XX	X			XX								
127.40		XX	XX	X			XX		X2					
137.64	XX	X	XX''						XX2			X		
146.77	X	XX		X					X	X				
148.40					XX		X		XX2	X				
149.18					XX		X		XX2	X				
165.88'						XX			X					
179.35	X	XX	XX						XX		X			
185.35					XX				X		X	X		
188.10		X				XX'''								
192.55	XX	X	X´´	X	X				XX2					
219.49			XX			XX'''			XX		XX			
239.70	XX	XX	X	X		XX			X					
269.90	X	X			XX		XX		XX2	X				
384.20	XX	XX	X	X					XX*					
392.43		XX	X						XX					
420.30		XX	X		X				XX2					
652.20	X	X	X						XX					
656.0	X					XXX'''								
842.50	X				X	XX'''			X					
KFM02	**Ca**	**Qz**	**Alb**	**Kfsp**	**Pre**	**Lau**	**Ana**	**Apo**	**Chl/Corr**	**Py**	**Hm**	**Ill**	**Ep**	**Fl**
102.75						XX'''			X			X		
111.0–111.15	X	(X)	XX'						X	X				
118.25		XX	X	X								X		
118.28	XX	X		X								X		
422.4	XX	XX	X	X					X					
423.65	X	XX	X	X					X					
476.75–477.0	X	XX						X	XX2,Bi			(X)		
486.0	XX#	X	X	X					X					
516.09–516.25	XX	X	X	X					XX2				(X)	(X)
516.60–516.65	XX	X	X	X					XX		X			
776.50–776.60		XX	X	X					X, Bi, (Sap)			(X)		
893.45–893.65								XX	X2					
903.65–903.70		XX	X						X2					
KFM03	**Ca**	**Qz**	**Alb**	**Kfsp**	**Pre**	**Lau**	**Ana**	**Apo**	**Chl/Corr**	**Py**	**Hm**	**Ill**	**Ep**	**Fl**
+0.50						XXX								
65.20–65.25	XX	X	X	X					XX2			X		
139.03–139.06	X	X						X (F)	XX2					
255.85–255.90	X	XX	X	X					X			XX Mu?		
381.70–381.86	XX								(Sap)					
388.50–388.60		XX	X	X					XX2					
643.80–644.17	XX	X	X	X					XX2		X			
803.85–804.05		XX	XX						XX, Bi					
813.88–813.97		X		XX				XX						
940.53–940.60	XX	XX	X	X				XX	(Sap)					
944.30–944.50	X	XX	X	X					XX			X		
986.60–986.70	X	XX	X	X										

Ca =Calcite, Qz= Quartz , Alb = Albite, K-fsp = K-feldspar, Pre=Prehnite, Lau=Laumontite, Ana= Analcime, Apophyllite, Chl=Chlorite, Corr=Corrensite, Py=Pyrite, Hm= Hematite. Ill=Illite, Ep=Epidote, Fl= Fluorite,
XX = main component; X=additional component; (X)= minor component.
This division is only valid for the sample and does not necessarily represent the fracture coating
2= Both chlorite and corrensite are present in the sample
´ = a small amount of hornblende is present in the sample but belongs probably to the fracture wall
´´ ="Calcian albite"
´´´= Laumontite-leonhardite (instead of only laumontite).
Bi = small amount of biotite has been identified
(Sap) = Saponite (smectite)
(F) = Fluoro-apophyllite

Oriented grain samples of fine fractions (<2 µm) for clay mineral identification

KFM01A	Chlorite	Corrensite	Illite	Mixed –layer clay	Smectite
105.30	X	X (regular)			
127.40	X	X (irregular)			
137.64		X (irregular) less swelling components that in 127.40	X		
148.40		X (more swelling components than in 148,4			
149.18		X (similar to 149.18)			
165.88		(X)			
185.35	X		X	Mixed layer clay of low crystallinity probably chlorite/illite	
192.55		X			
269.90		X (similar to 149.18 but somewhat less swelling)			
384.20	X	X (regular)	(X)		
420.30	X	X			
KFM02A	**Chlorite**	**Corrensite**	**Illite**	**Mixed –layer clay**	**Smectite**
102.75		X			
111.0–111.15	X	X			
118.25				Illite-smectite ratio 3:2	
118.28				Illite-smectite ratio 3:2	
422.40	X	X			
476.75–477.0		X	X		
486.0	X	X (deviates from 1.1 structure)			
516.09–516.25	X	X			
516.60–516.65	X	X			
776.50–776.60			(X)		X
903.65–903.70	X	X (deviates from 1:1 structure)			
KFM03A+B	**Chlorite**	**Corrensite**	**Illite**	**Mixed –layer clay**	**Smectite**
65.20–65.25	X		X	Illite-smectite	
139.03–139.06	X		(X)		X
255.85–255.90		X	X (Musc?)		
381.70–381.86					X
388.50–388.60	X				X
643.80–644.17	X	X			
803.85–804.05	(X)	X	(X)		
813.88–813.97		X			
940.53–940.60					X
944.30–944.50	X		X		

X=additional component; (X)= minor component.
This division is only valid for the sample and does not necessarily represent the fracture coating.

Appendix 5

ICP analyses of fracture coatings samples

	KFM01A							KFM02A				
Length	127.40	148.40	149.18	179,35–179.4	185.35	188.10–188.20	269.90	118.25	423.65	476.75–477.00	516.09–516.25	893.45–893.65
XRD mineral composition	Analcime, Quartz, K-feldspar, Corrensite	Prehnite, Corrensite, Analcime, Pyrite	Prehnite, Corrensite, Analcime,Pyrite	Quartz, Albite, Chlorite, Calcite, Hematite	Prehnite, Chlorite, Illite, Hematite, Mixed layer clay	Laumontite, Quartz	Prehnite, Analcime, Corrensite, Calcite, Quartz, Pyrite	Quartz, Albite, K-fsp, Illite	Quartz, Albite, K-fsp, Calcite, Chlorite	Quartz, Corrensite, Apophyllite, Calcite	Calcite, Chlorite, Corrensite, Quartz, Albite, K-fsp	Apohyllite, Chlorite
SiO_2 (wt%)	59.4	44.7	40.9	51.6	38.9	53.8	32.6	71.8	70.6	40.1	40	51
TiO_2	0.0904	0.0391	0.0199	0.919	0.0356	0.0152	0.0263	0.125	0.296	0.558	1	0.119
Al_2O_3	15.3	20.3	18.9	16.7	19.4	21.5	15	14.2	12.5	11.9	16.4	1.2
Fe_2O_3	10.7	6.73	10.8	11.6	10.5	1.02	10.2	2.03	5.91	14.2	9.06	1.43
MnO	0.0567	0.0851	0.17	0.167	0.141	0.0065	0.15	0.0233	0.124	0.301	0.286	0.0411
MgO	1.52	3.44	7.8	4.54	6.18	0.162	6.45	0.82	2.26	12.1	7.68	0.848
CaO	0.724	17.7	12.7	3.04	9.75	11.1	19.2	0.453	0.877	6.79	12.4	22.7
Na_2O	5.14	1.14	0.394	5.07	0.203	0.349	1.15	1.07	2.13	0.181	2.37	0.211
K_2O	3.01	1.29	1.6	1.74	1.48	0.392	0.654	8.1	5.19	4.73	1.61	4.61
P_2O_5	0.0228	0.0098	0.0073	0.226	0.0098	0.0078	0.0123	0.0822	0.0815	0.11	0.129	0.0208
SUM	96	95.4	93.3	95.6	86.6	88.4	85.4	98.7	100	91	90.9	82.2
Be (mg/kg)	1.27	5.45	9.89	3.79	14.7	2.06	5.01	2.07	1.38	1.24	5.12	<1
Sc	1.64	<1	<1	36.2	<3	<1	<1	2.81	6.59	31.8	41.6	<2
V	21.2	87.9	177	100	100	<2	50	38.2	14.6	183	156	5.19
Cr	18.2	24	17.9	21.9	<30	<10	57	242	<10	617	294	<20
Co	<6	<6	<6	21.5	<10	<6	<6	<7	<6	21.6	17.8	<10
Ni	<10	<10	<10	19.1	<30	<10	13.8	<10	<10	90.3	41.3	69.3
Cu	37.2	13.8	7.05	11.4	96.2	6.17	39.7	20.5	16.1	606	37.1	1490
Zn	21.8	32.1	73.7	109	133	<10	93.9	56.5	87.5	285	196	194
Ga	16.7	32.5	37.9	31.4	7.36	26.7	21.6	32.8	42.5	30	32.8	<2
Rb	99.5	39.1	47.9	106	141	20.6	26.5	254	133	340	48.5	439
Sr	52.3	22.6	54	193	79.7	338	53	50.4	60.7	27.6	359	20.3
Y	13.1	8.94	18	34.3	28.2	2.14	12.3	25.4	39.1	35.4	54.2	212
Zr	47.1	2.36	6.8	97.7	6.57	12.4	10.6	250	353	24.9	197	87.3
Nb	6.7	3.24	0.933	8.73	<0,5	0.959	0.882	9.8	30.4	20.6	36.1	2.82
Mo	<2	<2	14.5	50.7	<5	<2	5.05	<3	<2	<2	<2	<5
Sn	1.56	2.45	<1	6.05	2.77	<1	<1	1.42	3.73	25.4	16.3	21.5
Cs	32.7	9.21	3.02	n.d.	11.3	n.d.	8.58	15.7	0.305	9.7	0.367	0.277
Ba	554	180	340	161	76.3	128	117	1220	1430	317	207	247
Hf	2.31	0.416	0.818	2.38	0.907	0.264	0.666	7.26	11.5	0.942	6.93	3.26
Ta	0.53	0.367	0.137	0.771	<0,1	0.0987	0.094	1.12	2.72	23.1	5.15	0.209
W	6.18	4.6	1.85	2.95	11.3	1.04	2.56	1.54	7.9	1.79	2.07	12.6
Th	1.51	0.247	0.53	2.9	<0,3	0.853	1.18	2.39	10.8	1.12	7.2	4.1
U	6.68	6.69	5.46	12.1	8.4	0.461	3.41	4.54	39.7	1.37	20.9	1.7
La	30	4.52	10.8	41.8	45.6	6.6	25.3	12.9	38.4	43.8	37	815
Ce	56.1	13.1	24.9	62.4	182	15.2	47.9	25.6	74.6	44.4	57	1060
Pr	5.08	1.41	2.43	8.27	12	1.46	5.16	2.97	7.8	4.79	6.82	97.2
Nd	18.3	6.4	10.6	32.7	43.3	4.57	22.2	11	34.1	23	27.2	373
Sm	3.97	1.69	4.24	6.39	8.69	0.817	3.34	2.72	7.23	4.88	6.87	58.4
Eu	0.501	0.177	<0,05	1.08	0.949	<0,05	0.262	0.383	0.909	<0,04	0.609	9.4
Gd	3.21	1.54	3.32	6.36	10.1	0.96	2.79	1.72	6.26	4.73	6.41	58.8
Tb	0.468	0.14	0.414	0.799	1.1	0.119	0.222	0.373	1.07	0.684	1.06	7.2
Dy	2.26	1.17	2.46	4.47	4.3	0.574	1.53	3.03	6.99	5	7.65	32.4
Ho	0.467	0.219	0.526	0.961	0.981	0.107	0.317	0.828	1.52	1.08	1.74	5.58
Er	1.17	0.52	1.18	3.13	3.24	0.588	0.939	2.76	4.76	3.94	6.27	12.9
Tm	<0.1	0.142	0.227	0.491	<0,3	<0,1	<0,1	0.496	0.783	0.486	1.12	1.5
Yb	1.51	0.911	1.13	3.34	2.21	<0,2	0.896	3.8	4.65	5.37	9.84	6.38
Lu	0.148	0.0964	0.121	0.537	0.177	<0,03	0.0616	0.641	0.634	0.686	1.54	0.85

The mineralogical composition is obtained from XRD (cf Appendix 4).

The minerals are given in order of abundance.

Appendix 6

Gamma ray spectrometry data

			Average					
Drillhole-ID	Secup (m)	Seclow (m)	K [%]	U [ppm]	Th [ppm]	Natural exposure [micro-R/h]	Rock group	Rock type
KFM01								
KFM01A	109.60	110.06	2.3	5.8	19.2	13.0	B8	Metagranite-granodiorite
KFM01A	242.25	242.55	2.2	4.3	16.6	11.1	C	Meta-granodiorite
KFM01A	315.85	316.25	3.2	5.0	23.0	15.0	B8	Metagranite-granodiorite
KFM01A	355.30	355.50	1.0	2.4	3.1	3.8	B4	Amphibolite
KFM01A	432.96	433.15	1.6	1.7	1.5	3.8	B4	Amphibolite
KFM01A	473.53	473.71	0.8	0.2	2.9	2.1	B4	Amphibolite
KFM01A	477.10	477.50	1.2	5.4	18.0	10.7	B8	Metagranite-granodiorite
KFM01A	521.10	521.40	0.8	4.7	6.9	6.2	C	Metagranodiorite-tonalite
KFM01A	704.69	705.10	2.5	6.3	18.3	13.3	B8	Metagranite-granodiorite
KFM01A	947.40	947.80	2.7	2.2	15.0	10.0	B8	Metagranite-granodiorite
KFM01A	970.10	970.50	4.0	6.0	42.4	22.8	C	Metagranite
KFM02								
KFM02A	245.55	245.75	4.2	2.2	22.4	14.5	B8	Metagranite-granodiorite
KFM02A	263.35	263.68	3.4	3.7	22.1	14.3	Bepi	Episyenite
KFM02A	277.29	277.60	4.5	5.0	18.7	15.6	Bepi	Episyenite
KFM02A	295.64	295.81	4.6	5.9	23.2	17.8	Bepi	Episyenite
KFM02A	316.85	317.05	3.5	3.6	16.7	12.7	B8	Metagranite-granodiorite
KFM02A	317.05	317.45	3.0	5.0	13.2	11.7	B8	Metagranite-granodiorite
KFM02A	350.80	351.00	3.0	4.0	17.2	12.3	B8	Metagranite-granodiorite
KFM02A	351.45	351.85	3.5	6.8	15.4	14.3	B8	Metagranite-granodiorite
KFM02A	552.66	552.86	3.6	8.2	29.4	19.6	C	Metagranite
KFM02A	712.05	712.25	3.5	7.6	16.4	15.1	B8	Metagranite-granodiorite
KFM02A	916.85	917.05	1.2	2.0	9.5	6.0	C	Metatonalite
KFM02A	949.90	950.10	1.0	19.0	19.0	19.3	B8	Metagranite-granodiorite
KFM02A	953.25	953.45	3.0	4.6	15.2	12.0	B8	Metagranite-granodiorite
KFM03								
KFM03B	62.09	62.28	4.9	12.1	37.7	26.5	D2	Pegmatitic granite
KFM03A	157.20	157.40	4.2	8.2	22.1	18.2	D?	Leucogranite
KFM03A	165.70	165.90	3.5	2.1	13.7	10.8	B8	Metagranite-granodiorite
KFM03A	239.64	239.84	1.4	1.2	11.2	6.3	B5	Metatonalite
KFM03A	310.75	310.96	1.4	2.4	7.1	5.7	C	Metatonalite
KFM03A	433.07	433.27	2.7	6.5	11.0	11.5	B8	Metagranite-granodiorite
KFM03A	504.20	504.40	3.3	3.3	20.3	13.3	B8	Metagranite-granodiorite
KFM03A	620.00	620.20	2.8	4.3	19.9	13.0	B8	Metagranite-granodiorite
KFM03A	860.32	860.52	3.5	0.8	13.7	10.0	B8	Metagranite-granodiorite
KFM03A	957.40	957.60	3.4	7.4	22.6	16.8	B8	Metagranite-granodiorite